# SKELETAL BIOMECHANICS OF THE FLORIDA MANATEE
(*Trichechus manatus latirostris*)

By

KARI BETH CLIFTON

A DISSERTATION PRESENTED TO THE GRADUATE SCHOOL
OF THE UNIVERSITY OF FLORIDA IN PARTIAL FULFILLMENT
OF THE REQUIREMENTS FOR THE DEGREE OF
DOCTOR OF PHILOSOPHY

UNIVERSITY OF FLORIDA

2005

to all those—people and animal alike—who have loved, supported, encouraged, instructed, amazed, inspired, and empowered me

ACKNOWLEDGMENTS

This project was an enormous undertaking–one that I could not have completed alone. First I would like to acknowledge my supervisory committee chair (Roger Reep) and co-chair (Jack Mecholsky). I thank Roger for his unqualified generosity, encouragement, and guidance; and for feeding the spirit with food and wine. I benefited greatly from being allowed to wander off the path in pursuit of new ideas. I thank Jack for his patience in teaching a biologist to think like an engineer, and for the tailgates. My supervisory committee members (MaryBeth Horodyski, Donna Wheeler, and Tom Wronski) provided guidance, instruction, and support for which I am grateful.

Many individuals contributed to the success of this project. While I was working at the Florida Department of Environmental Protection, Dr. Sentiel Rommel suggested I take a look at manatee bone. He and Dr. Tom Koob at the Shriners Hospital for Children introduced me to the field of bone mechanics. The Save the Manatee Club funded a pilot study that led to the inception of this project. I am indebted to Maggie Stoll for her invaluable technical expertise and administrative support. To my fellow graduate students in the fracture mechanics group, I am grateful for the weekly discussions of ceramics and other things. I learned a great deal about fractography and bone mechanics from Jiahau Yan.

From the College of Engineering, Chuck Broward provided access to the air cannon, as well as his expert engineering skills. Billy Schultz performed the strain gauge testing. Bryan Conrad from the Department of Orthopaedics taught me to operate the

biomechanical testing equipment, and provided invaluable technical support. Joan Yonchek lent her amazing expertise in hard and soft tissue histology. I thank Allyson Barrett and Ben Lee from the Department of Dental Biomaterials for their assistance with technical issues and data collection. This project made great strides forward with the help of veterinary students Julia Golden and Beth Carson; and undergraduate volunteers Johnattan, Rebecca, Jessica, Stephanie, Jaime, Travis, and Chris.

Tissue samples were provided by the FWC's Marine Mammal Pathobiology Lab in St. Petersburg, and by Sea World of Florida. I extend my thanks and appreciation to Dr. Sentiel Rommel, Mr. Tom Pitchford, Mr. Ken Arrison and the staff of the MMPL, and to Dr. Beth Chittick of Sea World.

I wish to thank the college of Veterinary Medicine, the Marine Animal Health program, and in particular Dr. Charles Courtney for his interest and enthusiasm for my project. This project was funded by a College of Veterinary Medicine Consolidated Faculty Research award and a Marine Conservation Trust Fund award. Additional funding was provided by grants from the Sigma Xi Scientific Research Society, a College of Veterinary Medicine Graduate Student Seed Grant, and a Merck-Merial Veterinary Scholars Research Grant. The University's Graduate Student Council and Graduate School provided travel awards so that I could attend conferences.

Last, but not at all least, I would like to express my gratitude and appreciation for the love and support of my family throughout my many years of schooling. I am indebted to my nephews David, Adam, and Brain, for never, ever letting me get a lick of work done while at their house. There are, after all, more important things in life.

TABLE OF CONTENTS

LIST OF TABLES

LIST OF FIGURES

Abstract of Dissertation Presented to the Graduate School
of the University of Florida in Partial Fulfillment of the
Requirements for the Degree of Doctor of Philosophy

SKELETAL BIOMECHANICS OF THE FLORIDA MANATEE
(*Trichechus manatus latirostris*)

By

Kari Beth Clifton

December 2005

Chair: Roger L. Reep
Cochair: John J. Mecholsky, Jr.
Major Department: Veterinary Medicine

Watercraft-related mortality of the Florida manatee (*Trichechus manatus latirostris*) accounts for 25% of all deaths from 1974-2004, comprising 85% of anthropogenic-related deaths. Of those, the proportion of deaths due to impact accounts for 67% of all watercraft fatalities. Reducing this preventable source of mortality is a high priority in state and federal manatee recovery efforts, which focus primarily on regulating boating activities. However, with more boats using the waterways, the potential threat posed by watercraft continues to increase. To establish safe boat speeds for manatee protection, an estimate of the forces required to fracture their bone is needed. This study is the first to quantify the biomechanical effects of boat strikes on manatees. Our goal was to estimate material and structural properties of manatee rib bone. To measure bone material properties, machined specimens were tested in 3-point flexure. Strength, toughness, modulus, and work of fracture were determined for three size classes, by sex. Mean flexural strengths ranged from 62–160 MPa, fracture toughness

from 1.4–2.9 MPa·$m^{1/2}$, elastic moduli from 4–18 GPa, and work of fracture 3–6 MJ·$m^{-3}$, indicating that manatee bone is less strong and tough than other mammalian bone, including human. There were no differences in mechanical variables between the sexes. Density and mineral content increased with body size, suggesting that material properties are likely correlated bone tissue quality, as well as to microstructure. For whole bone structural tests, ribs were impacted to estimate failure stress and kinetic energy needed to cause fracture. Fractographic analysis was used to calculate the stress at failure. Strengths ranged from 106–179 MPa. Strain gauges were used to validate these calculations. Fractal geometry was used to calculate the fractal dimensional increment (D*). Values for manatee bone (.08–.22) were at the lower end of the range for ceramics, suggesting that a low amount of energy is needed to cause fracture. There was no relationship between D* and age. The ability to resist bone fracture does not appear to increase as animals grow. Impact energy calculations suggest that boats may inflict fatal injuries to manatees at speeds of 13–15 mph.

# CHAPTER 1
# INTRODUCTION

The West Indian manatee (*Trichechus manatus*) is one of four extant species belonging to the order Sirenia. It occurs throughout the Caribbean, from the southeastern United States to northeastern Brazil. Manatees inhabit shallow, coastal estuarine or riverine waters, feeding primarily on seagrasses and other aquatic vegetation. Their reliance on shallow-water habitats has resulted in two distinct, geographically isolated subspecies: the Florida manatee (*Trichechus manatus latirostris*) is found primarily in Florida, whereas the Antillean manatee (*Trichechus manatus manatus*) is found in disjunct populations in eastern Central America, the Greater Antilles, and northeastern coastal South America (Marmontel, 1993).

The Florida manatee is listed as endangered by the U.S. Department of the Interior, and is considered one of the most endangered marine mammals found in U.S. waters (U.S. Fish and Wildlife Service, 1996). Manatees are protected by state and federal legislation. Florida provided the first protection in 1893, when a law was passed prohibiting the killing of manatees (Reynolds and Odell, 1991). The Florida Manatee Sanctuary Act of 1978 established the entire state of Florida as a manatee refuge, and mandated the creation of boat speed regulatory zones (Reynolds and Odell, 1991). The Marine Mammal Protection Act of 1972 established federal guidelines for maintaining marine ecosystems, including marine mammals (Reynolds and Odell, 1991). The Endangered Species Act of 1973 mandates the development and implementation of recovery plans for wildlife identified as threatened or endangered with extinction. The

main objective of the Florida manatee recovery plan, first released by the U.S. Fish and Wildlife Service in 1989, is to downlist, and to ultimately delist the species when the population has reached maximum sustainable levels, and threats to the habitat and mortality are controlled (Eberhardt and O'Shea, 1995). The plan also identifies the actions needed to meet those criteria. However, the rapid growth of the human population in Florida, and the continued decline in manatee habitat and increasing numbers of deaths makes it unlikely that the species will be downlisted.

Sources of manatee mortality have been documented in Florida since 1974 (O'Shea et al., 1985; Ackerman et al., 1995; Wright et al., 1995). Watercraft-related mortality, caused by propeller wounds or by impact with a boat's hull, accounts for 25% of all deaths from 1974 through 2004, and comprises 85% of anthropogenic-related deaths (Florida Fish and Wildlife Conservation Commission, 2005). Wright et al. (1995) examined necropsy records for 406 manatees killed by boats from 1979 through 1991. Deaths were broken down into three sub-categories: deaths from propeller wounds; from impact-related injuries; or from a combination of propeller and impact injuries. The proportion of impact-related mortality has increased over time, and now accounts for more than half (66%) of all watercraft-related deaths (Florida Fish and Wildlife Conservation Commission, 2005). Regardless of cause of death, most manatees bore scars of healed propeller wounds. Fatal propeller wounds were usually more severe than non-fatal wounds, and animals killed by propeller cuts rarely suffered skeletal damage. Conversely, approximately 66% of the carcasses attributed to impact injuries had fractured and/or luxated ribs. In addition, healed fractures were rarely observed in any

carcasses. These data suggest that while many propeller wounds are sub-lethal, impact injuries sufficient to inflict skeletal damage are usually fatal.

The number of watercraft-related deaths has increased at a rate of 7% annually from 1992 to 2004 (Florida Fish and Wildlife Conservation Commission, 2005). Reducing watercraft-related mortality is identified as a high priority in the manatee recovery plan. To date, recovery efforts have focused primarily on regulation of boating activities by establishing speed zones in areas where manatees and boats coexist. The Florida Fish and Wildlife Conservation Commission (FWC) is responsible for establishing boat speed regulatory zones in any body of water in Florida where manatee protection is warranted (Florida DNR, 1989). The Florida Manatee Sanctuary Act of 1978 and subsequent amendments give the FWC the authority to regulate boat speeds and to limit boating activities in areas essential to manatees. The 1989 "Recommendations to Improve Boating Safety and Manatee Protection for Florida Waterways" identified 13 key counties and gave them the option to develop site specific speed zones, adopt 300 foot buffer slow speed zones within all inshore/coastal waters, or adopt 30 mph in channels and 20 mph outside the channels. Predominantly, the counties chose to develop their own zones, and most were adopted and approved by the state of Florida by the early 1990s.

To designate boat speed zones, the FWC primarily uses manatee aerial survey data, mortality records, satellite telemetry, and boat use data. Based on these datasets, speed zones are delimited by visual estimation of the areas used by manatees. Maximum speed limits are typically established by examining the number and pattern of manatees that utilize the area and the nature and extent of watercraft usage (e.g., a nearby boat

channel indicates frequent, high speed use) if known. The proposed speed zones are then reviewed and modified in a series of public and legal hearings. The speed zones that are ultimately implemented by law are a compromise of the rules originally proposed by the FWC and the affected parties (e.g., commercial boating industries, recreational boaters). Thus, creation of boat speed zones is a highly subjective process, not based on any information pertaining to the biological effects of boat strikes on manatees.

Although boat speed regulatory zones have been in existence since the inception of the Florida Manatee Sanctuary Act, the increasing human population along the Florida coastline has resulted in more boats utilizing the waterways. From 1996 through 2004, the number of watercraft on Florida waters has increased by 3% per year (U.S. Coast Guard, 2005). Florida is the fastest-growing recreational boating state in the U.S., ranking number 1 in the number of registered boats. In 2004, there were over 928,000 registered boats in the state (Florida Department of Motor Vehicles, unpublished data). Furthermore, new boat and engine designs allow boaters to utilize shallow areas once inaccessible (Wright et al., 1995). Thus, the potential threat to manatees posed by watercraft continues to increase, and regulatory efforts to date have not been successful in reducing the number of watercraft-related deaths. It is of considerable interest, to conservationists and boaters alike, to identify ways to reduce this major source of manatee mortality.

In an effort to improve the efficacy of boat speed zones, the second revision of the U.S. Fish and Wildlife Service's manatee recovery plan calls for research on mechanical characteristics of manatee bone (U.S. Fish and Wildlife Service, 2000). As discussed above, two-thirds of manatee deaths attributed to boats are a result of impact with some

part of the vessel. Ribs broken by the impact damage the surrounding soft tissues severely enough to result in death. Information on the amount of force needed to break manatee ribs would be valuable in refining boat speed zones to reduce lethal impacts. Currently, there is no information on the amount of energy needed to break manatee ribs in impact.

Manatee bone is unique in the animal kingdom. The ribs are solid cortical bone. They are pachyostotic, osteosclerotic, and appear to have a unique microstructure. It is these features that likely make manatee bone susceptible to fracture when struck by boats. The bony tetrapod endoskeleton first appeared some 400 million years ago (Carter and Beaupré, 2001). Throughout evolution, the basic form was constrained by genetics. However, nature has allowed a great deal of latitude in the details. Genetic mutations and also epigenetic and environmental factors have altered the mechanical environment of the skeleton (Carter and Beaupré, 2001). The result is immense variation in skeletal form and function, at both the gross structural level and the microscopic level. The remainder of this chapter presents a brief overview of the tremendous variety in bone tissues found among the vertebrates. It provides the framework for understanding where the manatee falls in the spectrum, and why we find it worthy of study.

## Skeletogenesis

The bones of the skeleton are formed one of two ways. Intramembranous bone forms directly within the mesenchyme (Hall, 2005). There are a few exceptions, but generally the craniofacial bones and cartilages, as well as dentine and alveolar bone, are all formed intramembranously, and are derived from neural crest. In contrast, endochondral bone forms by ossification of a pre-existing cartilaginous model. The bones

of the limbs, vertebral column, and the ribs are endochondral in origin. Endochondral bones are derived from mesoderm.

Dermal bones are derived from the dermis of the skin, and are present in some members of every vertebrate class except birds (Kent and Miller, 1997). They are membrane bones, although they are derived from ectoderm or endoderm, unlike intramembranous bone which originates from mesoderm (Hall, 2005). Meckel's cartilage and some bones of the chondrocranium are dermal bones. The pectoral girdle in most vertebrates is comprised of both dermal and endochondral bone (Romer and Parsons, 1977). Other dermal bones in modern vertebrates take the form of scales or plates. Dermal bones in fishes are comprised of various combinations of lamellar bone (cellular or acellular), dentin, and an enamel-like substance; all of which may be covered with epidermis (Kent and Miller, 1997). A few fishes possess bony plates. Some tetrapods have minute bony scales called osteoderms (Kent and Miller, 1997). Caecilians and some tropical toads have them. Crocodilians have osteoderms below cornified epidermis (Romer and Parsons, 1977). Some lizards have osteoderms that fuse with the skull shortly after birth, and lizards and crocodilians both possess abdominal ribs that are remnants of ventral bony scales (Romer and Parsons, 1977). The carapace and plastron of turtles are comprised of bony plates with immobile sutures (Kent and Miller, 1997). Armadillos and some whales are the only mammals that normally form dermal bone (Romer and Parsons, 1977; Kent and Miller, 1997). The armor of armadillos consists of polygonal bones with immobile sutures that are covered with epidermal scales.

Heterotopic bones are not part of the endoskeleton proper. They typically form in fibrous connective tissues and are endochondral, intramembranous, or dermal in origin

(Romer and Parsons, 1977; Kent and Miller, 1997). In mammals, sesamoids are heterotopic bones that form in tendons at points of friction, such as where they pass over joints. Sesamoid bones are also common in reptiles (Hall, 1984). Tendons in the legs of turkeys and pheasants often ossify (Currey, 1984; Kent and Miller, 1997). Kangaroos have ossified tendons on the mid-ventral surface of the tail (Murray, 1936). The baculum is a heterotopic bone found in insectivores, bats, rodents, carnivores, and in nonhuman primates (Romer and Parsons, 1977). Crocodilians have a bony plate in the eyelids, called the os palpebrae. The os cordis forms in the heart of deer and bovids. Rostral bones are formed in the snout of some mammals, such as the pig (Romer and Parsons, 1977; Kent and Miller, 1997). The os falciforme functions as a supernumerary digit in the digging hand of moles (Romer and Parsons, 1977). In birds, heterotopic bones are found in the gizzard of some doves and in the syrinx of others. Some lizards possess a cloacal bone in the ventral wall of the cloaca. One species of bat has a bone in its tongue, and bone is found in the diaphragm of camels (Kent and Miller, 1997). Some heterotopic elements are cartilaginous. Cartilage and bone have been reported in the hearts and aortae of snakes, turtles, crocodiles, alligators, birds, rats, and hamsters (Hall, 1984; Lopez et al., 2003). Hyaline cartilage is normally found in the aorta of rats, and fibrocartilage is found in the hearts of dogs and humans (Hall, 1984).

## Bone Shape and Macrostructure

Bones are classified into four groups, based on their shape (Marieb, 1995). Long bones are roughly cylindrical in shape. They are generally longer than they are wide. The ends of the bones (epiphyses) are more expanded than the shaft (diaphysis). Bones of the limbs are long bones (such as the femur and humerus; as well as smaller bones like the metacarpals, metatarsals, and phalanges). Short bones such as carpals and tarsals are

somewhat cuboidal in shape. Bones with complicated shapes (such as vertebrae and bones of the pelvic girdle) are classified as irregular. Flat bones, such as the frontal and parietal, are comprised of cancellous bone sandwiched between two layers of compact bone.

At the gross structural level bone is classified into two types based on its density (Carter and Hayes, 1976; Hayes and Bouxsein, 1997). Compact, or cortical bone ranges in density from 1.6–2.0 g/cm$^3$, and has a porosity of 5–30%. Cortical bone forms a shell around the outside of bones, encasing the inner cancellous bone, and constitutes the bulk of the shaft of long bones (Martin and Burr, 1989). Cancellous, or trabecular bone is much more porous (30–90% porosity), with density from 0.07–1.0 g/cm$^3$. Cancellous bone is found in the interior of flat, short, and irregular bones and in the ends of long bones. It takes the form of needles or plates called trabeculae (Jee, 1988). The pores are generally filled with bone marrow.

## Microscopic Structure of Bone

Bone, whether compact or cancellous, is comprised of two types of bone tissue: primary bone, of which there are two types- woven and lamellar; and secondary bone (Jee, 1988). Woven bone is found in sites of initial bone formation, during early stages of development. It forms directly in mesenchyme (intramembranous bone), or by ossification of a cartilaginous model (endochondral bone). Woven bone forms rapidly, but as a result it is structurally inferior to secondary bone (Martin and Burr, 1989). Collagen fibers are randomly oriented within the matrix, and osteocytes are distributed irregularly. It is generally low in mineral content, although it has the potential to become more highly mineralized than lamellar bone (Martin and Burr, 1989). Woven bone can be formed *de novo*, with no previous bone or cartilage model (Martin and Burr, 1989). It

forms the callus during fracture repair, and is formed in disease processes that involve the skeleton. It is also formed on the periosteal surfaces of bones that have been subjected to excessive strains (Martin et al., 1998).

Primary lamellar bone, whether cortical or cancellous, must be laid down on a pre-existing surface of either cartilage or bone (Martin and Burr, 1989). Trabeculae are thickened by deposition of lamellae on woven bone. Compact bone is formed by continued deposition until the intertrabecular spaces are filled in (Jee, 1988). There are three major patterns (Jee, 1988) of lamellar arrangement in cortical bone: 1) Circumferential lamellae surround the internal and external surfaces of the bone (inner and outer circumferential lamellae, respectively), 2) Haversian systems, and 3) Interstitial lamellae, fragments of previous Haversian systems and circumferential lamellae that have been partially resorbed, fill in the gaps between secondary Haversian systems. Primary Haversian systems, or osteons, are formed by compaction of woven bone, or when blood vessels on the periosteal surface become incorporated into new bone as a result of appositional growth. Bone is deposited in concentric rings around the vessel, forming a vascular channel.

Plexiform bone is another type of primary bone that contains both woven and primary lamellar bone (Currey, 1960; Enlow and Brown, 1956, 1958; Martin and Burr, 1989; Martin at el., 1998). It forms on either periosteal or endocortical surfaces. Subperiosteal or subendosteal bone forms buds perpendicular to the bone surface that grow for a short time, then join laterally, creating vascular spaces. The vascular spaces are then filled in with primary lamellar bone. The resulting tissue has the appearance of a

brick wall. Plexiform bone is most commonly found on the periosteal surface of the diaphysis of long bones (Martin and Burr, 1989).

Over time, bone must adjust to variable loading conditions and it must repair fatigue damage, a result of repetitive loading (Martin at al., 1998). Secondary lamellar bone is a result of bone remodeling, the replacement of existing bone with new bone. The secondary Haversian systems of remodeled bone are formed by tandem processes of bone removal and replacement (Jee, 1988). In cortical bone, groups of cells collectively referred to as a bone multicellular unit (BMU) first remove existing bone; then new bone is deposited in concentric lamellae, leaving a canal in the center. The lamellae are separated from the surrounding interstitial bone by the cement line, a layer of mineralized matrix devoid of collagen fibers (Jee, 1988; Martin and Burr, 1989). The resulting structure is a secondary Haversian system. So like primary lamellar bone, secondary lamellar bone is comprised of parallel sheets of lamellae. However, this bone is formed more slowly and is more organized than primary bone (Martin et al., 1998). Osteocytes are more regularly arranged. Within each lamella, the collagen fibers are all parallel, but the fibers in adjacent lamellae are oriented at 90° angles (other patterns of collagen fiber arrangement have also been documented). Primary and secondary Haversian systems can be distinguished from one another by their size and structure (Martin and Burr, 1989). Primary osteons have a smaller canal, fewer concentric lamellae, and no cement line. The trabeculae of cancellous bone are also lamellar in structure. In contrast to cortical bone, trabeculae are remodeled on the surface. The remodeled trabecular packets have a lamellar construction similar to secondary osteons (Jee, 1988).

## Mechanical Properties of Bone Related to Microscopic Structure

Three mechanical properties are typically measured in bone: elastic modulus, strength, and toughness. The elastic modulus, or the Young's modulus, is a measure of the stiffness of the material; it is a measure of the relationship between the external load applied, expressed in terms of stress; and the deformation response, in terms of strain. The strength of a material is the load capacity at fracture per unit area. For this calculation, knowledge of the type of loading and geometry of the structure is critical to proper comparison of strengths among different investigators. Toughness is a measure of the energy absorbed before fracture and released during fracture. With isotropic, monolithic materials, there is a direct relationship between the elastic modulus and toughness. Because of the complex, composite nature of bone, the relationships among elastic modulus, toughness, and strength may not be the same as with monolithic materials. Additionally, because bone is a hierarchical structure, these properties may vary as a function of scale of measurement. This section gives a brief overview of the mechanical properties of bone as related to its organization.

The mechanical properties of bone are affected by its porosity and degree of mineralization (Martin and Burr, 1998). Porosity affects bone strength: the more porous the bone, the weaker it is. Hence cancellous bone is weaker than compact bone. Bone strength and stiffness increase with increased mineral content. Currey (1969) found that a small increase in mineralization results in a large change in modulus, a result of the organization of the mineral crystals. He showed that the optimal mineral content is about 66–67%. Above this, toughness decreases with increased mineralization.

The organization of both cortical and cancellous bone influences its strength, stiffness, and toughness (Martin et al., 1998). Woven bone is weaker than lamellar bone,

because of its randomly arranged collagen fibers, osteocytes, and mineral crystals (Martin and Burr, 1998). However, the random arrangement makes it behave as an isotropic material. This makes it an ideal tissue for structures that must be equally strong in all directions, such as rapidly growing bones that will soon be remodeled (Wainwright et al., 1982).

The parallel collagen fibers of lamellar bone make it stronger than woven bone, but strength is affected by the orientation of the fibers in relation to the direction of the applied load (Martin and Burr, 1989). Generally, fibers parallel to the applied load are strongest in tension, and fibers perpendicular to the load are strongest in compression (Martin and Burr, 1989). Thus, anisotropic bone is stronger and stiffer in the direction of the predominant orientation of the collagen fibers. In most long bones, the fibers, lamellae, and osteons are parallel to the long axis. Hence they are stronger in that direction, but may be significantly weaker when loaded in other directions (Wainwright et al., 1982). In the transverse plane, plexiform bone is weaker when loaded radially (perpendicular to lamella) than tangentially (in the plane of the lamella). In the tangential plane plexiform bone fails near the interlamellar blood vessels. However, Haversian bone is equally strong in all orientations in the transverse plane, due to the concentric arrangement of the lamellae. Therefore, osteonal bone is transversely isotropic (Reilly and Burstein, 1974).

Plexiform bone confers two mechanical advantages on structures (Martin and Burr, 1989). The rapid increase of the surface area for primary lamellar bone deposition greatly increases the strength of the bone in a short period of time. Second, adding this

bone on the periosteal surface quickly increases the diameter of the structure; which increases its rigidity, thereby increasing its resistance to bending.

Remodeled bone (i.e., that containing Haversian systems) is weaker than purely lamellar bone in compression, tension, shear, and bending (Martin and Burr, 1989). There are three possible reasons for this (Currey, 1984). First, Haversian bone is younger than the bone it replaced: therefore, it is less mineralized. Second, the creation of Haversian canals increases the porosity of the bone. Third, the cement lines surrounding Haversian systems do not contain collagen, so they are lower in strength than the lamellae. The fact that cement lines fracture easily imparts another important property to remodeled bone– toughness (the ability to resist failure). The tougher a material, the more energy required to break it (Gordon, 1978). The low-strength cement lines dissipate energy and stop cracks from propagating (Currey, 1984; Martin et al., 1998).

The strength of cancellous bone is affected by the structure of the individual trabeculae, and by the arrangement of the trabeculae (Martin et al., 1998). Primary trabeculae may be stronger than remodeled ones, as the cement lines associated with trabecular packets of remodeled bone decrease its strength. Orientation of the trabeculae is also important: they are stronger when oriented parallel to applied loads (Martin et al., 1998). The trabeculae in the ends of long bones are oriented either along the lines of stress or in support of those that are (Thompson, 1942; Hildebrand, 1988; Martin et al., 1998). The porosity and trabecular structure of cancellous bone that make it weaker than cortical bone also make it more compliant, thus making it a good shock absorber (Martin and Burr, 1989).

## Variations in the Microscopic Structure of Vertebrate Bone

Most vertebrates do not possess highly remodeled Haversian bone structure (Foote, 1916; Enlow and Brown, 1956, 1957, 1958; Currey, 1960). Foote (1916) made a histological comparison of the diaphysis of 440 femurs (294 nonhuman) encompassing all tetrapod vertebrate classes. He found that primary lamellar bone was the predominant type in the 39 species of amphibians examined. A small number had some plexiform bone, and a larger number had secondary Haversian systems. In general, the cortex was thin relative to the size of the bone. Among the 34 reptiles examined, primary lamellar bone predominated in the lizards, while Haversian bone was found in the turtles. Plexiform bone was found in the alligator and in some turtles. Most turtles follow the typical vertebrate pattern of long bone development. However, all turtles, whether terrestrial or aquatic, had medullary cavities densely filled with dense cancellous bone (Foote, 1916; Rhodin et al., 1981). In contrast, there was no cancellous bone in the lizards.

Dinosaur bone was more similar to mammalian bone than to reptilian bone (Reid, 1984). Primary osteonal or plexiform bone was the most common types present. Secondary remodeling did occur, although the number and distribution of Haversian systems was highly variable. The degree of remodeling varied from none at all to extensive. Haversian distribution patterns ranged from randomly scattered to discreet regional concentrations. Areas with high densities of Haversian systems were associated with sites of muscular attachment, which is corroborated by the presence of Sharpey's fibers near these regions (Reid, 1984). Areas where tendons insert on bones are subject to heavy local stresses (Hildebrand, 1988). The diaphyseal medullary cavity was either empty or contained cancellous bone (Reid, 1984). Some of the trabeculae of primary

cancellous bone were not remodeled, but rather lamellar bone was deposited onto the surfaces of primary endochondral trabeculae, and the cartilage core remained (Reid, 1984).

Considerable variation in bone structure was noted among the 40 birds examined by Foote (1916). Although primary lamellar and Haversian bone were present in numerous species, he considered plexiform bone to be the most characteristic of the group. Cortical bone thickness varied considerably among species. He calculated that birds with "empty" bones (i.e., containing air sacs, no marrow) had thinner cortices relative to bone diameter than those with marrow, or those that had marrow cavities filled with cancellous bone, of similar size. There is relatively little variation in bone structure among birds compared to other vertebrate groups (Bellairs and Jenkin, 1960).

The 188 mammals (nonhuman) examined by Foote (1916) were characterized by a great deal of structural diversity. Overall, secondary Haversian systems were present in a greater proportion of mammals than in any other class. However, some mammals were extensively remodeled, while others such as bats experienced little or none. Similarly, plexiform bone was found more often in mammals than in other classes.

Among mammals, plexiform bone is found most commonly in the artiodactyls (Foote, 1916; Enlow and Brown, 1958; Martin and Burr, 1989). Manatees and their close relatives the elephants both have plexiform bone (Foote, 1916; Enlow and Brown, 1958; Marmontel, 1993). Deer antlers are plexiform, as are some long bones of large-breed canines, cats, and bears (Enlow and Brown, 1958; Currey, 1960). Plexiform bone has also been identified in the human mandible, and in the long bones of children who are under some degree of dietary stress (Martin and Burr, 1989). Foote (1916) found plexiform

bone in many human fetal and juvenile femora. Currey (1960) reported a thin layer of plexiform bone on the periosteal surface of an adult human femur. Currey generalized that in many mammals larger than rats, some bones grow by deposition of plexiform bone at some stage of development.

The extent to which primary bone is replaced by Haversian systems varies enormously from species to species, as well as with age, sex, and health, both within and among individuals (Foote, 1916; Currey, 1960). Haversian systems are almost completely absent from rodents and bats. Most bats possess primary lamellar bone except for the large *Pteropus* species, which do have some Haversian systems (Foote, 1916). Cats do not begin to remodel their bone until after reaching sexual maturity (Currey, 1960).

Foote (1916) indicated the presence of cancellous bone in the femora of a number of large terrestrial and semi-aquatic mammals, such as the elephant, hippo, white rhino, tapir, otter, polar bear, bearded seal, and a number of artiodactyls. Wall (1983) also noted the presence of cancellous bone in the medullary cavities of the white rhino and the hippo. Bones in the bat wing have little or no medullary cavity and are poorly mineralized, making them less dense and stiff than most mammalian bone (Swartz and Watts, 1999).

In contrast to terrestrial mammals, cetaceans have a reduced bone mass and density (de Buffrenil et al. 1990). The outer cortical layer of the humerus and radius were found to vary in thickness, but were relatively thin compared to terrestrial vertebrates, and the medullary cavities were filled with porous spongy bone (Felts and Spurrell, 1965, 1966). The forelimb is not a weight-bearing structure, nor is it used for propulsion, but rather it functions for maneuvering and attitude control (Felts and Spurrell, 1965, 1966;

Domning and de Buffrenil, 1991). As such, it is exposed to significant tensile and compressive loads in the medio-lateral plane. The bones are correspondingly broad and flattened medio-laterally, modified from the tubular form typical of most animals.

Foote (1916) observed that while all bones consist of the same structural units, they are combined in many different combinations and proportions. Because of this, he suggested that the lamella be considered the structural unit of bone. Other authors concur that bone tissues and their organizational patterns form a continuum rather than discreet categories (Currey, 1960; Moss, 1961; Martin et al., 1998). Moss (1961) stated that confusion arises when we try to "classify skeletal tissue types in terms applicable to mammals alone." Many variations from what is considered the "typical" vertebrate bone structure exemplified by humans have been examined in detail. Some modifications characterize an entire class, while others are shared by species from more than one group. Some of these variations are described below.

Three significant deviations from the classical vertebrate bone structure are found among the fishes. Elasmobranchs (sharks, skates, and rays) have a cartilaginous skeleton that is not replaced by endochondral bone (Budker, 1971; Compagno, 1999). In most elasmobranchs, however, the skeleton is strengthened by calcification of the cartilage. Calcified polygons of hydroxyapatite cover the surface of bones, and the vertebral centra are partially calcified in the interior (Compagno, 1999). There are three general patterns of vertebral calcification, and these patterns are so consistent that they have been used to classify sharks taxonomically (Goodrich, 1930; Budker, 1971). Additionally, the degree of calcification somewhat reflects age and habitat preference (Compagno, 1999). Skeletons of older animals are generally more calcified than younger ones. Inshore

demersal sharks possess the most heavily calcified skeletons, while deep-water and some oceanic and inshore sharks are variably less calcified.

The teleosts, or bony fishes, are unique in that their bone is largely acellular (Moss, 1961). Acellular bone is distinguished from cellular bone by the absence of osteocytes. It can be formed by two different mechanisms, through modified osteogenesis or chondroidal osteogenesis (Moss, 1961). During endochondral ossification, osteoblasts secrete matrix around themselves and become embedded. However, soon afterward the nuclei become pycnotic and die. The lacunae are subsequently filled in with bone. In appositional bone deposition the osteoblasts at the periosteal surface secrete matrix, but they continually "withdraw" from the surface. As a result, they never become embedded in the matrix, thereby producing consecutive layers of acellular bone (Moss, 1961). The process of acellular bone formation is not well understood, but it appears that there is a buildup of calcium salts inside the pycnotic cells. This "intracytoplasmic mineralization" leads to the death of the embedded cells (Moss, 1961).The mechanical properties of acellular bone are unknown (Wainwright et al., 1982; Currey, 1984).

Chondroid bone, produced by a modified form of intramembranous bone formation, has characteristics of bone and cartilage (Fang and Hall, 1997; Kawakami et al., 2001; Witten and Hall, 2002). Chondroidal osteogenesis is a process of bone formation found primarily in fish (Moss, 1961). Cellular and acellular bone are formed from chondroid. The kype that appears in the Atlantic salmon during breeding season is composed of chondroid bone (Witten and Hall, 2003). This structure develops rapidly, and is structurally similar to bone formed under pathological conditions in humans such

as periosteal osteosarcomas. Additionally, there is evidence that bone morphogenetic proteins are involved in the production of chondroid bone (Kawakami et al., 2001).

Adventitious (secondary) cartilage forms on membrane bone in response to mechanical stimulation (Fang and Hall, 1997). This type of cartilage is found in skulls of birds and mammals, however, it does not form in amphibians and it is unclear whether or not it forms in reptiles. Additionally, amphibians do not form a cartilaginous callus in response to fracture, and whether or not reptiles do is unknown (Hall, 1984). It is also unclear whether these groups lack adventitial cartilage because their periostea have a reduced osteogenic potential compared to birds and mammals, or because the required mechanical stimulus for its formation is lacking (Hall, 1984).

Reptiles commonly form metaplastic bone, in which chondrocytes are transformed into osteoblasts and cartilaginous matrix becomes bone (Hall, 1984). Additionally, metaplastic bone is also formed by chondrification and subsequent ossification of tendons and ligaments (Reid, 1984). It is possible that reptiles form metaplastic bone to compensate for the reduced bone- and cartilage- forming capabilities of the periosteum (Hall, 1984). Metaplastic bone similar to that in reptiles was also found in dinosaurs, typically in ossified tendons, but occasionally in the periosteal regions of limb bones (Reid, 1984). Osseous metaplasias have also been documented in a variety of soft tissues in humans, where the condition is always pathological (Dayoub et al., 2003; Siomin et al., 2003).

A skeletal adaptation in birds is pneumatization, the inclusion of air sacs in the bones. Many bones of the skull and postcranial skeleton are hollow and contain air sacs lined with epithelium, which are continuous with the nasal sacs, tympanic cavities, or the

bronchial system (Bellairs and Jenkin, 1960). The post-cranial skeleton is pneumatized by extensions of the respiratory air sacs. Typically, an extension of an air sac enters a bone through a pneumatic foramen. The sac extends into the marrow cavity, and as it grows around the degenerating trabeculae, it becomes broken up into a network of branching tubes. The trabeculae and marrow disappear from the bone shaft, but remain in the epiphyses in small quantities. The branches of the air sacs reunite to form a single sac that occupies the entire bone cavity (Bellairs and Jenkin, 1960).

Pneumatization lightens the skeleton, and therefore is widely believed to be an adaptation for flight (Bellairs and Jenkin, 1960). The extent of pneumatization varies widely among species, but appears to be related to body size and lifestyle. Small birds, and aquatic birds such as penguins, are poorly pneumatized (Goodrich, 1930; Bellairs and Jenkin, 1960). In smaller species, the ratio of air sac volume to body surface area is small, so extensive pneumatization may not be economical. Diving in aquatic, flightless birds may be hindered by pneumatization. For larger, flighted birds the benefit of pneumatization may be significant, and this is especially beneficial because their skeleton is subjected to greater stress during flight (Bellairs and Jenkin, 1960). However, the cortical bone layer is about the same thickness in non-pneumatized bones of similar size. To compensate for this, pneumatized bones have a larger diameter than non-pneumatized bones of similar length, which increases its resistance to bending. Additionally, long bones of some large birds have extra internal support in the form of struts.

Pneumatization has been documented in animals other than birds. The centra of some dinosaurs exhibit an unusual remodeled structure in which a few thin sheets of compact lamellae formed the external shell and a series of internal longitudinal partitions

(Reid, 1984). The internal vertebral spaces were filled with air (Goodrich, 1930). This structure resulted in a substantial lightening of the centrum (Reid, 1984). Similarly, elephants have air-filled sinuses in the skull to lighten it (Feldhamer et al., 1999).

In fishes, amphibians, reptiles, and birds, chondrocytes of the epiphyseal cartilages do not organize into vertical columns as seen in mammals (Bellairs and Jenkin, 1960; Moss, 1961; Rhodin et al., 1981; Hall, 1984). In reptiles and birds the epiphyses ossify differently from mammals (Bellairs and Jenkin, 1960; Hall, 1984). In small lizards, an area of epiphyseal cartilage never ossifies. In other lizards, there is no secondary center of ossification at all in the epiphysis, so ossification proceeds from the diaphysis. In these animals the articular cartilage functions as the growth plate. Most lizards do have secondary centers of ossification. However, ossification proceeds laterally, from the perichondreal surface inward (Hall, 1984). In contrast, the ossification patterns of large varanid lizards (e.g., Komodo dragon) are nearly identical to mammals. Unlike mammals, varanids retain the cartilage canals surrounding blood vessels of the epiphyses. Lizards that retain some cartilage in the epiphyses are capable of indeterminate growth (Hall, 1984). Like some other reptiles, turtles never develop secondary ossification centers in the epiphyses. As a result these animals are capable of continual endochondral growth throughout adulthood (Rhodin et al., 1981; Hall, 1984). Birds only have secondary centers of ossification at the proximal end of the tibia, which may be related to the invasion of the air sacs (Bellairs and Jenkin, 1960). Presence of secondary ossification centers might interfere with penetration of the sacs, and blood vessels associated with the ossification centers influence the arrangement of the chondrocytes.

Pachyostosis is defined as an increase in cross-sectional area of bones by increasing the thickness of the periosteal cortices, and the absence of a free medullary cavity (Domning and de Buffrenil, 1991). Osteosclerosis refers to the replacement of cancellous bone with cortical bone (de Buffrenil et al., 1990; Domning and de Buffrenil, 1991). Increased bone density, mineralization, and reduced porosity are characteristic of this condition. Domning and de Buffrenil (1991) pointed out that the term pachyostosis is often, though erroneously, used to refer to both conditions simultaneously. The bones of some sirenians are, in fact, osteosclerotic without being pachyostotic.

Fawcett (1942a, b) described the compact bone of manatee ribs as structurally less differentiated than that of other mammals; largely non-lamellar, periosteal bone laid down in an eccentric pattern, and the periosteum of the ribs continues to lay down new bone well after the animal has stopped growing. Large amounts of endochondral (primary) bone remain unabsorbed, and calcified cartilage matrix persists. The non-lamellar bone described by Fawcett (1942b) was later classified as plexiform bone by Enlow and Brown (1958). De Buffrenil and Schoevaert (1989) quantified pachyostosis in the dugong. They found that rather than being uniform, density and mineralization were greatest in the skull, anterior (cranial-most) vertebrae and ribs, and decreased caudad. A similar gradient existed in the forelimb, with greatest degree of pachyostosis in the scapula and humerus, and a lesser degree in the forearm and in the phalanges. In a review of sirenian phylogeny, Savage (1976) identified pachyostosis as the only truly autapomorph characteristic among the Sirenia. All sirenians, which first appeared in the middle Eocene, exhibited pachyostosis to some degree.

Pachyostosis and osteosclerosis are not unique to sirenians. Pachyostosis is found in many species that are at least partially adapted to the aquatic environment (Wall, 1983). Nopsca (1923) identified the condition in dinosaurs. Pachyostotic bones have been described in pelicans and penguins (Foote, 1916; Meister, 1962). Walruses have a very dense rostrum, while the rest of the skull is comprised of spongy bone. This is hypothesized to aid the animals in diving for food (Kaiser 1965, 1967). De Buffrenil et al. (1990) described pachyostotic bone in two archaeocetes. Wall (1983) found that limb bone density was significantly greater in aquatic and semi-aquatic mammals than in terrestrial mammals. Stein (1989) compared limb bone densities among 15 species of marsupials and rodents. Fish and Stein (1991) compared the limb bone densities of several mustelids. Both studies reported that densities of limb bones of semi-aquatic species were significantly greater than those of terrestrial species. When Fish and Stein (1991) combined their data with that of Wall (1983), they found that some semi-aquatic mammals exhibited increased limb bone densities similar to fully aquatic mammals while others did not differ from terrestrial animals (Fish and Stein, 1991). Pachyostotic bone has also been found in a wide variety of fossil artiodactyls (Morales et al., 1993).

Pachyostosis is believed to be an adaptation to promote reduced buoyancy in aquatic and semi-aquatic animals (Nopsca, 1923; Meister, 1962; Kaiser 1965, 1967; Felts and Spurrell, 1965, 1966; Rhodin et al., 1981; Wall, 1983; de Buffrenil and Schoevaert, 1989; Domning and de Buffrenil, 1991). Bone density in semi-aquatic animals appears to be related to the extent to which the animals are adapted to the aquatic environment (Wall, 1983; Stein, 1989; Fish and Stein, 1991). Wall (1983) postulated that selection for increased limb bone density occurred when total body submergence became a habitual

part of the animals' lifestyle. However, some fully aquatic mammals such as the cetaceans likely underwent a secondary reduction in bone density as they developed other methods of buoyancy control related to deep diving.

The occurrence of pachyostotic bone in manatees has been likened to pathological conditions observed in humans. Fawcett (1942b) described it as resembling Albers-Schönberg disease, or marble bone disease, an autosomal dominant form of osteopetrosis. Increased bone density is a primary feature of the sclerosing diseases. However, many forms of osteopetrosis and osteosclerosis are accompanied by skeletal architectural deformities and a suite of soft tissue and physiological defects (Shapiro, 1993; Tolar et al., 2004) that are not present in manatees or other species exhibiting pachyostosis. Autosomal dominant osteopetrosis lacks the pathologies of other forms. Another candidate for the cause of pachyostosis is the recently discovered role of the LRP5 gene in skeletal mineralization. Some mutations of the gene have been shown to result in high bone mass, accompanied by an increase in bone volume and reduced marrow spaces, but without any other evident pathologies (Johnson et al., 2002; Koay and Brown, 2005).

## Manatees in Perspective

Manatees share a number of developmental features with other marine animals that are not found in terrestrial vertebrates. Manatees (Fawcett, 1942a, b), cetaceans (Felts and Spurrell, 1965, 1966), penguins (Meister, 1962), and the marine turtle *Dermochelys* (Rhodin et al., 1981) all develop amedullary long bones that retain some endochondral bone that is not remodeled. In all these species except manatees the medullary cavity is filled with coarse-cancellous bone; manatees fill the cavity with compact bone. Additionally, these aquatic animals vascularize their epiphyses both perichondrally and transphyseally. Some pinnipeds (Versaggi, 1977) and extinct

amphibians (Rhodin et al., 1981) also show similar patterns of development. Manatees and penguins both have an unusually thick periosteum that adheres tightly to the bone surface (Fawcett, 1942b; Meister, 1962). In manatees the periosteum of the ribs continues to lay down new bone well after the animal has stopped growing (Fawcett, 1942b).

Felts and Spurrell (1965, 1966) identified some common structural and developmental characteristics of cetacean limb bones. They found that although cetaceans retain the typical mammalian pattern of fusion of ossification centers, the process is delayed. The zones of cartilage maturation are not as distinct or as organized as they are in terrestrial mammals. At no time during development are regular columns of chondrocytes observed near the growth plates, a feature shared with fishes, amphibians, reptiles, and birds. Secondary ossification of all cetacean limb elements begins after birth. Furthermore, there is an extended lag time between cartilage calcification and endochondral ossification. All of these features have been described in manatees (Fawcett, 1942b).

Sirenians (e.g., manatees and dugongs) and cetaceans (e.g., whales) are the only fully aquatic marine mammals. As a result of their aquatic lifestyle, they are free of the mechanical constraints that influence limb bone architecture in animals that spend at least part of their time on land. In contrast to the cetaceans, manatees and dugongs are the only herbivorous, fully aquatic mammals (Domning and de Buffrenil, 1990). As herbivores, they are tied to the shallow waters of the euphotic zone, which has likely hindered them from taking advantage of the same hydrodynamic mechanisms of buoyancy control utilized by cetaceans (Domning and de Buffrenil, 1990). Domning and de Buffrenil (1991) offered reasonable evidence that pachyostosis and osteosclerosis in the manatee

are adaptations to increase skeletal ballast for buoyancy control. Increased bone diameter, density, mineralization, and compactness all serve to increase the mass of the skeleton to offset the positive buoyancy of the lungs.

Although increased mineralization will increase the mass of the bones, Currey (1969) demonstrated that as mineral content rises beyond a certain point, bone becomes more brittle in static and impact loading. Increasing bone diameter may offset the reduction in strength somewhat, by increasing flexural stiffness. In manatee ribs, pachyostosis is accomplished by the addition of plexiform bone, largely to the lateral surface. Mechanically, this may be advantageous compared to purely lamellar bone. When a load is applied to plexiform bone, the woven bone will experience less stress than the lamellar bone due to its lower modulus (Wainwright et al., 1982). Additionally, remodeling rates appear to be low in manatee ribs, as indicated by the low number of Haversian systems. This may be because manatees, being aquatic animals, do not experience loads that influence remodeling to the same degree as terrestrial animals. The crack-stopping ability of osteons increases bone toughness (Martin et al., 1998), so the low number of osteons in manatee bone may contribute to its low toughness compared to other bone.

Most developmental and structural traits of manatee bone are shared with other animals, a result of phylogenetic relatedness and common evolutionary problems associated with the return to the marine environment. Other features such as long bones constructed of solid compact bone likely result from the manatee's unique ecological niche. Although the material properties of bone types have been studied, manatees provide a unique combination of structure and function. There are two articles that

qualitatively describe the histology of manatee bone (Fawcett, 1942b; Domning and Myrick, 1980). Marmontel (1993) qualitatively assessed remodeling rates in a number of bones. Domning and de Buffrenil, 1991 measured density, mineral content, and porosity for manatee rib bone for a range of animal sizes. Yan (2002) and Yan et al. (2005) calculated fracture toughness for rib bone. There is no information on the mechanical properties of whole bone, or of manatee bone tested in impact. This study is the first to comprehensively measure mechanical properties of manatee bone.

The overall goal of this project was to quantify the biomechanical effects of boat strikes on manatees. This was accomplished by integrating basic research data on bone biomechanics with data from impact tests, which have a more practical application. We conducted two kinds of tests to measure both material properties and structural properties of manatee bone. Material properties are those of the tissue itself, independent of whole bone size or shape. Structural properties are those properties conferred by the size and shape of whole bones, in addition to the properties of the material. For example, a block-shaped vertebra will behave differently from a long, slender rib when tested in compression, even if they are constructed out of the same material. In Chapter 2, the objective was to conduct 3 point flexure tests using standard test protocols to measure material properties of manatee rib compact bone. Two hypotheses were tested: 1) manatee bone is less strong and tough compared to other species when loaded statically, and 2) the biomechanical properties of manatee bone vary between sexes and among age classes. We measured strength, Young's modulus, fracture toughness, and work of fracture for both sexes, in three age classes. Chapter 3 addresses the hypothesis that forces generated by most watercraft under normal operation are sufficient to inflict fatal

skeletal injuries to manatees. Impact tests were used to estimate the energy needed to fracture whole ribs and the stress at failure. The work presented here provides the first detailed information about material and structural properties of manatee bone. Data generated by the studies herein will contribute to our understanding of manatee-boat interactions, and will be instrumental in shifting the focus to a more objective approach for establishing regulatory boat speed zones adequate to reduce watercraft-related mortality.

# CHAPTER 2
# MATERIAL PROPERTIES OF MANATEE RIB BONE

## Introduction

The Florida manatee (*Trichechus manatus latirostris*) is listed as endangered by the U.S. Department of the Interior, and is considered one of the most endangered marine mammals found in U.S. waters (U.S. Fish and Wildlife Service, 1996). Sources of manatee mortality have been documented in Florida since 1974 (O'Shea et al., 1985; Ackerman et al., 1995; Wright et al., 1995). Watercraft-related mortality, caused by propeller wounds or by impact with a boat's hull, accounted for 25% of all deaths from 1974 through 2004, and comprised 85% of human-related deaths. The proportion of deaths due to impact accounts for more than half (55%) of all watercraft-related deaths (Wright et al., 1995). Animals killed by propeller wounds rarely suffer skeletal damage. Conversely, approximately 66% of the carcasses attributed to hull impact injuries have fractured and/or luxated ribs (Wright et al., 1995). Furthermore, healed fractures are observed infrequently. This suggests that while many propeller wounds are sub-lethal, hull impact injuries sufficient to inflict skeletal damage are usually fatal.

The number of documented watercraft-related deaths increased at a rate of 7% annually from 1992 through 2004 (Florida Fish and Wildlife Conservation Commission, 2003). Attempts at reducing watercraft-related mortality have focused primarily on regulation of boating activities, such as creating speed zones in areas where manatees and boats coexist. However, the increasing human population along the Florida coastline has resulted in more boats utilizing the waterways. From 1996 through 2004, the number of

watercraft on Florida waters increased by 3% per year (U.S. Coast Guard, 2005). In 2004, with over 928,000 registered boats in the state; Florida moved ahead of California and Michigan to be ranked the number one recreational boating state in the U.S. (Florida Department of Highway Safety and Motor Vehicles, unpublished data; U.S. Coast Guard, 2005). Additionally, new boat and engine designs allow boaters to utilize shallow areas once inaccessible. Thus, the potential threat to manatees posed by watercraft continues to increase. Creation of boat speed zones is a highly subjective process, not based on any information pertaining to the biological effects of boat strikes on manatees. A major goal of the U.S. Fish and Wildlife Service's manatee recovery plan is to refine the boat speed zones rules to reduce boat strike deaths (U.S. Fish and Wildlife Service, 2000). Toward this goal, the plan calls for research on mechanical characteristics of manatee bone. The data from this study will be useful in shifting the focus to a more objective approach for establishing regulatory boat speed zones adequate to reduce watercraft-related mortality.

Manatee bone is unusual compared to that of other marine mammals. Compared to terrestrial mammals, the general trend in marine mammals has been a reduction of bone mass and density (de Buffrenil et al., 1990). In contrast to most marine mammals, the manatee skeleton exhibits pachyostosis, characterized by thickening of bone tissue, replacement of cancellous bone with compact bone, and absence of a free medullary cavity (Fawcett, 1942b; de Buffrenil et al., 1990; Domning and de Buffrenil, 1991). The mechanical properties of bone have been well studied for humans and some domestic animals (Wainwright et al., 1982; Currey, 2002); however, mechanical studies on the bones of marine mammals have been few. Mechanical property data are available for fin whale (*Balaenoptera physalus*), dense-beaked whale (*Mesoplodon densirostris*), narwhal

(*Monodon monocceros*), polar bear (*Ursus maritimus*), walrus (*Odobenus rosmarus*), and dugong (*Dugong dugon*) (Currey, 1979a; Currey and Brear, 1990; Evans et al., 1990; Brear et al., 1993; Currey et al., 1994; Zioupos et al., 1997; Currey, 1999).

Some information on the composition of manatee bone exists (Fawcett, 1942a, b; Domning and Myrick, 1980; Domning and de Buffrenil, 1991; Marmontel, 1993). Fawcett (1942b) and Domning and Myrick (1980) provide qualitative reports on the microstructure of rib bone. Domining and de Buffrenil (1991) measured density, mineral content, and porosity (measured as its inverse, compactness). They found that mineral content and density increased with body size through the subadults, and leveled off in adults. Additionally, de Buffrenil and Schoevaert (1989) examined bone density in the dugong, a close relative of the manatee. They found a bone density gradient that increased from craniad to caudad, and from dorsad to ventrad. In developing an aging technique for manatees, Marmontel (1993) examined histological sections of various bones. She reported differences in the number of osteons in males and females of similar age, and inferred that there may be differences in remodeling rate between the sexes. We recently reported on the use of fractography and Chevron notch beam tests to measure fracture toughness (Yan, 2002; Yan et al., 2005). The present study is the first comprehensive measure of the mechanical properties of manatee bone.

The first step in quantifying the biomechanical effects of boat strikes on manatees was to measure some material properties of manatee rib compact bone. Based on the limited information on manatee bone available in the literature, we hypothesized that manatee bone is less strong and tough compared to other species when loaded statically, and that the material properties of manatee bone vary between sexes and among age

classes. The objectives were to calculate flexural strength, toughness, Young's modulus, and work of fracture in bending for rib bone, and to measure density and mineral content for manatees of both sexes in three age classes.

## Materials and Methods

### Bone Sample Collection

Bone tissues were obtained from the Florida Fish and Wildlife Conservation Commission's Marine Mammal Pathobiology Laboratory. Collection and use of tissues for research was conducted under U.S. Fish and Wildlife Service permit #MA067116-0 issued to the University of Florida. Animals of both sexes in three age classes (calf, subadult, adult) were tested. Because it is difficult to age manatees, there is little age data available. By convention, total body length (cm) is used as a proxy for age (O'Shea et al, 1985). Calves were defined as ≤ 175 cm total body length, subadults were 176–275 cm total body length, and adults > 275 cm total body length (O'Shea et al., 1985). Three ribs were obtained from fresh carcasses at the time of necropsy. One rib was taken from the cranial, middle, and caudal thoracic regions (Figure 2-1). Ribs were taken from the same positions whenever possible, and stored frozen in plastic bags until machining. Freezing and thawing of bone does not significantly alter the mechanical properties of bone (Sedlin and Hirsch, 1966; Currey, 1988b; Pelker et al., 1984). They were brought to room temperature for machining and testing.

### Specimen Preparation

A band saw was used to rough cut 60 mm segments from the proximal and middle 1/3 sections of the ribs under a constant spray of water, to keep the bone from heating and to keep it wet. Specimens with dimensions of 50 x 3 x 3 mm were machined with a diamond-edged band on a wet saw (Exakt Technologies, Hamburg, Germany), with the

long axis of the test pieces parallel to the long axis of the rib. Dimensions were verified with digital calipers (Mitutoyo, Tokyo, Japan) to the nearest 0.01 mm. Machined specimens were stored in physiological buffered saline until testing, and they were tested wet.

**Material Properties Testing**

Three point bending tests were performed with a Mini-Bionix materials testing machine following ASTM standard D790M-92 for flexural testing of plastics (MTS Systems, Eden Prairie, MN; ASTM, 2001). For each specimen, a 10-cycle, 10-Newton preload was applied, then loaded to failure using a standard 3-point bending fixture at a displacement rate of 1mm/min. The load was applied to the surface that corresponded to the lateral surface of the rib (i.e., tested in the transverse orientation). Load and displacement were recorded at 5 Hz, and output to a personal computer for analysis.

Mechanical variables measured were flexural strength, Young's modulus (i.e., elastic modulus) in bending, fracture toughness, and work of fracture. The flexural strength of a material is the load required to break a piece of the material in bending (Wainwright et al., 1982). Flexural strength in 3-point bending was calculated as

$$\sigma = \frac{3FL}{2BD^2} \tag{2-1}$$

where F is peak load (Newtons) at failure, l is the distance (meters) between the supports of the bending fixture, B is the specimen width (m), and D is the specimen depth (m). A correction factor was applied to the strength calculation if the specimen fractured somewhere other than opposite the point at which the load was applied (Riley et al., 1999).The correction factor was calculated as

$$\sigma_{corr} = \left( \frac{2((L/2) - x)}{L} \right) \cdot \sigma \tag{2-2}$$

where $\sigma_{corr}$ is the corrected flexural strength, L is the original length of the test specimen, and x is the length of the shorter of the two halves after testing, and σ is the flexural strength from Eq. 2-1. Young's modulus is an indication of how easily the material strains elastically under a given stress; it is a measure of the stiffness of the material (Jackson, 1992). Young's modulus in bending was calculated as

$$E = \frac{(F/x)L^3}{48I} \tag{2-3}$$

where F/x is the slope of the load-displacement curve, l is the distance between the supports of the bending fixture (m), and I is the moment of inertia, calculated as

$$I = \frac{BD^3}{12} \tag{2-4}$$

Yan et al. (2005) showed that, unlike typical bone, manatee bone behaves more as a ceramic. Therefore, fractographic analysis and fracture mechanics can be used to calculate fracture toughness. Fracture toughness is the ability to resist fracture, measured as the critical stress intensity factor ($K_C$). This is an estimate of the amount of energy required to propagate a macrocrack that leads to fracture (Mecholsky, 1996); it is a measure of the behavior in the pre-yield region. The critical stress intensity factor was calculated as

$$K_C = Y\sigma(c)^{1/2} \tag{2-5}$$

where Y is a geometric factor based on crack shape and loading conditions, σ is flexural strength, and c is the crack size ($m^2$). Crack size is calculated as

$$c = (a \cdot b)^{1/2} \tag{2-6}$$

where a and b are crack depth and half-width (m), respectively, as measured from the fracture surface with a light microscope. A correction factor was applied if the failure did not originate from the surface of the specimen (Mecholsky, 1993). Scanning electron micrographs were taken of some fracture surfaces for detailed examination and validation of light microscope measurements. The work of fracture is another measure of energy. Like fracture toughness, work of fracture is that energy required to propagate a crack through a specimen (Aksel and Warren, 2003). It is calculated from the area under the stress-strain curve; it is a measure of the behavior in both the pre- and post-yield regions. For materials that have little or no post-yield deformation, work of fracture and fracture essentially measure the same property, i.e., toughness. However, for materials that have post-yield deformation, or exhibit some inelasticity in the pre-yield region, the two variables may be different. For those materials, work of fracture gives a more complete picture of the behavior. Work of fracture was calculated [cf. Appendix B] for specimens tested in 3-point flexure as

$$\mathrm{WOF} = \frac{3W}{2BD^2} \tag{2-7}$$

where W is the area under the load displacement curve (N m).

**Bone Density and Mineral Content Determination**

Extra bone from the middle sampling region of each rib was used to measure Young's modulus with ultrasound to compare to calculated values, and to measure density and mineral content. Since calculation of Young's modulus from the load-displacement curve is prone to error, ultrasound was used to as a check for the calculated modulus (Vincent, 1990). Specimens were defatted with ammonia, dried at 95° for 48 h, and weighed to the nearest 0.001 g. Density was determined using an Accupyc 1330

helium pycnometer (Micromeritics Instrument Corp., Norcross, GA). Ultrasound measurements were made with a Nuson Ultrasan (Nuson, Boalsburg, PA). Samples were then incinerated at 800°C for 10 h, and weighed to the nearest 0.001 g. Mineral content was expressed as a percent of ash weight over dry weight (Kaufman and Siffert, 2001).

**Statistical Analyses**

Statistical analyses were conducted both within and among animals. For each individual, specimens within each sample site were compared (Figure 2-1B) to look for differences within sample sites. Next, specimens for each sample site were pooled to compare among sample sites within individuals. To examine ontogenetic changes in material properties, specimens were pooled across sites to calculate means by animal. For each variable, animal means were regressed against total body length to examine ontogenetic patterns. Analysis of covariance (ANCOVA) was performed, with length as the covariate, to look for differences between the sexes (Zar, 1996). For all tests, results were considered significant if $p<0.05$. Analyses were performed with Statistical Analysis Systems using Proc GLM (SAS Institute, Inc., 1989).

## Results

Six males and six females were tested for the subadult and adult age classes (Table 2-1). Tissues were obtained from only two calves. Owing to their small size, it is difficult to recover calf carcasses in fresh condition. The ribs of the smallest calf (total body length 102 cm, a newborn calf) were too small to obtain more than one or two specimens each. Additionally, some ribs of the smaller subadults were too small to obtain samples from both the proximal and middle regions. For these animals, only the proximal region was taken.

**Within-Animal Comparisons**

A total of 3,220 specimens from 26 animals were tested in 3-point bending. Fracture toughness was determined for 1,650 of those. At each sample site, no significant differences were found among samples, indicating that the bone at each sample site was homogeneous. Specimens for each sample site were pooled Analyses comparing sampling locations within animals did not reveal any consistent patterns, either cranio-caudal or dorso-ventral, for any variable. Therefore, specimens were pooled for each animal for analyses by sex and total body length (a proxy for age). Mean values for each variable, by animal, are reported in Table 2-1.

**Material Properties Tests**

Figures 2-2 to 2-4 and 2-6 show the relationship of each mechanical variable to total body length. For each mechanical variable, ANCOVA indicated no difference between the sexes. Therefore, sexes were pooled for regression analyses of variables against total body length. For all variables, linear regression did not adequately describe the relationships between variables and total body length. Rather, the relationships were curvilinear; a second order polynomial regression was the best fit, and highly significant, in all cases. Flexural strength increased with body length up to 267 cm, then reached a plateau ($R^2 = 0.79$, $p<0.0001$, Figure 2-2). Fracture toughness exhibited a similar pattern ($R^2 = 0.73$, $p<0.0001$, Figure 2-3).

Work of fracture increased with body size through the subadult size class, just as flexural strength and toughness ($R^2 = 0.50$, $p = 0.0004$, Figure 2-4). Unlike the other variables, work of fracture showed a strong decline with increasing body length for animals 265 cm total length or greater. Although there was a large amount of scatter among the subadults, the value for the smallest calf MEC0033 was much less than the

others. The regression was run minus this animal to determine if it was responsible for the parabolic shape; it was not. Fracture energy, as measured by work of fracture, was greatest in animals of intermediate body length, about 200–267cm total length (i.e, the large subadults).

Young's modulus showed a different pattern, increasing with body length over the entire range of body sizes ($R^2 = 0.86$, $p < 0.0001$, Figure 2-5). Ultrasound was used to measure modulus of 13 bone samples from 11 animals. On average, the ultrasound modulus was 1 GPa greater than that calculated from the load-displacement curves. The good agreement between the ultrasound results and our calculated values indicates that our modulus values are reasonably accurate. Currey (2004) has shown that, in general, Young's modulus and flexural strength are highly correlated ($R^2 = 0.86$). Our data reflected the same positive correlation, although the relationship was not as close ($R^2 = 0.67$, Figure 2-6). Figure 2-7 shows some example load-displacement curves for the small sample specimens tested here. Representative curves for each size class are given. To facilitate comparison among age classes, the values for ultimate load, Young's modulus, and work of fracture are given for each curve.

**Bone Density and Mineral Content**

Extra bone was available to measure density and mineral content for 20 animals (Table 2-1). Mean density by animal was 2.17 g/cm$^3$ (± 0.04 SD, range 2.10–2.22 g/cm$^3$), and mean mineral content was 69% (± 2% SD, range 64–71%). Density showed a weak positive correlation with total length, however, the correlation was not significant ($R^2 = 0.19$, $p = 0.0517$, Figure 2-8). Percent mineral content also correlated weakly to total body length, although the relationship was significant ($R^2 = 0.27$, $p = 0.0198$, Figure 2-9) In contrast, density showed a strong, positive correlation with elastic modulus with the

removal of one outlier ($R^2 = 0.64$, $p<0.0001$, Figure 2-10). Percent mineral content also showed a strong correlation with modulus ($R^2 = 0.61$, $p<0.0001$, Figure 2-11). Our results show that while modulus was highly correlated to both bone tissue density and mineral content, only mineral content increased with total body length.

## Discussion

Reducing watercraft-related manatee mortality is identified as a Level 1 high priority in the Florida Manatee Recovery Plan of the U.S. Fish and Wildlife Service (U.S. Fish and Wildlife Service, 2000). The recovery plan calls for research on mechanical characteristics of bone to obtain a better understanding of the effects of watercraft-related impacts To meet this objective, the goal of this study was to measure some material properties of manatee rib compact bone. Based on the limited information available in the literature, we hypothesized that manatee bone is less strong and tough compared to other species when loaded statically, and that the material properties of manatee bone vary between sexes and with the size of the animal.

### The Material Properties of Manatee Bone

The main finding of this study is that manatee bone is on average less strong and tough than other mammals. Mean flexural strength by animal ranged from 62–160 MPa. In comparison, typical flexural strengths for human and bovine bone specimens tested in 3-point bending are 209 MPa and 224 MPa, respectively (Martin et al., 1998). Flexural strengths have been reported for horse radius (154-249 MPa), black bear tibia (211–328 MPa), and ox femur (227–264 MPa) (Schryver, 1978; Wainwright et al., 1982; Reilly and Currey, 1999; Batson et al., 2000; Harvey and Donahue, 2004). We would expect normally manatee bone to have a bending strength comparable to that of other animals with similar organization. However, we predicted that out values would be lower than

values for other species, based on the high mineral content reported by others. We did find higher than average mineral content, is likely the reason for the low strengths (see below).

The Young's modulus, or the modulus of elasticity, is the measure of the stiffness of a material. Mean modulus ranged from 4–18 GPa, which was similar to that for equine metacarpals (14 GPa), horse radius (14–21 GPa), human femur (15 GPa), cow femur (20 GPa), and black bear tibia (16-30 GPa) (Martin et al., 1998; Zioupos and Currey, 1998; Currey, 2001; Les et al., 2002; Harvey and Donahue, 2004).

Fracture toughness is the ability to resist fracture, one measure of which is the critical stress intensity factor ($K_C$). Toughness is an important property because a tough bone is more resistant to fracture, and this is most important when bone is impacted (Wainwright et al., 1982; Martin et al., 1998). Because bone is viscoelastic, it will behave differently when loaded at different rates (Martin et al., 1998). Generally, the more rapidly bone is loaded, the greater the modulus, and the less energy it is able to absorb. The bone mineral content and density previously described in manatees led us to predict that manatee bone may be on average less tough than other bone (Domning and de Buffrenil, 1991). As predicted, data reported here indicate that manatee bone (1.4–2.9 $MPa \cdot m^{1/2}$) is generally less tough than other bone such as human tibia (2.2–5.7 $MPa \cdot m^{1/2}$), bovine femur and tibia (2.2–5.5 $MPa \cdot m^{1/2}$), and equine metacarpus (4.4–7.5 $MPa \cdot m^{1/2}$) (Martin et al., 1998; Malik et al., 2003). The ontogenetic pattern in fracture toughness mirrored the pattern seen in flexural strength. Since fracture toughness is proportional to both the flexural strength and the flaw size (Equation 2-5), our results suggest that the flaw size is similar over the range of body sizes tested here. A plot of

mean crack size by animal vs. total body length indicated that there was no difference in crack size in relation to body size ($R^2 = 0.0009$, $p = 0.8886$, Figure 2-12).

For both strength and fracture toughness, the regressions may indicate a slight decline for the largest animals. It appeared as though the largest animal, MSW0245, may be responsible for this. This animal had been aged at 25, and many of the test specimens had a qualitatively different look from those of other adults. It may be that this possible decline in strength and toughness in the largest animals is a result of age-related decreases in material properties similar to those well-documented in humans. However, without more ages available for the other larger animals, and without more animals of advanced age, this cannot be determined conclusively.

Another measure of toughness is work of fracture. The work of fracture for manatee bone varied from 3.0–6.0 $MJ/m^3$, which is considerably lower than the 28–46 $MJ/m^3$ for human femur, but well within the range of values reported for other mammals (Currey and Pond, 1989). Harvey and Donahue (2004) recorded values of 3.2-9.4 $MJ/m^3$ for black bear tibia. Currey (2002) reported works of fracture between 0.3–15.6 $MJ/m^3$ for a wide variety of terrestrial and marine animals. Typically, young bone has a low work of fracture that first increases with age, then declines. Manatee bone followed the same pattern.

Mean manatee rib bone density of 2.17 $g/cm^3$ was greater than that reported for humans, which is typically 1.7–1.9 $g/cm^3$, but equal to that of cow femur (2.1 $g/cm^3$) and baboon femur (1.90–2.17 $g/cm^3$) (Yeni et al., 1998; Phelps et al., 2000; Currey, 2002). De Buffrenil and Schoevaert (1989) reported densities of 1.79–2.10 for ribs from three dugongs (2 subadults and 1 adult), a close relative of manatees who also exhibit

pachyostosis of the skeleton. In similar fashion, mineral content for the manatee bone averaged 69%, greater than what is commonly reported for other species. With one exception, all values were between 68-71%. Even greater values of up to 75% mineral content (range 67–75%) were reported for dugong ribs (de Buffrenil and Schoevaert, 1989). According to Martin et al. (1998), mineral content is typically 65 ± 3% for cortical bone. Currey and Butler (1975) reported mineral contents of 60–66% for human femora aged 2–48 years, and 64–67% for black bear tibias from animals 2–14 years (Harvey and Donahue, 2004).

It is important to clearly define the terms density and mineral content. Density can be measured two ways, as the weight per unit volume of only the constituent material, or of the volume inclusive of the spaces, or voids (Martin et al., 1998). The latter is termed apparent density. Thus, bone that is highly porous will have low apparent density. If, however, just the bone tissue is considered, the true tissue density of the porous sample would be just as high as a volume completely filled with the same material. The pycnometer used for this study forces helium gas, under pressure, into the sample chamber to determine volume. In concept, this fills the sample voids if the permeability is adequate, thereby measuring true density. In similar fashion, mineral content can be construed as either the amount of mineral per unit sample volume (i.e., volumetric mineralization), or per volume of bone matrix, exclusive of voids (i.e., specific mineralization). Ashing bone, as done here, is a measure of specific mineralization. A more complete picture of manatee bone density and mineralization patterns may have been drawn if we had also calculated apparent density and volumetric mineralization.

We can summarize our findings about manatees bone as follows: flexural strength was less than for other species; both stiffness and fracture toughness were roughly equal to or less than other species; and work of fracture was similar to values reported for a number of species. Material properties of manatee cortical bone increased with total body length up to about 267 cm, then leveled off, or declined as for work of fracture, with increasing body size. We expected this pattern to be related to an increase in density and/or mineral content with increasing body length. This appears to be what happened, as density and mineral content increased with body size. However, the relationship between density and body size was not significant. This is likely due to two things: that the variation in density was slight, and that comparatively our values were at the high end of the spectrum of values reported in the literature. Mineral content showed greater variation, and increased significantly with body size. Importantly, mineral content was higher than that seen in most mammalian bone. The high mineral contents, coupled with densities at the high end of published values may explain the patterns of the mechanical variables to total body length in animals greater than 265 cm. To better understand the material behavior of manatee rib bone, additional factors need to be evaluated, such as its plexiform structure, collagen content/quality, and its reportedly low remodeling rate (Marmontel, 1993).

We can look to Domning and de Buffrenil (1991) to gain insight into our findings. The authors determined density, mineral content, and compactness of manatee rib for 12 animals. Compactness is the percent of the total cross sectional area that is occupied by bone; it is the inverse of porosity. Total body lengths were missing for the three largest animals. Of the nine animals of known body length, only one was an adult (324 cm TL);

the others were calves and subadults (141–254 cm TL). It is important to note that the authors calculated apparent density, whereas we calculated the material density. They reported densities of 1.59–2.07 g/cm$^3$ (mean 1.85 g/cm$^3$), lower than our densities. However, mineral content for those animals was 67–70%, essentially identical to our data. There was a strong correlation between mineral content and total length, and apparent density and total body length. However, that was related to the fact that those animals were primarily calves and subadults (i.e, less than 275 cm TL); we saw a similar pattern in our data over the same size range. The authors noted that there seemed to be no relation of mineral content and density to body size greater than 275 cm. Compactness varied from 84–94%, which translates to 6–16% porosity. Porosity declined with increasing body length ($R^2 = 0.53$). The authors concluded that mineralization was not dependent on size, and that the increase in apparent density with size was due to the decrease in porosity. Considering both datasets together, we can draw some conclusions about the relationship between mineral content and material properties. Manatee bone tissue density, consistently high, varies little over a wide range of body sizes. The increase in apparent density and mineral content with body size, along with a decrease in porosity, indicates an increase in bone tissue volume. Furthermore, there appears to be little change in the quality of the material. As the animals grow, the interstitial spaces are filled in with more bone. Some additional mineral is added to the existing bone. However, because the existing bone is already so highly mineralized, the resulting bone has reduced strength and toughness. Thus, the ontogenetic patterns in mechanical variables appears to be related to the amount of material present, but the overall low values for strength and toughness are related to the quality of the material.

**The Effect of Mineral Content on the Material Properties of Bone**

Bending strength of compact bone is primarily determined by the Young's modulus (Currey, 1999). In turn, the primary determinant of modulus is mineral content and to a lesser extent, porosity and bone architecture (Schaffler and Burr, 1988; Currey, 1998, 2003, 2004). The effect of mineral content on bone material properties has been well studied, both in terms of changes with age (Currey and Butler, 1975; Currey, 1979b) and interspecific variation (Currey, 1969, 1988, 1999, 2002, 2004a, b). Dramatic changes in material properties result from a relatively small change in mineral content. Generally, for mineral contents of 63–68%, static strength, toughness, and modulus increase as mineral is deposited in the collagen. However, above 68%, strength may actually decrease as mineral content rises, due to the fact that the hydroxyapatite crystals coalesce and are therefore unable to stop cracks from propagating (Currey, 1969). Additionally, the impact strength of highly mineralized bone is less than its static strength, and impact strength drops more precipitously than static strength as mineralization increases (Currey, 1969). A decrease in toughness is generally associated with an increase in mineral content (Currey, 1969; Malik et al., 2003). Specifically, toughness, as measured by work of fracture, increases with mineral content up to 66–67%, and then declines precipitously as mineral content continues to rise (Currey, 1969). Our mineral content ranged from 64–71% (mean 69%). This may be why we saw the decrease in strength and toughness for the largest manatees.

Degree of bone mineralization is known to increase with age in humans, and there is a corresponding increase in strength and stiffness, and a decrease in absorption of impact energy (Currey, 1979b, 1984, 2002; Currey et al., 1996). Although this pattern is well documented in humans, this is not the case for all animals. Harvey and Donahue

(2004, 2005) found that although mineral content, hence modulus, increased in black bear tibia from animals aged 2–14 years, there was no decline in strength, toughness, or porosity with age. Furthermore, they found no reduction in bone mechanical properties attributable to long periods of hibernation. Phelps et al. (2000) examined age-related changes in mechanical properties of the baboon femur, which is known to resemble human bone in microstructure. Although significant decreases in fracture toughness were noted for adult animals aged 6–27 years, they found no variation in bone density, mineral content, or porosity with age.

**Other Factors Influencing Bone Material Properties**

Material properties of cortical bone are determined in large part by mineral content, but also by porosity, histological architecture, and amount and quality of collagen (Martin et al., 1998). One deficit of this study is that we did not include a histological examination of our bone. This would have allowed us to measure porosity, and both quantitatively and qualitatively describe the type and arrangement of bone and collagen. Yan (2002) measured porosity from scanning electron micrographs for a few rib bone samples from one calf and four subadult manatees. Porosity varied from 3–44%, and was strongly correlated to flexural strength ($R^2 = 0.88$) and fracture toughness ($R^2 = 0.89$). However, porosity varied as much as 26% within the same rib, and was not significantly correlated to total body length. Although the very highest porosity (44%) was for the neonate MEC0033, some values for other animals were still somewhat greater than those reported by others, including 1–10% for both human femur and baboon femur, 4% for cow femur, and 2–7% for black bear tibia (Schaffler and Burr, 1988; Currey and Pond, 1989; Phelps et al., 2000; Harvey and Donahue, 2004). In a second set of measurements, Yan (2005) reported an average porosity of 7% for manatee rib and 4%

for cow femur, values more in line with other published values. The average porosity for manatee rib reported by Domning and de Buffrenil (1991) was 10%. De Buffrenil and Schoevaert (1989) reported porosities of 16% for 1 subadult, to <1% for the adult.

Increasingly, researchers are examining the influence of collagen on the mechanical properties of bone, as variations in structure, mineral content, and density are not sufficiently able to explain the decline in properties with age. Wang et al. (2001) found that collagen denaturation resulted in decreased strength and toughness of the human femur. They also found that modulus was constant irrespective of the degree of collagen degradation. In a related study, Wang et al. (2002) examined collagen content and quality in human femora aged 19–89 years. They found that age-related changes in collagen were associated with decreased strength, toughness, and work to fracture of bone. Moreover, the deterioration of collagen with age was significantly correlated to the post-yield deformation. Phelps et al. (2000) found that the organic fraction showed a significant, positive correlation with fracture toughness for baboon femora. The exact mechanism by which changes in collagen alter mechanical properties is not known. However, it has been speculated that changes in the amount of collagen or to either the inter- or intra-molecular stability of the collagen are responsible (Zioupos et al., 1999; Burr, 2002). Age-related changes in cross-linking have been shown to alter collagen structure, which in turn may alter its hydration (Lucchinetti, 2001; Wang et al., 2002). To date, studies on the effects of collagen cross linking have been contradictory. Regardless of the specific mechanism, there is growing evidence that collagen degradation with age is primarily responsible for the post-yield decrease in toughness and work of fracture, and that these declines are independent of mineral content or density (Lucchinetti, 2001; Burr,

2002; Wang et al., 2001). In support of this, we found no relationship between work of fracture and mineral content for manatee rib bone ($R^2 = 0.02$).

Bone type and degree of remodeling influence material properties. Mineral content for mature primary lamellar bone is 67% versus 63% for Haversian bone (Currey, 1969; Vincent, 1990). Bone remodeling replaces mature, mineralized bone with material that is initially less mineralized. Haversian bone has decreased strength and modulus compared to lamellar bone, but increased toughness. Remodeling may decrease strength by as much as 20% (Martin et al., 1998). That the mineral content of manatee bone is high relative to most lamellar bone may be indicative of low remodeling rates. Possible evidence for this may be from Fawcett (1942b), who conducted the only detailed examination of manatee bone histology to date. He described what is now known as plexiform bone, as well as endochondral (primary) bone that remained unremodeled, and some persistent calcified cartilage matrix. He did not quantify the extent of remodeling, only remarking that Haversian systems are predominantly located in the innermost third of the cross section, and their numbers diminish rapidly toward the outer edge. He also did not comment on whether the osteons were primary or secondary. Furthermore, the descriptive histology was based on one rib from one fresh adult animal, one dried humerus from a museum, and two preserved fetuses. Based on the limited information provided about the adult, its true age is ambiguous, and it was likely not skeletally mature.

Marmontel (1993) examined histological sections of various manatee bones, including ribs. She estimated that bone resorption increased significantly with total body length. In addition, females had significantly greater numbers of Haversian systems than

males. Her work suggested that there are age differences in manatee bone structure and composition that may directly influence its mechanical behavior. This pattern is different from what is seen in humans. It is generally thought that remodeling slows in older individuals, resulting in an increase in the amount of older, more mineralized bone. Hence, the modulus increases, and this contributes to the elevated susceptibility to fracture with age (Currey, 1979b). However, there is evidence to demonstrate that this is not true. Bone turnover has been found to increase in the elderly human population, compared to middle-aged adults (Gallagher et al., 1998; Gundberg, 2002). The scenario for manatees may be similar: an increase in remodeling with age may be partly responsible for the slight decline in strength seen in the largest individuals, as Haversian bone is weaker than lamellar. Similarly, sex differences in remodeling might result in significant variation in mechanical properties between males and females. In contrast to Marmontel (1993), we did not find any significant differences between the sexes for any mechanical variable. Histological examination of manatee bone will tell us whether or not remodeling differences exist.

Manatee rib bone is composed of plexiform bone, which is a mix of primary lamellar and woven bone. Preliminary observations of undecalcified histological sections show that, in addition to plexiform bone, there appears to be a central area of woven bone. This may be what Fawcett (1942b) referred to as disorganized, primary endochondral bone. Woven bone, although less organized than lamellar, has the potential to become more mineralized (Currey, 1998; Martin et al., 1998). For manatees, the preponderance of woven bone, in conjunction with a low remodeling rate, likely accounts for the elevated bone density and high mineral content.

**Summary**

Manatees fill a unique aquatic niche. As the only herbivorous marine mammal, they inhabit shallow, coastal estuarine or riverine waters, feeding primarily on seagrasses and other aquatic vegetation. The pachyostotic long bones of the Florida manatee are hypothesized to regulate buoyancy in shallow water and serve as a means of attitude control (Domning and de Buffrenil, 1991). Because the ribs and long bones are not weight bearing in the aquatic environment, development of pachyostosis may have been evolutionarily advantageous. However, the arrival of the engine-driven watercraft to Florida waters has left the manatee ill-suited to cope with their encounters. Every year, 25–30% of all manatee deaths are due to injuries that result from bones broken in collisions with watercraft. To begin to understand the injuries from a bone mechanics perspective, we measured some material properties of manatee rib bone. We found that this bone is less strong and less tough than most other mammalian bone. We also found that, although the bone increases in static strength as the animals grow, the bone is not able to absorb more energy. In fact there is a strong indication that the ability to absorb energy (measured as work of fracture) declines with increasing size in animals over 265 cm total body length (i.e., large subadults). This decline is due in part to the bone's high density and mineral content. Finally, we found no differences in mechanical properties between males and females. The pachyostotic nature of the bone, which makes the manatee well-adapted to its environment, also leaves it highly susceptible to fatal injuries from boats.

Table 2-1. Mean material properties for 26 manatees

| Animal | Sex | TL (cm) | Age class | N | σ (MPa) | E (GPa) | WOF ($MJ/m^3$) | $N_{KC}$ | $K_C$ ($MPa \cdot m^{1/2}$) | Density ($g/cm^3$) | Mineral content |
|---|---|---|---|---|---|---|---|---|---|---|---|
| MEC0033 | F | 102 | C | 5 | 62 | 4.0 | 3.1 | 5 | 1.4 | — | — |
| MSTM0109 | M | 166 | C | 30 | 134 | 12.8 | 3.8 | 60 | 2.5 | 2.14 | 69 |
| MSW0033 | M | 178 | S | 31 | 136 | 12.0 | 6.0 | 29 | 2.1 | — | — |
| MSW0164 | M | 182 | S | 25 | 105 | 9.4 | 4.0 | 24 | 2.2 | 2.22 | 64 |
| MNW0207 | F | 188 | S | 37 | 127 | 11.6 | 3.5 | 34 | 2.4 | 2.10 | 67 |
| MSW0227 | F | 190 | S | 48 | 124 | 12.3 | 4.2 | 44 | 2.4 | 2.16 | 67 |
| SWFTM0114 | M | 196 | S | 66 | 122 | 11.2 | 4.6 | 48 | 2.3 | — | — |
| MSW0057 | M | 201 | S | 36 | 153 | 9.6 | 5.5 | 21 | 2.7 | — | — |
| MSW0134 | F | 205 | S | 58 | 130 | 11.5 | 5.5 | 54 | 2.1 | — | — |
| MSE0205 | M | 238 | S | 114 | 135 | 12.6 | 4.4 | 63 | 2.6 | 2.11 | 68 |
| MSW0160 | F | 246 | S | 131 | 159 | 14.9 | 5.6 | 50 | 2.8 | 2.18 | 68 |
| MSTM0102 | F | 265 | S | 169 | 157 | 15.4 | 4.3 | 155 | 2.6 | — | — |
| MSW0165 | F | 267 | S | 157 | 152 | 14.5 | 4.6 | 59 | 2.7 | 2.15 | 68 |
| MEC0220 | M | 275 | S | 139 | 144 | 14.4 | 3.6 | 59 | 2.6 | 2.11 | 69 |
| MSW0251 | M | 276 | A | 142 | 160 | 17.7 | 3.6 | 114 | 2.8 | 2.20 | 71 |
| MSW0225 | F | 282 | A | 160 | 151 | 16.0 | 3.8 | 114 | 2.7 | 2.18 | 69 |
| MSW0223 | F | 294 | A | 184 | 153 | 15.5 | 4.0 | 60 | 2.8 | 2.20 | 69 |
| MSW0208 | F | 299 | A | 175 | 154 | 16.0 | 4.2 | 60 | 2.8 | 2.22 | 70 |
| MEC0213 | F | 314 | A | 143 | 143 | 16.0 | 3.2 | 60 | 2.6 | 2.16 | 68 |
| MSW0226 | M | 315 | A | 156 | 151 | 16.6 | 3.2 | 60 | 2.7 | 2.18 | 69 |
| MSW0239 | M | 321 | A | 181 | 150 | 16.4 | 3.7 | 60 | 2.8 | 2.21 | 70 |
| MSW0331 | F | 326 | A | 173 | 150 | 17.2 | 3.2 | 118 | 2.6 | 2.19 | 68 |
| MSW0253 | M | 327 | A | 189 | 149 | 15.7 | 3.8 | 119 | 2.6 | 2.19 | 69 |
| SWFTM0414 | F | 335 | A | 189 | 158 | 17.4 | 3.6 | 60 | 2.9 | 2.20 | 69 |
| MNW0208 | M | 343 | A | 178 | 159 | 18.0 | 3.0 | 60 | 2.9 | 2.22 | 70 |
| MSW0245 | M | 344 | A | 307 | 143 | 15.6 | 3.1 | 93 | 2.3 | 2.16 | 68 |

Variables are: sex, male (M) or female (F); total body length (TL); age class, calf (C) subadult (S), or adult (A); sample size for strength, modulus, and work of fracture (N); flexural strength (σ); Young's modulus (E); work of fracture (WOF); number of toughness samples ($N_{KC}$); fracture toughness ($K_C$); density; and percent mineral content. — indicates no data for that variable.

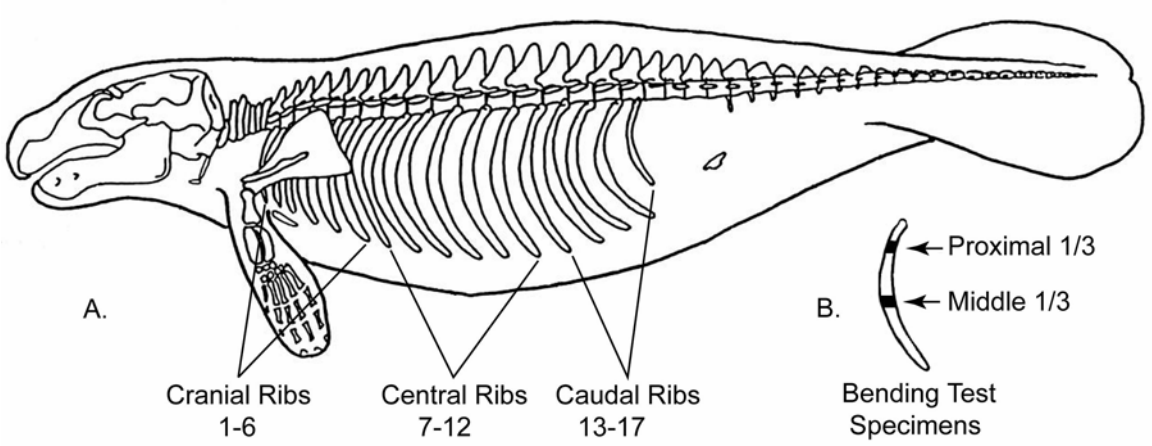


Figure 2-1. Sample sites for biomechanical analyses. A) Ribcage is divided into three regions: cranial, middle, and caudal. One rib from each region was used for bending tests. B) Sample sites for bending tests within each rib are indicated.

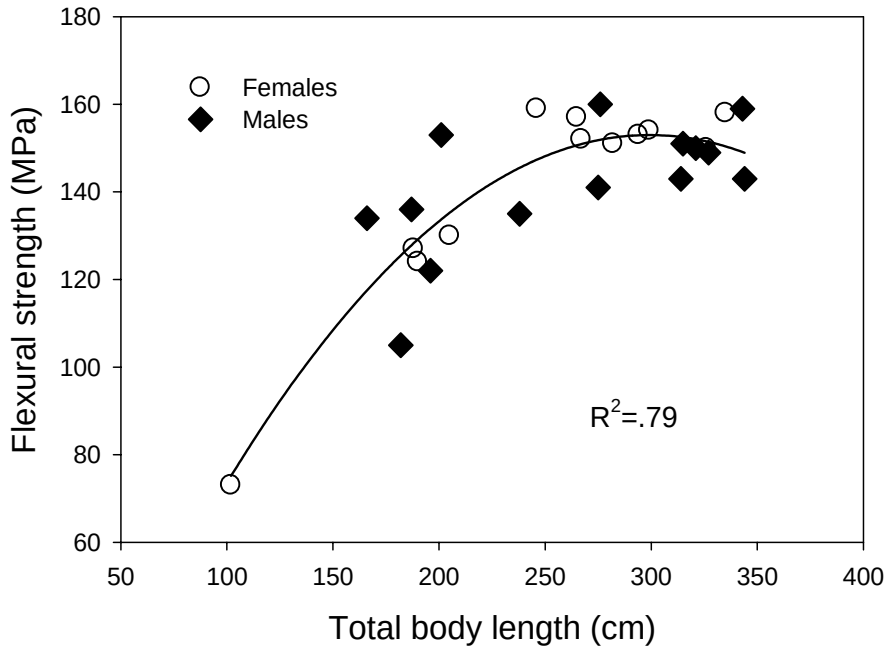


Figure 2-2. Flexural strength vs. total length. Strength increases with body length in the subadults and plateaus in the adults. There was no significant difference in strength between sexes (ANCOVA, $p = 0.93$).

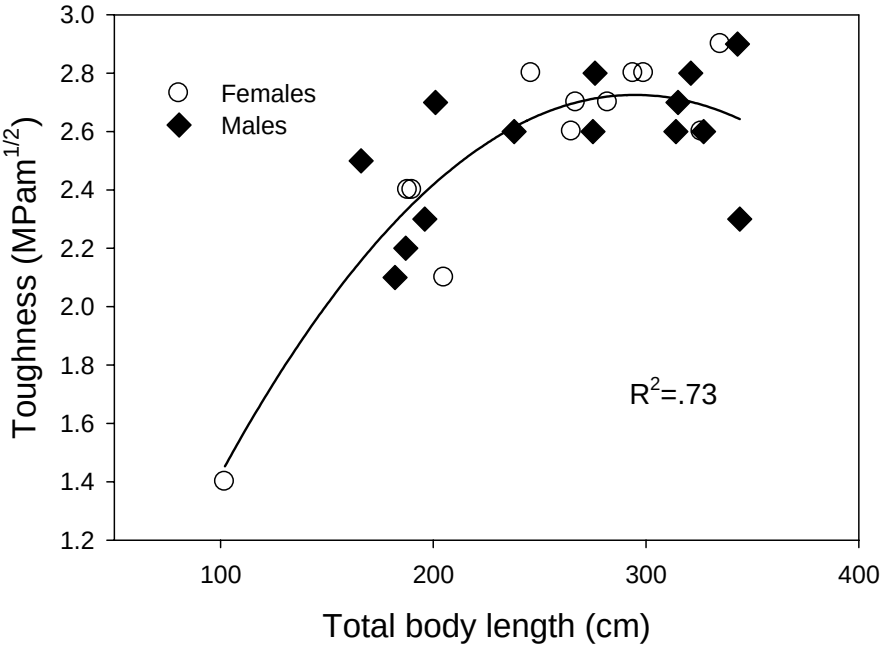


Figure 2-3. Fracture toughness vs. total length. Fracture toughness peaks in the subadults and thereafter plateaus in the adults. There was no significant difference between sexes (ANCOVA, p = 0.81)

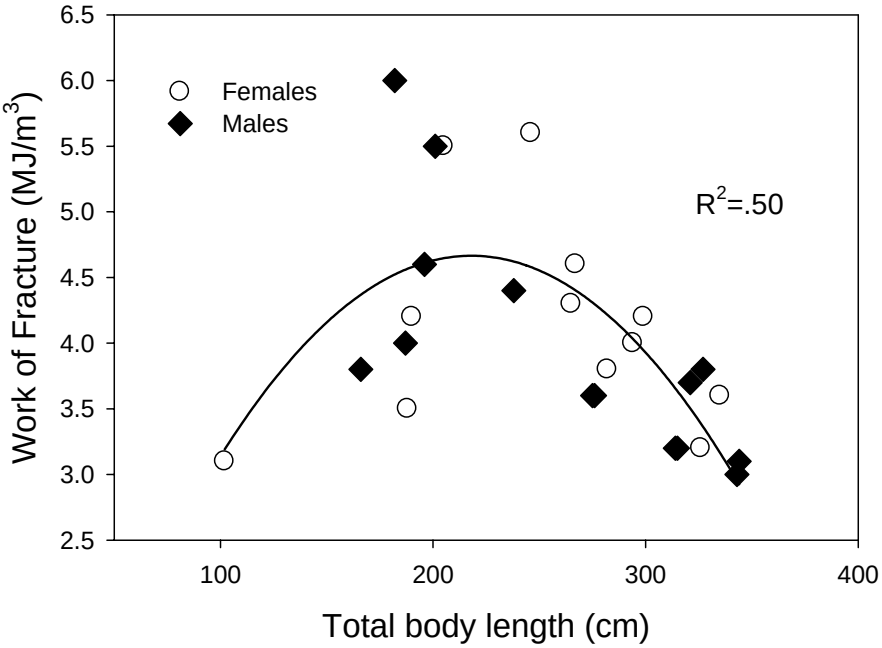


Figure 2-4. Work of fracture vs. total length. Work of fracture peaked in the subadults, and thereafter declined with increasing body length. There was no significant difference between sexes (ANCOVA, p = 0.96).

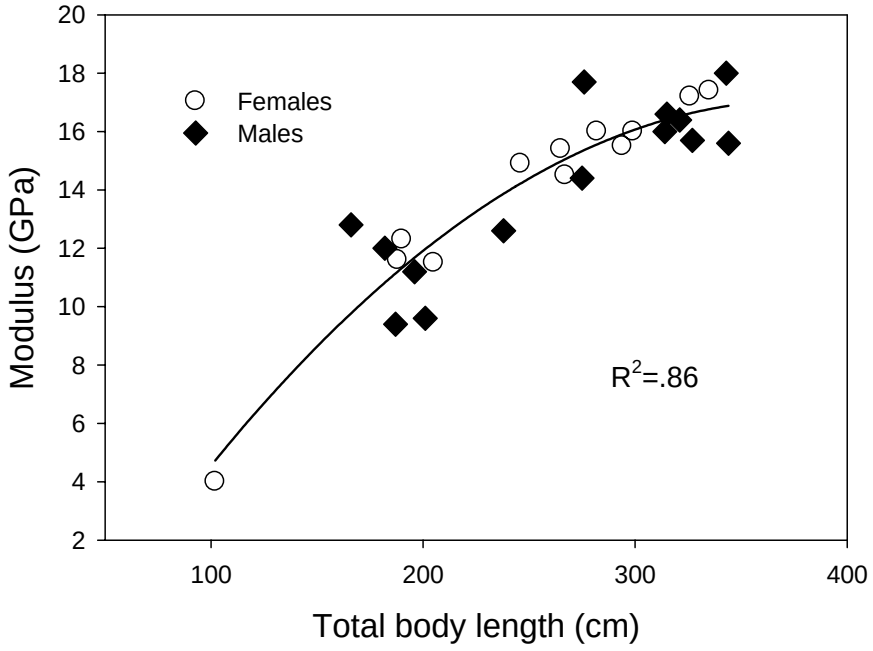


Figure 2-5. Elastic modulus vs. total length. Elastic modulus increased with increasing body length. There was no significant difference between sexes (ANCOVA, $p = 0.70$).

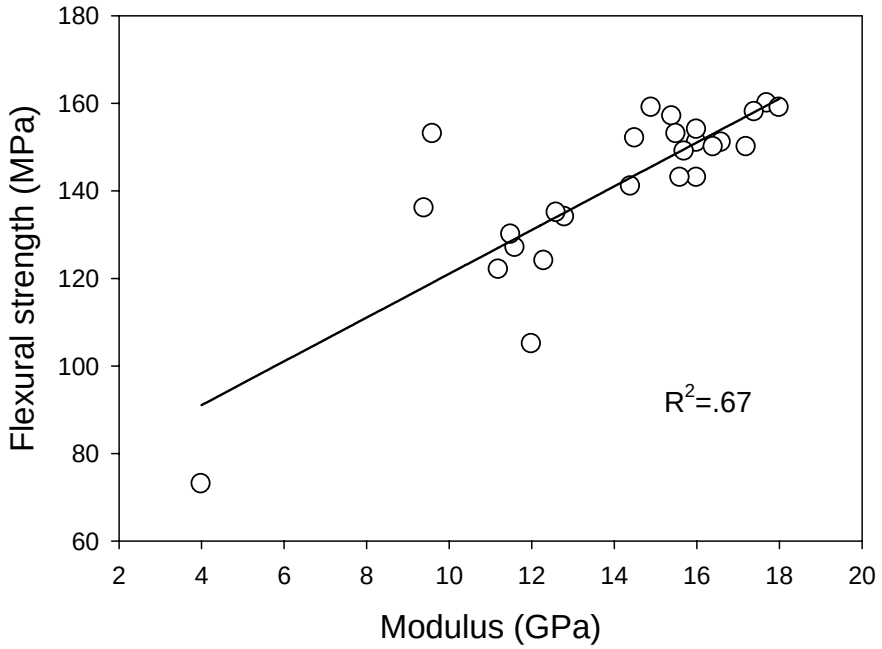


Figure 2-6. Flexural strength vs. modulus. Flexural strength is significantly correlated to the elastic modulus ($p<0.0001$).

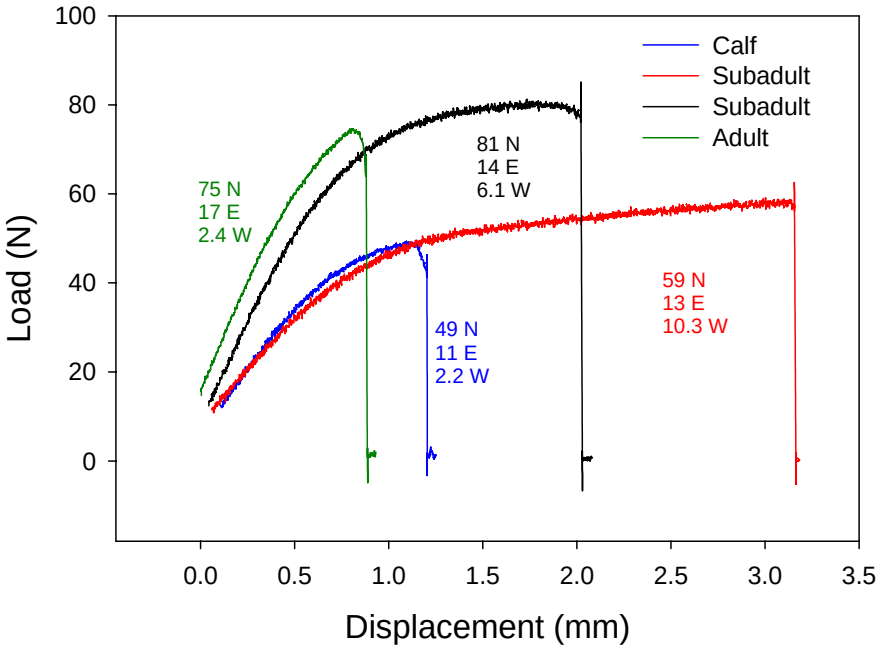


Figure 2-7. Load-displacement curves for small sample specimens tested in 3-point flexure. Values given for each curve are: ultimate load, N (Newtons); modulus, E (GPa); and work of fracture, W ($MJ/m^3$). Three age classes are represented: calves (MNW0207); subadults (MSW0160); and adults (MNW0208). Two curves for the subadult MSW0160 are shown. The red curve is an example of the high work of fracture obtained for some subadult specimens. The black curve is a more typical curve for a large subadult.

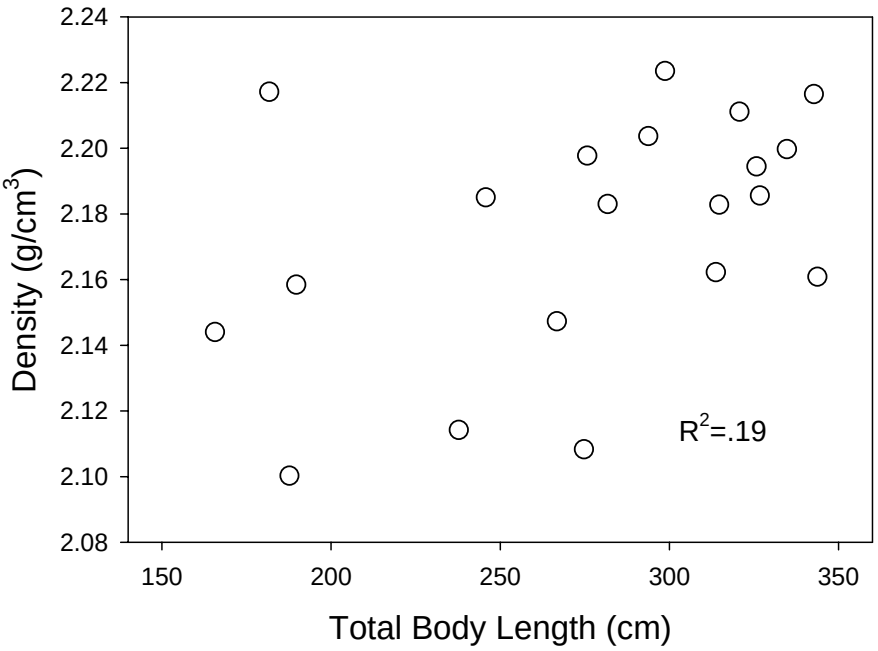


Figure 2-8. Density vs. total body length. There was no significant relationship between bone tissue density and body size ($p = 0.0517$).

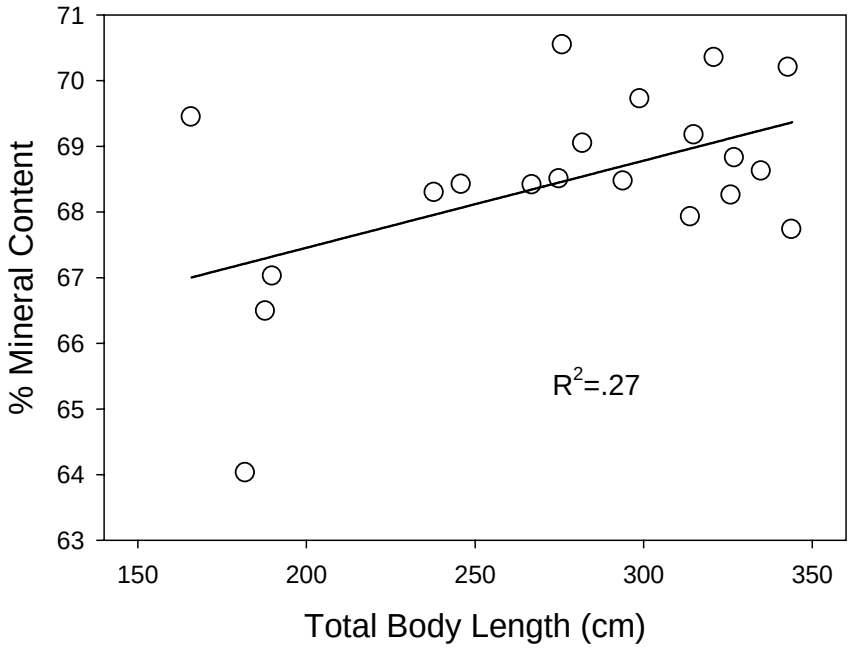


Figure 2-9. Percent mineral content vs. total body length. There was a significant increase in percent mineral content with total body length ($p = 0.0198$), although the correlation was weak.

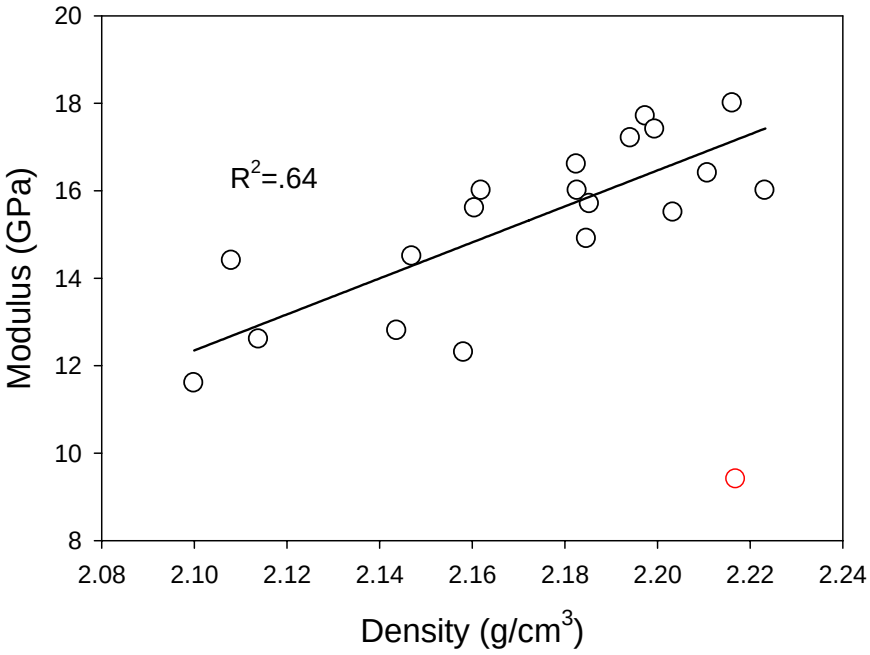


Figure 2-10. Modulus vs. density. With one outlier (shown in red) removed, modulus is significantly correlated to density ($p<0.0001$).

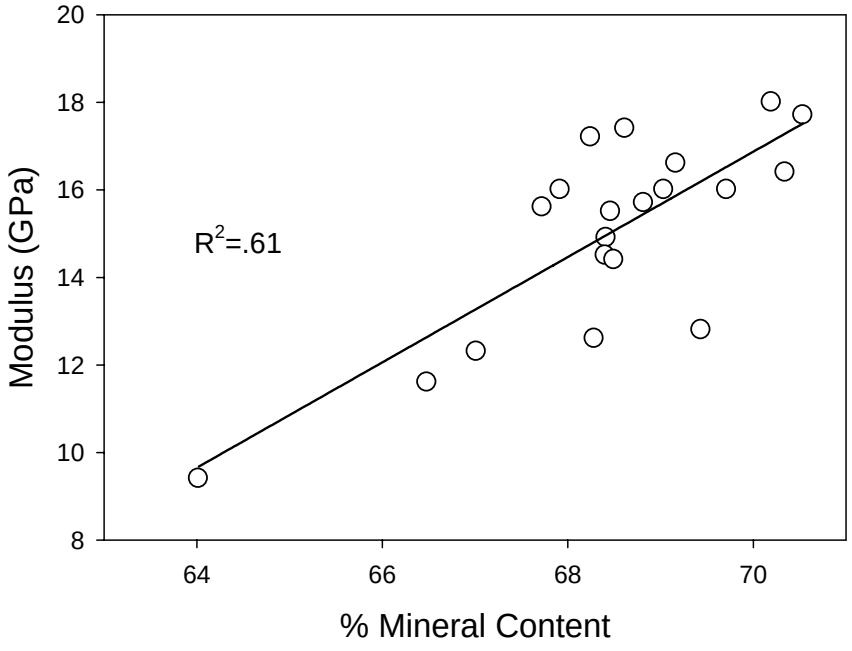


Figure 2-11. Modulus vs. percent mineral content. Modulus is significantly correlated to mineral content ($p<0.0001$).

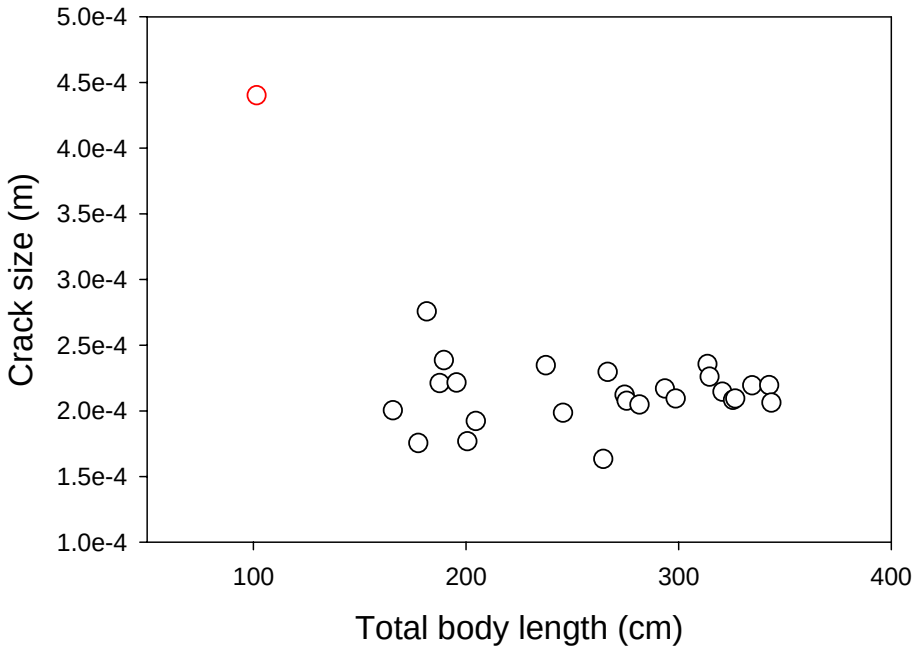


Figure 2-12. Small sample crack size vs. total body length. The neonate calf MEC0033 was an outlier (shown in red). With the outlier removed, there was no change in crack size with total body length ($R^2 = 0.0009$, $p = 0.8886$).

# CHAPTER 3
# STRUCTURAL PROPERTIES OF MANATEE RIBS TESTED IN IMPACT

## Introduction

The endangered Florida manatee shares its nearshore, coastal habitat with an ever increasing number of boats. Each year, 25–30% of all manatee deaths are a result of collisions with watercraft. Boat speed zones are the primary tool for ameliorating the lethal interactions. However, existing limits are not based explicitly on information pertaining to the nature or severity of the injury, including bone fractures. In an effort to establish safer boat speeds for manatees, the Florida manatee recovery plan calls for research on the mechanical characteristics of manatee bone to better understand the effects of watercraft-related impacts (U.S. Fish and Wildlife Service, 2000). This study is the first to estimate mechanical properties of whole manatee bone.

Quantitative fractography is a technique which uses principles of fracture mechanics and fractal geometry to analyze fracture surfaces of brittle materials such as ceramics (Mecholsky, 1993, 2001). The strength of a material is determined by the size of the fracture initiating crack, or flaw, and the fracture toughness of the material. Location of the crack can be determined by examining the markings on the fracture surface. In similar fashion, the topography of a fracture surface is also a record of fracture parameters and is fractal in nature. The fractal dimensional increment (D*) is a quantitative measure of the tortuosity of a brittle fracture surface, and is related to parameters such as the fracture toughness and elastic modulus West et al., 1999).

Two features of manatee bone allowed us to use quantitative fractography to measure its mechanical parameters. First, all its ribs and long bones are constructed of solid cortical bone; there are no marrow cavities or spongy bone. This feature, unusual for mammalian bone, is thought to be an adaptation to aid in hydrostasis (Domning and de Buffrenil, 1989). Second, manatee bone often undergoes brittle fracture in static tests (Chapter 2; Yan et al., 2005). Bone typically behaves as a quasi-brittle solid (Zioupos, 1998). However, fully mineralized bone from adult manatees does not undergo any post-yield plastic deformation.

The goal of this study was to estimate the stress at failure and the fracture toughness of whole manatee ribs fractured in impact. Fracture toughness is the ability to resist fracture, one measure of which is the critical stress intensity factor ($K_C$). This is an estimate of the amount of energy required to propagate a macrocrack that leads to fracture (Mecholsky, 1996). Toughness is an important property because a tough bone is resistant to fracture, and this is most important when bone is impacted (Wainwright et al., 1982; Turner and Burr, 1993). Since adult manatee bone fails in a brittle manner when loaded statically, it is likely that fracture resistance measured by $K_C$ is approximately similar to the work of fracture as a measure of toughness in manatee bone loaded in impact. We also addressed the hypothesis that forces generated by most watercraft under normal operation are sufficient to inflict fatal skeletal injuries to manatees.

## Materials and Methods

### Bone Sample Collection

Ribs from 20 animals of both sexes, in three age classes (i.e., calf, subadult, and adult) were obtained from the Florida Fish and Wildlife Conservation Commission's Marine Mammal Pathobiology Laboratory. By convention, total body length was used as

a proxy for age, and individuals were assigned to age classes based on established size definitions (O'Shea et al., 1985). Bones were obtained from fresh carcasses at the time of necropsy. One rib from the mid-thoracic region of each animal was collected and stored frozen until testing. Bones were cleaned of soft tissues and tested at room temperature.

**Whole Rib Impact Testing**

Whole ribs were impacted using a compressed air gun at the Structures Laboratory in the Department of Coastal and Civil Engineering, at the University of Florida (Fig. 3-1). The barrel is 20' in length with a 4" inner diameter. The gun is equipped with a compressor that allows projectiles to be fired at a range of speeds, and two photocells and an oscilloscope to record the speed of the projectile as it exits the barrel. Ribs were positioned vertically in a fixture that was mounted on a steel frame, so that the lateral (convex) side of the rib faced the gun, and the concave side faced the frame. They were impacted perpendicular to their long axis, in the middle of the lateral side with a 2" x 4" x 4'pine projectile. The leading end of the projectile was equipped with a hemispherical nosepiece coated in fiberglass. The mass of the projectile was 13 kg. The distance between the end of the barrel and the rib was 2.3 m. The projectile was fired between 23-28 m/s. Kinetic energy (KE) of the projectile was calculated as

$$KE = \tfrac{1}{2}mv^2 \tag{3-1}$$

where m is the mass of the projectile (kg), and v is velocity (m/s).

Quantitative fractography was used to identify the fracture origin and measure crack size for each rib (Figure 3-2). The failure stress was calculated as

$$\sigma = \frac{K_C}{Y(c)^{1/2}} \tag{3-2}$$

where $K_C$ fracture toughness ($MPa \cdot m^{1/2}$), measured as the critical stress intensity factor. Y is a geometric factor based on crack shape and loading conditions, and c is the crack size ($m^2$). Values for $K_C$ were taken from the middle region of the adjacent rib, which was used to determine bone material properties in Chapter 2. The value used was the mean for the adjacent section. Crack size was calculated as

$$c = (a \cdot b)^{1/2} \tag{3-3}$$

where a and b are crack depth and half-width (m), respectively, as measured from the fracture surface with digital calipers to the nearest 0.1 mm.

**Strain Gauge Testing**

To validate the failure stress calculations, three additional ribs were outfitted with strain gages to directly measure strain during impact. For each rib, a uniaxial gauge (CEA-06-250UN-350, Vishay Micro-Measurements, Raleigh, NC) was placed on the lateral (convex) surface, and a uniaxial gauge and a rosette gauge (CEA-06-125UR-350) were placed on the pleural (concave) side. Gauges were placed along the midline, parallel to the long axis, either above or below the center of the rib. The center element of the rosette was oriented parallel to the long axis of the bone. Signals were output to an 8 channel signal conditioner and sampled at 50 kHz. Raw data were converted to microstrain, which were used to calculate the principal strains using standard formulae. Failure stress was calculated as

$$\sigma = E\varepsilon \tag{3-4}$$

where E is Young's modulus (GPa) measured with ultrasound (Nuson, Inc., Boalsburg, PA), and $\varepsilon$ is the maximum principal strain.

As a check of the strain data, an additional rib was outfitted with gauges and loaded to failure in quasi-static 3 point bending at a load rate of 4.448 N/s. The signal

was sampled at 20 Hz. Failure stress was calculated using the standard formula for a curved beam in bending. For all gauged ribs, the fracture origin was identified fractographically, and $K_C$ was determined using Equation 3-2. Toughness values calculated for whole ribs were compared to those from the materials test specimens to assess the validity of using the materials values from Chapter 2 in the failure stress calculations.

**Fractal Dimensional Increment**

The fractal dimensional increment (D*) was calculated using a modified slit island technique (Hill et al., 2001). The technique involves making an epoxy replica of the fracture surface (Figure 3-3). The replica is ground down to the plane of fracture to produce fracture surface contours, or islands. The island perimeter, represented by a line, is measured with rulers of different lengths. A log-log graph of perimeter length versus the ruler length produces a line whose slope is related to the fractal dimension, D (i.e., slope = 1-D). The non-integer, or fractional portion, of the slope is equal to D*, which is a measure of the fracture surface tortuosity. The higher the value of D*, the more tortuous (rough) the surface. For example, a fractal dimension (D) of 2.08 (D* = .08) would be a surface which is relatively smooth, and a D of 2.40 (D* = .40) would be a "rough" surface, with much tortuosity.

For each rib, a negative impression mold of the fracture surface was made in dental putty and latex, and then double cast in epoxy. The cast was made such that the fracture origin was horizontal. The fracture surface of the positive cast was sputter coated (Denton Desk II cold sputter coater, Denton Vacuum, Moorestown, NJ) with gold-palladium for contrast, and the second cast was poured. Replicas were ground down to the fracture origin on a grinding wheel using increasingly finer grit sanding papers, then

polished with 0.3µm alumina slurry. Composite images of the fracture surface contours were made from high resolution images (200X) taken with a digital camera mounted on a light microscope (Figure 3-4). D* was calculated from the composite images using the Materials Pro® Analyzer software add-on for the Image Pro-Plus® software (Media Cybernetics, Inc., Silver Spring, MD).

Ideally we would like to be able to calculate whole bone fracture toughness from the measured fractal dimension. The two parameters are related in the equation

$$K_C = Ea_0^{1/2}D^{*1/2} \quad (3\text{-}5)$$

where E (GPa) is the elastic modulus, $a_0$ (Å)is a proportionality constant, and D* is the fractal dimensional increment. The variable $a_0$ is a material constant that has been proposed as a measure of the average intermolecular strained bond length (Mecholsky, 2001). It is not directly measurable, but must be calculated from other, independently measured parameters or estimated using quantum mechanics models. Although $a_0$ has been established for a number of materials, there is no experimentally determined value for cortical bone. Using our measured D* values, $K_C$ values calculated from the strain gage data and fractographic measurements, and the ultrasonic modulus, we estimated $a_0$ for manatee cortical bone.

**Kinetic Energy Calculations**

The most common recreational watercraft in operation in Florida waters is a 17' vessel (Wright et al., 1995) which is typically equipped with a single outboard engine of 100–115 HP. A typical 17' vessel at idle speed (i.e., no wake) is traveling at 2–3 mph (depending on vessel configuration), and 10–12 mph corresponds to a boat traveling at or near hull speed (i.e., on a plane). Maximum speed is approximately 35–40 mph. Weights for a few common 17' vessels with the recommended engines were taken from the

specifications posted on manufacturers' websites. Kinetic energy was calculated for speeds of 2, 10, and 35 mph. We assumed one adult operator (200 lbs.) and one half–tank of fuel. The soft tissues overlying bone have been shown to absorb and dissipate impact energy, thereby decreasing the energy transferred to the skeleton (Currey, 1968; Nikolić et al., 1975; Parkkari et al., 1994, 1995; Robinovitch et al., 1995). To estimate the energy damping ability of the tissues overlying the ribs, soft tissue thickness (e.g., skin, blubber, muscle) was measured approximately one third of the way down from the head of the ribs on some whole body sections. Robinovitch et al. (1995) measured the amount of impact energy transferred to the femoral trochanter with overlying soft tissues of varying thickness. They regressed tissue energy absorption against soft tissue thickness to determine the threshold of tissue thickness needed to prevent femur fracture during falls in the elderly. We used their regression to estimate the amount of energy dissipated by manatee soft tissues. Kinetic energy curves for the boats were visually compared to the kinetic energy of the projectile used to impact the bare rib, as well as to the estimate for ribs with overlying soft tissues.

### Statistical Analyses

Failure stress and D* were compared between sexes and age classes in separate one-way ANOVAs (Zar, 1996). Fractal dimension was regressed against total body length (a proxy for age) to examine the relationship of D* to age. Analyses were performed with SAS (SAS Institute, Inc., 1989).

## Results

### Whole Rib Impact Tests

Mechanical and fractal dimension data from the impact tests are presented in Table 3-1 and Fig 3-4. A total of 22 ribs from 20 animals were tested. Only one calf was

tested, as the small size of the ribs made them difficult to test. Of the other 19, eight were subadults (i.e., juveniles) and 11 were adults. The sexes were represented equally, ten females and ten males. Mean failure stress was 47 MPa, varying from 37–67 MPa. Mean adjusted failure stress (see below) was 139 ± 21 MPa (range 106–179 MPa), and mean D* was 0.13 ± 0.04 (range 0.08–0.22). Means by sex and age class are reported in Table 3-2. We tested 4 ribs from animal MNW0208, which was a large adult. Three of those were tested in impact and one in quasi-static 3 point flexure. Values for D* were .09, .13, .13, and .20 (Tables 3-1 and 3-3). The variability in these numbers is similar to that for the entire dataset, and thus, not unexpected. This variability may represent natural variation in the ribs, or it may be an artifact of the replication or grinding processes. There were no statistically significant differences between the sexes for either failure stress ($p = 0.51$) or D* ($p = 0.18$). Similarly, no differences were found between age classes for either variable ($p = 0.19$ and $p = 0.63$ for failure stress and D*, respectively). The lone calf was omitted from the analysis by age class. The regressions of D* and failure stress against total body length indicated no relationship between either parameter to body size (Figures 3-5 and 3-6, respectively). These two independent measures both imply that the ability to resist bone fracture in impact does not increase as animals grow.

**Strain Gauge Tests**

Of the three ribs outfitted with strain gages for the impact tests, data were successfully collected for only one (Table 3-3). The rib tested in 3 point bending failed at a load of 4480 N. Peak strains for the impact and static tests were very similar (0.56% and 0.61% respectively). Fracture toughness calculated for the impacted rib was 7.7 $MPa \cdot m^{1/2}$, essentially identical to the 7.8 $MPa \cdot m^{1/2}$ for the rib from the static test. These values were much greater than those used for the failure stress calculations reported in

Table 3-1. Our results indicate that it is not appropriate to use the small specimen fracture toughness values of Chapter 2 to calculate whole bone failure stress. By doing so, our stresses were most likely underestimates. To adjust for this, we used 8 $MPa \cdot m^{1/2}$ to derive more appropriate estimates of failure stress, reported as $\sigma_W$ in Table 3-1 and Figure 3-6.

The material constant $a_0$ calculated for the two gauged ribs is reported in Table 3-3. The value for rib 14 is twice that for rib 6, 13,000 and 6,700 Å, respectively. Values for classes of ceramics are much lower, typically 1-100 Å, but our values lie in the range reported for various polymers, from 2,700-14,000 Å (West et al., 1999; Mecholsky, 2001). Much more work needs to be done to determine whether it is possible to estimate $a_0$ for a complex material such as cortical bone.

**Kinetic Energy Calculations**

Projectile velocity, as measured exiting the barrel, was 23-28 m/s. To make conservative estimates of the threshold for fracture we used the maximum projectile velocity (28 m/s) for calculations. Vessel configurations and kinetic energies are presented in Tables 3-4 and 3-5, and Figure 3-7. Based on the configurations selected, rib fracture can occur at speeds of 7–8 mph, or just below hull speed. This is speed at which boats generate kinetic energy equal to that of the projectile, as determined by the point at which the regression curves cross the kinetic energy line for the projectile. This estimate is for bare bone, which of course is not a realistic scenario. Human impact studies indicate that for some body sites, soft tissues absorb and dissipate as much as 90% of impact energy (Nikolić et al., 1975). The maximum thickness of manatee soft tissues (i.e., skin, blubber, and muscle) was 58 mm. Robinovitch et al. (1995) measured impact energy absorption for soft tissues up to 43 mm thickness. Using their regression, we extrapolated the amount of energy dissipated by the manatee soft tissues to be 70%. That

is, only 30% of impact energy is transferred to the bone. This projection is plotted on Figure 3-7. At this energy absorption estimate, boat speeds of 13–15 miles per hour are sufficient to fracture manatee ribs (i.e., where the regression curves cross the "with skin" kinetic energy estimate, indicated by the dashed lines on Figure 3-5).

## Discussion

Fractals are geometrical objects with fractional dimensions (Mecholsky, 1986). Mandelbrot was the first to recognize that natural structures and phenomena are fractal, and this includes fracture surfaces (Mandelbrot et al., 1984; Mecholsky et al., 1996). Fractal geometry provides a means of measuring the roughness, or tortuosity of a fracture surface. The fractal dimension (D) is a quantitative measure of the dimensionality of an irregular, or tortuous, surface. The fractional dimensional increment (D*, the fractional portion of the fractal dimension) is related to fracture parameters such as the fracture toughness and elastic modulus. Techniques were first applied to metals, and were subsequently applied to ceramics and some composites (Mandelbrot et al., 1984; Mecholsky et al., 1989; West et al., 1999; Czarnecki et al., 2001). Fractal geometry is now being used for trabecular bone as a means to quantify changes in bone quality and quantity (Majumdar et al., 1993). We have utilized the fractal dimension to quantify fracture parameters of manatee cortical bone using the same methods applied to structural materials.

### The Fractal Dimensional Increment

Although use of fractal analysis now can be found widely in the engineering literature, there are few examples of its application to biological composites. Fractal dimension is becoming a popular tool for quantifying changes in trabecular bone architecture related to disease conditions such as osteoporosis. In this body of literature,

its proposed use is singly as a diagnostic tool. Only two studies of biological composites have related fracture energy to fractal geometry. Currey et al. (1995) measured fractal dimension for cortical bone for a variety of species. Fractal dimensional increment was correlated to the work of fracture, from .05 for a highly mineralized, brittle fin whale tympanic bulla to .25 for very tough, young deer antler. Various types of cortical bone had intermediate fractal dimensions, which roughly correlated to their calculated works of fracture. Hill (2001) measured fractal dimensional increments for the conch shell of *Strombus gigas*. Means ranged from .16–.22 for specimens stored in different media. Our measured D* values for manatee cortical bone ranged from .08–.22, which is in general agreement with the other two studies. However, it is difficult to make detailed comparisons among studies because, although the same theory was used to calculate fractal dimension, different measurement methods were used. Additionally, biological composites, like some other materials, may be multi-fractal, making results sensitive to measurement length scale. Currey et al. (1995) found this to be true for bone with high work of fracture, fractal dimension decreasing with increased length scale in these tough materials.

A wide range of D* values exists for classes of materials (e.g., metals, polycrystalline ceramics, and glasses). However, since most of the data available in the literature are for essentially monolithic materials, we could only make a cursory comparison to our data. Aside from the two references to bone and shell, the most appropriate materials to compare to our data are the cement-epoxy composites. Czarnecki et al. (2001) measured fractal dimensional increments of .02–.08 for seven epoxy concretes. However, they used the vertical profile technique to calculate fractal

dimension, which is known to produce values consistently lower than those of the slit island technique (Hill et al., 2001).

**Fractal Dimensional Increment and Fracture Toughness**

Because of the large amount of variation in fractal dimension both within and among classes of materials, comparing D* values alone is not informative. It is more instructive to examine the relationship between the fractal dimension and fracture toughness. For most materials that fail in a brittle manner, there is a positive correlation between fracture toughness ($K_C$) and $D^{*1/2}$, and the slit island technique has been shown to produce a D* that is a more accurate predictor of $K_C$ than other techniques (Russ, 1994; Hill et al., 2001; Mecholsky, 2001). Over the range of D* values for manatee bone, fracture toughness only varied by 1 $MPa \cdot m^{1/2}$, which resulted in no significant relationship between fractal dimension and fracture toughness ($R^2 = 0.02$, $p = 0.5535$, Figure 3-8). There are a few possible explanations for the lack of correlation. It could be that there is no relationship between the parameters for cortical bone, or that the range of fracture toughness values was too narrow to detect a trend. A third possibility is that error was introduced into our technique. Calculation of the fractal dimensional increment using the slit island technique is sensitive to error in the polishing angle. Della Bona et al. (2001) showed that variation of 5° or greater from the fracture plane significantly underestimates D*. There may have been angle errors introduced in the production and grinding of the replicas that would account for some of the low values reported here. However, our methodology was consistent throughout, so this would not explain the non-significant relationship between fractal dimension and fracture toughness.

We hypothesize that the lack of correlation between fractal dimension and fracture toughness reflects the true relationship between these properties for manatee

bone. Critical crack size for the whole ribs was similar for all animals regardless of total body length ($R^2 = 0.10$, $p = 0.1538$, Figure 3-9) or cross sectional area of ribs. In Chapter 2 we reported that density and mineral content also did not vary significantly over the range of body sizes. If these values accurately reflect the material properties of rib bone, then our finding of non-significant variation in critical crack size and failure stress among animals is not anomalous. Despite the increase in rib size (340–1926 $mm^2$ cross-sectional area) with increasing body size in manatees, there is no concomitant increase in ability to resist crack formation because the material is essentially the same.

**R-curve Behavior and Viscoelasticity in Bone**

The greater fracture toughness values calculated from the strain data relative to the small specimen values of Chapter 2 may be indicative of R-curve behavior in manatee bone. A rising R-curve describes an increase in fracture toughness with the increase in crack extension (Vashishth, 2004). This behavior is characteristic of quasi-brittle materials such as some ceramics, and has now been documented in human, bovine, equine, and deer antler bone (Les et al., 2002; Malik et al., 2003; Nalla et al., 2004; Vashishth et al., 1997). If manatee bone exhibits R-curve behavior, then it is not appropriate to use toughness values from small sample material properties tests to calculate failure stresses of whole bones. Those values, measured from machined specimens tested in 3-point bending, ranged from 2.0–3.0 $MPa \cdot m^{1/2}$.

True brittle materials exhibit flat R-curve behavior (Vashishth et al., 1997; Zioupos, 1998). The material tests in Chapter 2 showed that adult manatee bone tested in static 3 point bending undergoes very little or no plastic deformation; it typically fails catastrophically near the yield point. This seemingly contradicts the toughness data presented here that suggests R-curve behavior. However, Vashishth et al. (1997) point

out that some ceramics do produce rising R-Curves. Like all bone, manatee bone is a ceramic-polymer composite of complex, hierarchical structure. Bone microstructure, mineral density, and collagen content all affect the R-curve behavior (Les et al., 2002; Malik et al., 2003; Nalla et al., 2004; Vashishth et al., 1997). Malik et al. (2003) reported lower R-curves in bone of increased stiffness, tested in tension. Nalla et al. (2004) reported an age-related decrease in both crack initiation and crack growth resistance. The high mineral content of manatee bone (mean 69%) likely has a similar effect. Appropriate testing needs to be done to characterize R-curve behavior in manatee bone.

The R-curve behavior of bone is due to its viscoelastic nature; its collagen component is partly responsible for the toughening mechanism of crack bridging. A larger sample allows for a greater crack size, and more collagen is available to contribute to the toughening, resulting in a larger fracture toughness. Therefore, absolute size most likely explains the greater fracture toughness of the whole ribs over the machined specimens. For some materials, including most bone, fracture toughness is strain rate dependent. As strain rate increases, so does strength, modulus, and $K_C$; a feature also attributable to viscoelasticity (Zioupos, 1998). However, note that work of fracture (WOF) will decrease with increased strain rate, also due to the viscoelastic nature of bone. The different behavior of $K_C$ versus WOF with strain rate is due to the method of measurement of both. Because we tested the whole bones and the small sample specimens at different rates, the effects of strain rate and specimen size were confounded in this study. However, in ceramics, fracture toughness is not strain rate dependent, as long as it is not strongly sensitive to stress corrosion processes. The impact tests provide

additional evidence that manatee bone behaves as a ceramic; the whole rib tested in quasi-static 3 point flexure had a crack size identical to the other ribs tested in impact.

**Impact Energy Absorption of Soft Tissues**

Impact testing of human bone is often done to determine the loads at which bones, such as the femur, break. The whole rib manatee tested in static 3 point bending failed at a load of 4480 N, which is only moderately greater than the critical trochanteric impact load of 4170 N, the average load required to fracture in impact the proximal femur in the elderly (Parkkari et al., 1995). Soft tissues overlying the bone absorb impact energy, thereby reducing the load transferred to the bone. Energy absorbed by soft tissues has been shown to be as high as 90%. In femoral impact tests conducted by Robinovitch et al. (1995), energy absorption varied from 6–58%. As tissue thickness increases, energy absorption increases, and the peak load transferred to the bone decreases. The authors found that for each millimeter of soft tissue thickness, peak load transferred to the bone decreased by 70 N, and soft tissue energy absorption increased by 1.7 J. In a different study, Parkkari et al. (1995) impacted artificial hips protected by soft tissues at high and low impact rates. They found that, regardless of impact rate, 80% of the total load was transferred to the bone. In these cited two studies, impact energies of 132 J and 140 J were sufficient to generate loads capable of creating fractures. Our projectile generated 5 kJ, so we likely could have created fractures in manatee ribs with much less force. Taking the soft tissues into consideration, our calculations indicated that a kinetic energy of 17 kJ is required to create rib fractures in manatees. Based on the regression of Robinovitch et al., (1995), 12 kJ of the 17 kJ (70%) would be dissipated by the soft tissues, and the remaining 5 kJ (30%) transferred to the skeleton. For a typical 17’ vessel, this translates to speeds of 13–15 mph. We needed to make a few assumptions to generate this estimate.

While our weights for the vessels are accurate, the total weight would likely be greater, as we did not include items such as the battery, safety equipment, coolers, other equipment, or additional passengers. Greater vessel weights would shift the curves up, effectively lowering the vessel speed able to create fractures. More importantly, it may not be valid to use the energy–soft tissue thickness regression based on human tissues for manatees. The dermis of manatee skin is different from that of humans, and from that other marine mammals (Kipps et al., 2002), and likely has different energy-damping capabilities. Additionally, manatees have a blubber layer. Blubber is different from fat in terrestrial animals. To more accurately determine the position of the "with skin" line in Figure 3-7, the compliance of manatee skin and blubber needs to be determined, and impact testing of ribs with the associated soft tissues in place needs to be performed.

**Summary**

The goal of this study was twofold: to estimate the stress at failure and the fracture toughness of whole manatee ribs fractured in impact, and to determine if the typical watercraft is able to generate enough force to break manatee ribs upon impact. The unique construction of manatee ribs enabled us to apply fractal geometry techniques to measure some fracture mechanics parameters. Adult manatee bone behaves more like a ceramic than other types of bone. Because of this, we were able to see many of the features observed for brittle fracture in ceramics. We were able to identify crack origins, and make quantitative measurements of crack size. Failure stress was constant across body size, indicating that the amount of force needed to break ribs does not change as the animals grow, despite the increase in rib size. There was no change in the amount of kinetic energy needed to fracture whole bone with total body length, measured as the fractal dimension (D*). The whole rib toughness and measured D* independently

corroborate the finding that flaw size is the same for all animals, regardless of body size. Just as for the material properties tests of Chapter 2, we found no differences between the sexes in their ability to resist fracture. Finally, we found that the boats typically found in Florida waters can easily generate enough impact force to break manatee ribs.

Table 3-1. Mechanical and fractal data for 20 manatee ribs fractured in impact

| Animal | Sex | TL (cm) | Age | D* | c ($m^2$) | $K_C$ ($MPa \cdot m^{1/2}$) | $\sigma_M$ (MPa) | $\sigma_W$ (MPa) |
|---|---|---|---|---|---|---|---|---|
| MSTM0109 | M | 166 | C | .13 | 1.9E-03 | 2.5 | 46 | 142 |
| MNW0207 | F | 188 | S | .09 | 1.9E-03 | 2.4 | 45 | 145 |
| MSW0227 | F | 190 | S | .09 | 2.5E-03 | 2.3 | 37 | 125 |
| MSTM0113 | M | 196 | S | .17 | 1.5E-03 | 2.0 | 41 | 159 |
| MSW0057 | M | 201 | S | .14 | 1.5E-03 | 2.2 | 46 | 163 |
| MSE0205 | M | 238 | S | .22 | 1.8E-03 | 2.5 | 48 | 149 |
| MSW0160 | F | 246 | S | .17 | 1.8E-03 | 2.7 | 52 | 148 |
| MSTM0102 | F | 265 | S | .13 | 1.5E-03 | 2.5 | 51 | 159 |
| MSW0165 | F | 267 | S | .11 | 2.7E-03 | 2.5 | 45 | 120 |
| MSW0251 | M | 276 | A | .12 | 2.4E-03 | 3.0 | 50 | 128 |
| MSW0225 | F | 282 | A | .12 | 2.4E-03 | 3.0 | 49 | 127 |
| MSW0223 | F | 294 | A | .14 | 2.2E-03 | 2.7 | 46 | 133 |
| MSW0208 | F | 299 | A | .17 | 2.7E-03 | 2.8 | 43 | 120 |
| MEC0213 | F | 314 | A | .08 | 1.5E-03 | 2.7 | 61 | 176 |
| MSW0226 | M | 315 | A | .11 | 2.8E-03 | 2.7 | 41 | 118 |
| MSW0239 | M | 321 | A | .17 | 1.6E-03 | 2.5 | 56 | 175 |
| MSW0253 | M | 327 | A | .11 | 2.3E-03 | 2.7 | 46 | 130 |
| MSTM0414 | F | 335 | A | .12 | 2.0E-03 | 2.8 | 50 | 138 |
| MNW0208#6 | M | 343 | A | .20 | 2.3E-03 | 2.9 | 48 | 129 |
| MNW0208#9 | M | 343 | A | .09 | 1.5E-03 | 2.9 | 67 | 179 |
| MNW0208#10 | M | 343 | A | .13 | 3.5E-03 | 2.9 | 40 | 106 |
| MSW0245 | M | 344 | A | .15 | 2.2E-03 | 2.4 | 41 | 133 |

Variables are: sex, male (M) or female (F); total body length (TL); age classes: calf (C), subadult (S), or adult (A); fractal dimensional increment (D*); crack size (c); fracture toughness from small specimens ($K_C$); and failure stresses ($\sigma_M$ calculated with fracture toughness data from machined, small specimen tests of Chapter 2, and $\sigma_W$ calculated from estimated whole bone fracture toughness). Three ribs were tested for animal MNW0208 (rib number indicated).

Table 3-2. Mean mechanical and fractal data by sex and age class

| Group | $\sigma_M$ (MPa) | $\sigma_W$ (MPa) | D* |
|---|---|---|---|
| Sexes (ages pooled) | | | |
| Females (10) | 48 ± 6 | 139 ± 18 | .12 ± .03 |
| Males (12) | 46 ± 8 | 143 ± 23 | .15 ± .04 |
| Ages classes (sexes pooled) | | | |
| Subadults (8) | 48 ± 5 | 146 ± 16 | .14 ± .05 |
| Adults (13) | 49 ± 8 | 137 ± 24 | .13 ± .03 |

Variables are failure stress ($\sigma_M$), adjusted failure stress ($\sigma_W$), and fractal dimensional increment (D*). Values are mean ± S.D. Sample sizes are reported in parentheses for each group. No groups were significantly different ($p>0.05$).

Table 3-3. Mechanical data for strain gauged ribs

| Rib # | Peak microstrain | Modulus (GPa) | Stress (MPa) | c ($m^2$) | Toughness (MPa·$m^{1/2}$) | D* | $a_0$ (Å) |
|---|---|---|---|---|---|---|---|
| 6 | 6075 | 21 | 128 | 2.3E-03 | 7.7 | .20 | 0.7E-06 |
| 14 | 5562 | 19 | 106 | 3.5E-03 | 7.8 | .13 | 1.3E-06 |

Ribs were from animal MNW0208. Rib #6 was tested in impact, rib #14 in quasi-static 3 point bending. Young's modulus was measured with ultrasound. Failure stress was calculated as $\sigma = E\varepsilon$. Crack size, c ($m^2$), as measured from the fracture surface. Fracture toughness calculated from Equation 3-3. Constant $a_0$ was calculated from Equation 3-5.

Table 3-4. Boat data for kinetic energy calculations

| Make | Length | Weight (kg) | Tank (gal) | Fuel (kg) | HP | Engine (kg) | Boater (kg) | Total (kg) |
|---|---|---|---|---|---|---|---|---|
| Maverick[1] | 17'0" | 684 | 40 | 53 | 115 | 162 | 91 | 989 |
| Mako[2] | 17'3" | 567 | 37 | 49 | 115 | 162 | 91 | 869 |
| Key West[3] | 17'6" | 454 | 40 | 53 | 100 | 161 | 91 | 758 |

Boat weights were taken from manufacturers' specifications posted on their official websites. Fuel weight is for one half tank. Total weight is equal to the sum of weights for the vessel, fuel, engine, and one passenger.

[1]Maverick Boat Company, Inc, 2004. Model: 17' Master Angler

[2]Mako Marine International, Inc. 2005. Model: 171 Center Console

[3]Key West Boats, Inc., 2005. Model: 1760 Stealth

Table 3-5. Kinetic energy calculations for vessel configurations and impact projectile

| Manatee | Kinetic Energy (kJ) | Boat | Kinetic Energy (kJ) 2mph | 10mph | 35mph |
|---|---|---|---|---|---|
| Bare bone | 5 | Maverick | 0.40 | 10 | 121 |
| With skin | 17 | Mako | 0.35 | 9 | 106 |
| | | Key West | 0.30 | 8 | 93 |

Energy for bare bone is the kinetic energy of the projectile. With skin is the minimum amount of kinetic energy needed to create a fracture based on the calculated 70% energy absorption by manatee soft tissues.

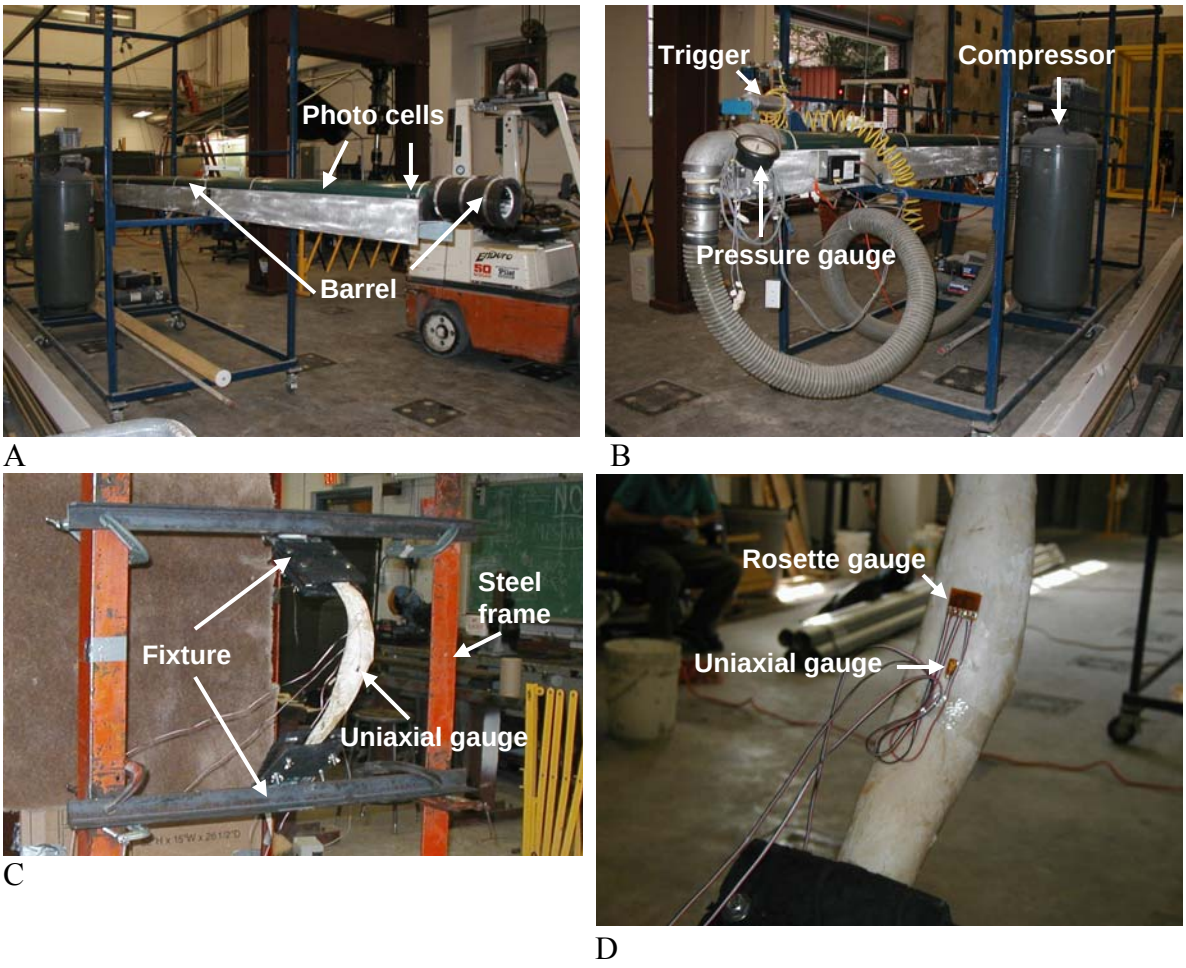


Figure 3-1. Setup for impact tests of whole manatee ribs. A) Compressed air gun assembly. The barrel is a 20' PVC pipe with a 4" diameter. The end of the barrel is equipped with 2 photocells to measure the velocity of the projectile. B) The gun is equipped with a compressor, pressure gauge, and trigger. C) Manatee rib positioned in test fixture, mounted on frame for impact testing. The rib is outfitted with a uniaxial strain gauge on the convex (lateral) surface. D) View of the concave (pleural, or medial) side. This side is outfitted with a uniaxial and a rosette strain gauge. The intended area of impact is between these two gauges.

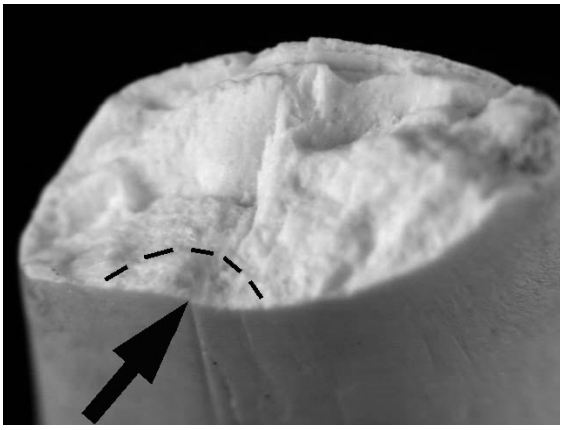

A

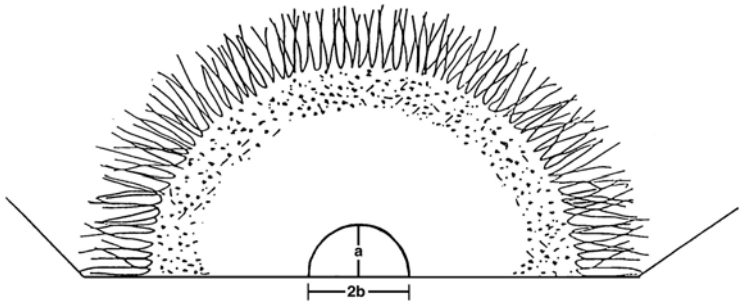


B

Figure 3-2. Fracture surface of a manatee rib fractured by collision with a boat. A) Examination of fracture surface indicated that the crack that led to failure (dashed line) originated at a groove on the medial surface (arrow). B) Schematic of fracture surface features used for fractography. Crack size (c) for a semi-elliptical surface crack is calculated by measuring crack depth, a, and half the crack width, b (i.e., ½(2b)).


Figure 3-3. Procedure for making epoxy replicas of manatee rib fracture surfaces. A) A negative impression of the fracture surface is made in dental putty and latex. B) A positive mold is made from epoxy using a PVC ring. C) The fracture surface of the positive epoxy cast is sputter coated with gold-palladium for contrast. The second layer of epoxy is then poured. D) The completed cast is ground down to the area of interest on a grinding wheel using sanding papers of increasingly fine grits. The cast is polished with an alumina slurry. E) The fracture contours, or "islands" (black arrows), are photographed at high magnification (200X). The composite photographs are used for fractal analysis.

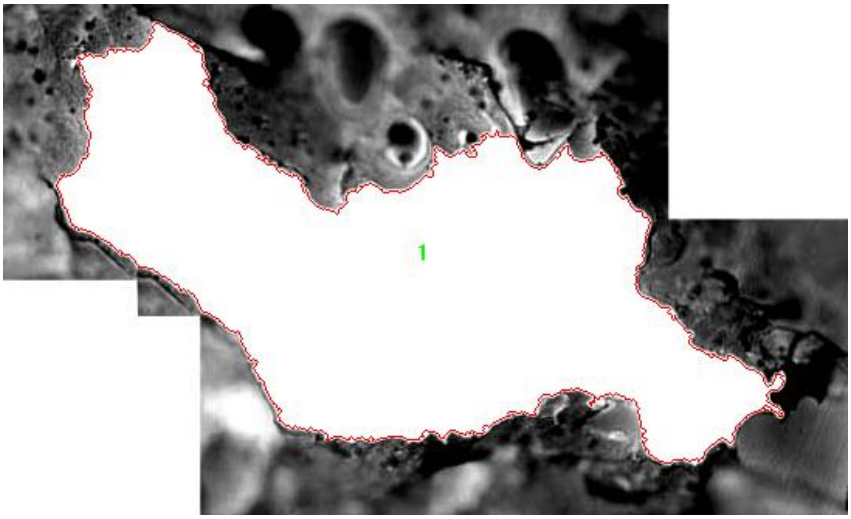


Figure 3-4. Example of a fracture surface contour used for calculation of fractal dimensional increment (D*). Image is a composite of photos taken at 200X. The computer traces the “island” contours (red line), and measures its length with different size rulers to calculate D*.

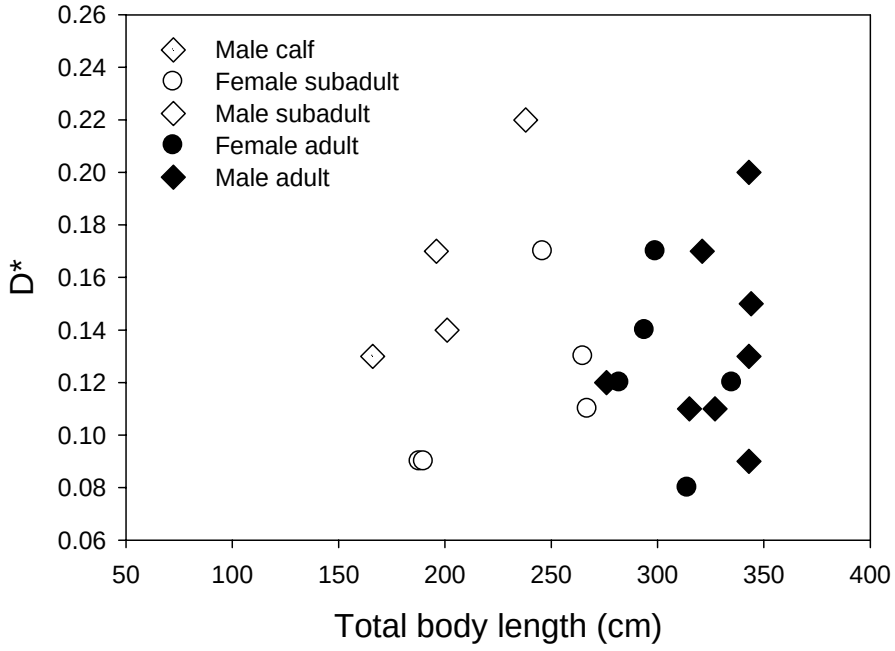


Figure 3-5. Fractal dimensional increment (D*) vs. total body length. There was no relationship between D* and animal size ($R^2 = 0.002$). Thus, the ability to resist bone fracture does not increase as animals grow. There were no significant differences between sexes or age classes.

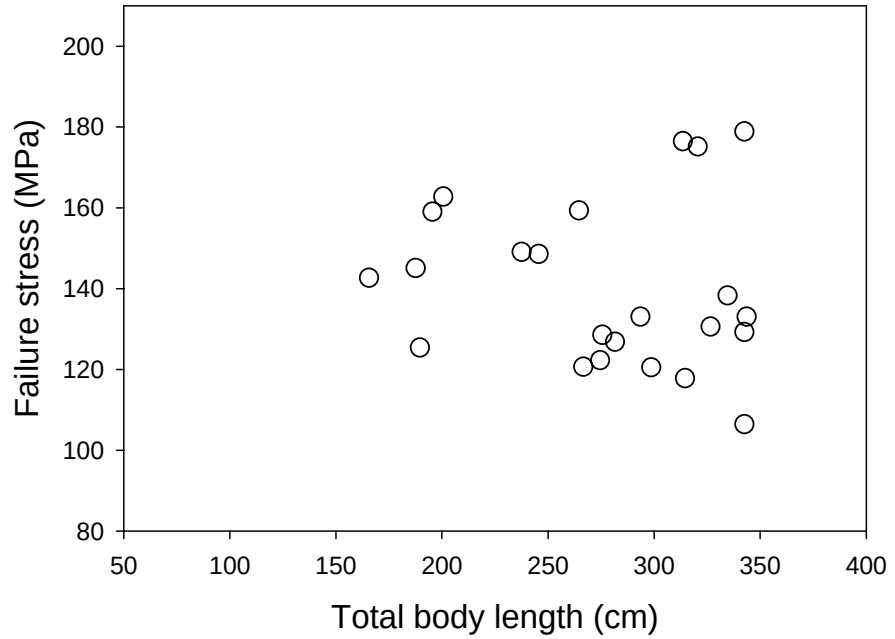


Figure 3-6. Failure stress vs. total body length. There was no relationship between adjusted failure stress ($\sigma_W$) ($R^2 = 0.012$, $p = 0.5535$).

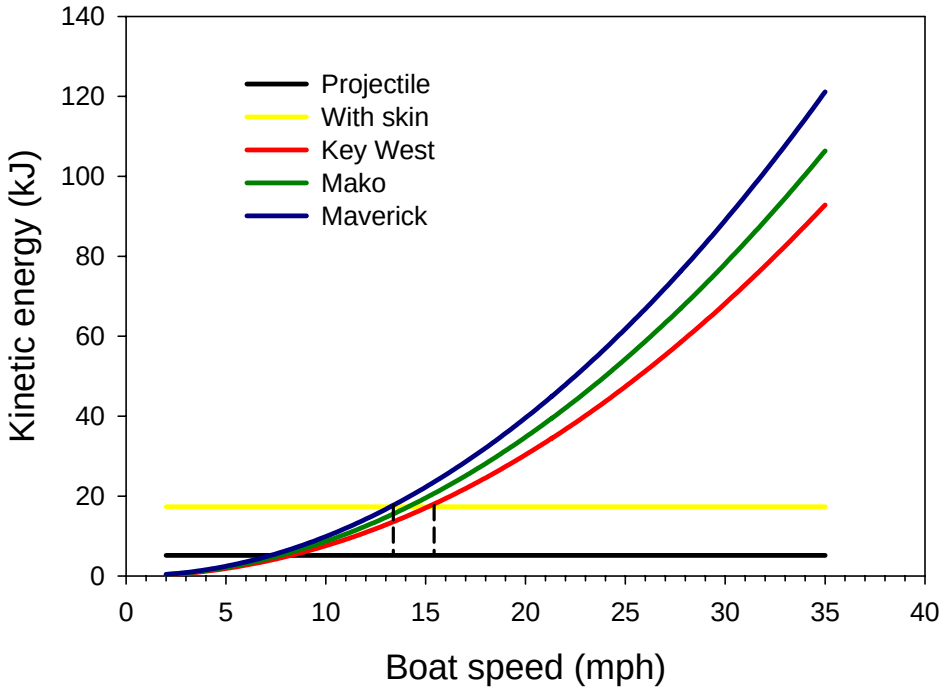


Figure 3-7. Kinetic energy as a function of boat speed. Three vessel configurations are presented. Calculated kinetic energy of the projectile is plotted, along with an energy estimate with overlying soft tissues in place. With an estimated 70% of the total kinetic energy being dissipated by the soft tissues, minimum boat speeds capable of producing rib fracture are 13–15 mph (dashed lines).

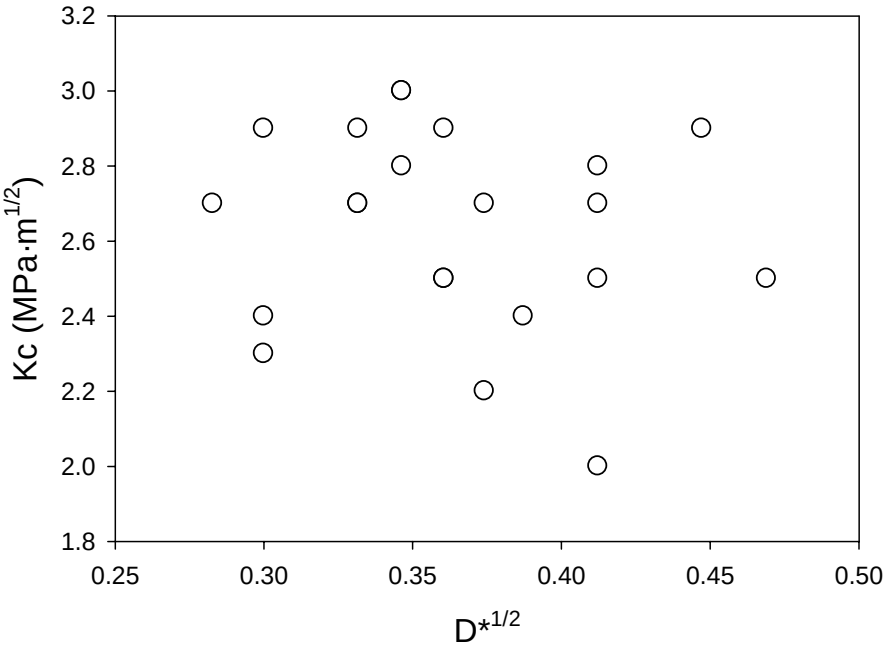


Figure 3-8. Fracture toughness ($K_C$) vs. fractal dimensional increment (D*). There was no relationship between the two variables ($R^2 = 0.0226$, $p = 0.5047$).

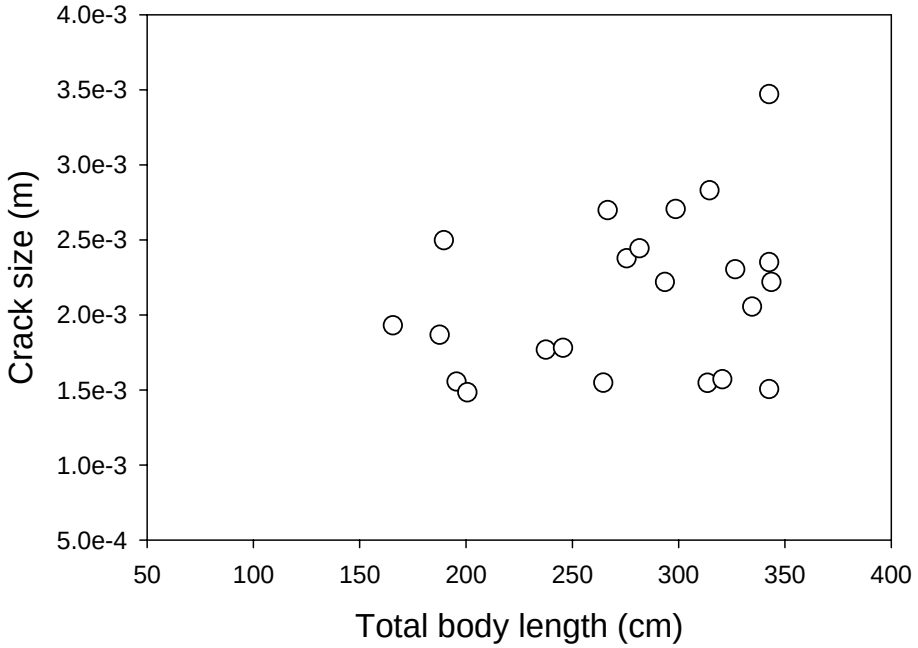


Figure 3-9. Whole rib crack size vs. total body length. There was no relationship between flaw size and total body length ($R^2 = 0.10$, $p = 0.1538$). Flaw size is the same regardless of rib cross sectional area, which increases with total body size.

# CHAPTER 4
# CONCLUSIONS AND FUTURE RESEARCH

## Summary and Conclusions

Based on the work presented here, the following conclusions can be drawn:

1. Measured as a material property, the strength of manatee bone is generally lower than that of other mammalian bone. This is likely due to three factors: its high mineral content (67–71%) and density (mean 2.17 g/cm$^3$); its microstructure; and its porosity. Strength is known to increase with increasing mineral content between 63% and 68%. When mineral content is above 68%, static strength decreases; we contend that this may be the case for manatee bone. Most other mammalian bone does not reach these large values of mineral content. We did not address microstructure and porosity in this study.
2. Manatee bone, as a material, is less tough than other mammalian bone. We calculated two measures of toughness, fracture toughness ($K_C$) and work of fracture (WOF). The first, $K_C$, is calculated from the ultimate strength and crack size. Because $K_C$ mirrored the flexural strength curve so closely, this implies that crack size varied little over the range of animals tested here. This is significant because for many ceramics, strength is usually crack size dependent. However, $K_C$ is a measure of the behavior in the elastic, or pre-yield region only. Because of this limitation, more than one measure is needed to fully characterize toughness. Work of fracture is the energy needed to propagate a crack, measured as the area under the entire stress-strain curve. Because

toughness is largely determined by the post-yield behavior, the decline in work of fracture seen in the adults may be due to age-related changes of the collagen matrix.

3. The age-related patterns in mechanical variables appear to be related to the amount of bone material present. Manatees grow quickly; appositional bone growth is by deposition of plexiform bone. In general, a scaffolding of woven bone is laid down first, then later the spaces are filled in by lamellar bone. So in young animals the bone is porous, but it becomes less so as they grow. This likely accounts for the ontogenetic patterns observed here, as an increase in bone volume results in an increase in strength.
4. There were no significant differences between the sexes for any mechanical variable. Marmontel (1993) described possible differences in bone resorption between the sexes, which we would expect to see reflected in the mechanical properties. However, we found no differences between the sexes.
5. Tests of whole ribs (i.e., structural tests) indicated that adult manatees are not able to better absorb and dissipate impact energy to prevent bone fractures than smaller animals. There was no change in the energy needed to fracture whole bone with total body length, measured as the fractal dimension (D*). Additionally, there was no relationship between the energy needed to initiate a crack ($K_C$) and D*. This last result is reasonable, since we found no significant change in mineral content or density with body size. Despite the fact that the ribs increase in cross sectional area as they grow, the tissue properties remain relatively constant. Regardless of rib size, it takes about the same amount of energy to create and propagate a crack. The whole rib

toughness and measured D* independently corroborate the finding that flaw size is the same for all animals, regardless of body size.

6. The typical watercraft found in Florida waters is able to generate enough kinetic energy to create fatal rib fractures in manatees. Vessel speeds of 13–15 mph were estimated to be sufficient to create fractures.
7. We successfully applied fractographic techniques to calculate fracture toughness for manatee rib bone. We were able to see many of the features observed for brittle fracture in ceramics.

Our study represents the first attempt to quantify the biomechanical effects of boat strikes on manatees; this information contributes significantly to our understanding of manatee-boat interactions. We think these data will be useful in shifting the focus to a more objective approach for revising boat speed regulatory zones. It is our hope that managers and policy makers will take into account the biology of the animal to devise speed zones that are adequate to minimize the chance of fatal impacts.

## Further Research

It became clear in the course of this research that a detailed histomorphometric analysis of manatee bone is needed to elucidate the relationship between manatee rib bone architecture and its material properties. In most mammalian bone, the relationship of material properties to age is largely dictated by bone mineral content. This was not the case for manatee bone, as mineral content and bone tissue density varied only slightly across the range of animals tested, from a newborn calf to a 25 year old animal. Material properties can vary widely at high mineral contents. Currey (1999) found that in bone with calcium content of 230 mg/g or higher, bending strength may be either high or low.

Other factors that contribute to material properties to a lesser degree in other mammals may have greater significance for manatees. For example, modulus (i.e., stiffness) is influenced by porosity and bone architecture as well as mineral content. Currey (1999) found that porosity and calcium content together explained 60% of the variability in modulus. However, for bone tested in bending, he found that porosity had no observable effect on strength (Currey, 1998).

Bone architecture is known to affect mechanical properties. Not only do the bone types (e.g. woven, lamellar) differ in mechanical properties, but even the orientation of fibers within lamellae will affect the mechanical competency of the whole tissue (Martin et al., 1998). Fawcett (1942b) described eccentric rings, or layers, visible to the naked eye on the lateral surface of the ribs. We too have observed these markings in our preliminary histological observations. Microscopic examination revealed that these rings mark the boundaries between layers among which the osteons are oriented obliquely. Fawcett (1942b) also described what he considered to be adult manatee bone as having a region of un-remodeled endochondral bone. This area, along with the manner in which plexiform bone is deposited, may result in a degree of porosity that persists regardless of age. It is likely that manatee bone architecture and porosity affect its mechanical behavior in a unique way; histology will bear this out.

The issue of manatee bone toughness needs to be examined further. We measured fracture toughness ($K_C$), both for the small sample specimens and the whole ribs from the impact tests. Yan (2005) also calculated fracture toughness for small sample specimens, but his samples were notched. As a result, his crack sizes were intermediate to ours. Correspondingly, his fracture toughness values of 4.1–5.5 $MPa \cdot m^{1/2}$ were intermediate to

our values for the small samples (1.4–2.9 $MPa \cdot m^{1/2}$) and the estimate for whole ribs (8 $MPa \cdot m^{1/2}$). These data indicate that fracture toughness is dependent on crack size; this is evidence for R-curve behavior in manatee bone.

Our investigation of fracture needs to be re-examined to determine the relative contributions of the pre- and post-yield regions to the total work. The factors influencing mechanical properties differ in the pre- and post-yield regions. Further analysis of our data might shed light on the relative importance of these factors for manatee bone. Yan (2005) calculated the J integral for manatee bone. The J integral is a measure of the energy used to propagate a crack; it is similar to the work of fracture. He found that, on average, 4 to 5 times more energy was consumed in the post-yield region than in the pre-yield region. This finding indicates that there are factors in addition to mineral content as having an important role in the mechanical behavior of manatee bone.

The whole bone impact tests of Chapter 3 were only the first step in modeling the effects of boat impacts on manatees. This study originally proposed measuring the compliance of the skin and soft tissues overlying the ribcage, as well as impacting large body sections to directly determine the amount of kinetic energy needed to fracture ribs. We believe that the composition of manatee skin allows a significant portion of the impact energy to be transferred to the skeleton. If we are correct, our kinetic energy threshold is an overestimate. It is likely that vessel speeds below hull speed are sufficient to create fatal bone fractures. Unfortunately, time constraints did not allow for these tests to be completed. This information is vital to accurately determining how much impact energy is transferred to the manatee, and how much of that is in turn transferred to the skeleton.

## Additional Avenues of Research

In the course of this research, three additional avenues of research possibly relevant to manatee bone have emerged: the influence of LRP5, VEGF, and cathepsin K on manatee bone. The purpose here is not to examine these topics in depth, but simply to put forth the ideas.

As mentioned in Chapter 1, the gene for LRP5, a low density lipoprotein receptor, plays a role in bone development. The LRP5 pathway is thought to play a role in mechanosensation in bone (Johnson et al., 2002). A single point mutation is known to result in high bone density in humans (Johnson et al., 2002). The mutation results in the hyperfunctioning of bone building cells, or osteoblasts. The high bone mass mutation in LRP5 is thought to produce bone that is overadapted to the loads being applied. Bone with this mutation experiences strains 40% higher than wild-type bone under the same applied load. In other words, it takes less of a load to elicit the same response in animals with this mutation. This may be the mechanism by which manatees are able to maintain high bone mass in non weight bearing bones. If this is the case with manatee bone, the exact mutation of the LRP5 gene, and the mechanism of altered function needs to be determined. In contrast, the sclerosing conditions, which also superficially resemble manatee bone, are all a result of osteoclast malfunctions. Again, it is important to determine which cell type has altered function if we are to elucidate the mechanism by which manatees are able to maintain high bone mass and density in the aquatic environment.

Nopsca (1923) speculated that pachyostosis is a neotenous condition that arose in response to submergence of air breathing animals. Sickenberg (1931) proposed a mechanism for development of pachyostosis, hypothesizing that it arose as a result of

thyroid and/or pituitary dysfunction caused by chronic oxygen deficiency as a result of entry into the aquatic environment. This idea had led to the generally accepted belief that manatees are hypothyroid, although there is no direct evidence for this. It may be possible that hypoxia can modify bone formation directly, without the influence of an altered metabolism. Vascular endothelial growth factor, or VEGF, may provide a mechanism by which this can occur. VEGF is expressed by many types of cells, including osteoblasts. VEGF production is stimulated by hypoxic conditions that arise during development, and as a result of bone fracture (Steinbrech et al., 1999; Warren et al., 2001). Maes et al. (2005) showed that overexpression of one isoform resulted in a thickened perichondrium and excessive bone formation within the diaphysis of the long bones.

Cathepsin K is a cysteine protease that plays a role in osteoclast-mediated collagen degradation (Meier et al., 2005). In mice, deficiency of Cathepsin K results in pycnodysostosis, a form of osteosclerosis, a condition which manatee bone resembles, at least superficially (Li et al., 2005a). In Cathepsin K deficient mice, femoral cortical bone area is increased by 30%, although mechanical properties such as ultimate load to failure and stiffness are not different from wild type animals (Li et al., 2005b). However, the bones were 60% more brittle as measured by post-yield deflection, and work to fracture was reduced by 40% overall. These bones had an altered matrix construction that was presumed to be the cause of the altered mechanical properties. Viewed under polarized light, the architecture resembles that observed in some preliminary histological observations of manatee bone. Cathepsin K deficiency may be responsible for the mechanical properties of manatee rib bone.

APPENDIX A
DATA TABLES

Table A-1. Mortality information for animals used in this study

| Field ID | Sex | Size (cm) | Date | County | Region | Probable cause of death |
|---|---|---|---|---|---|---|
| MEC0033 | F | 102 | 05/06/2000 | Brevard | Banana River | Perinatal |
| MSTM0109 | M | 166 | 02/04/2002 | Monroe | Lake Surprise | Watercraft |
| MSW0033 | M | 178 | 03/11/2000 | Lee | Caloosahatchee River | Undetermined, decomposed |
| MSW0164 | M | 182 | 05/18/2001 | Collier | Naples Bay | Cold stress |
| MNW0207 | F | 188 | 03/03/2002 | Pinellas | Boca Ciega Bay | Cold stress |
| MSW0227 | F | 190 | 02/20/2002 | Lee | Orange River | Cold stress |
| SWFTM0114 | M | 196 | 05/13/2001 | Brevard | Barge Canal | Watercraft |
| MSW0057 | M | 201 | 05/06/2000 | Charlotte | Gasparilla Sound | Watercraft |
| MSW0134 | F | 205 | 02/12/2001 | Collier | Faka Union Canal | Cold stress |
| MSE0205 | M | 238 | 01/26/2002 | Palm Beach | Loxahatchee River | Watercraft |
| MSW0160 | F | 246 | 05/14/2001 | Collier | North Rookery Bay Channel | Watercraft |
| MSTM0102 | F | 265 | 02/12/2001 | Collier | Halfway Creek | Watercraft |
| MSW0165 | F | 267 | 05/19/2001 | DeSoto | Peace River | Human, other |
| MEC0220 | M | 275 | 03/17/2002 | Indian River | Indian River | Watercraft |
| MSW0251 | M | 276 | 03/24/2002 | Sarasota | Forked Creek | Natural |
| MSW0225 | F | 282 | 02/18/2002 | Lee | Ten Mile Canal | Natural |
| MSW0223 | F | 294 | 02/10/2002 | Lee | Pine Island Sound | Watercraft |
| MSW0208 | F | 299 | 01/15/2002 | Lee | Orange River | Natural |
| MEC0213 | F | 314 | 02/03/2002 | Indian River | Indian River | Watercraft |
| MSW0226 | M | 315 | 02/20/2002 | Lee | Caloosahatchee River | Watercraft |
| MSW0239 | M | 321 | 03/15/2002 | Charlotte | Stump Pass | Natural |
| MSW0331 | F | 326 | 02/27/2003 | Collier | Faka Union Canal | Natural |
| MSW0253 | M | 327 | 03/25/2002 | Sarasota | Lemon Bay | Natural |
| SWFTM0414b | F | 335 | 05/26/2004 | St. Johns | Matanzas River | Natural |
| MNW0208 | M | 343 | 03/10/2002 | Citrus | Kings Bay | Natural |
| MSW0245 | M | 344 | 03/22/2002 | Sarasota | Blackburn Bay | Natural |

Source: Florida Fish and Wildlife Institute, 2005.

Table A-2. Means for four mechanical properties by body region

| Animal | Site | Mechanical variable | Rib position | | |
|---|---|---|---|---|---|
| | | | Cranial | Central | Caudal |
| MEC0033 | Proximal | S (MPa) | — | 87 (n/a, 1) | 59 (n/a, 1) |
| | | E (GPa) | | 4.8 (n/a, 1) | 3.1 (n/a, 1) |
| | | W ($MJ \cdot m^{-3}$) | | 4.0 (n/a, 1) | 2.2 (n/a, 1) |
| | | $K_C$ ($MPa \cdot m^{1/2}$) | | 1.6 (n/a, 1) | 1.2 (n/a, 1) |
| | Middle | S | 66 (n/a, 1) | 66 (n/a, 1) | 32 (n/a, 1) |
| | | E | 3.6 (n/a, 1) | 3.1 (n/a, 1) | 1.1 (n/a, 1) |
| | | W | 2.3 (n/a, 1) | 4.0 (n/a, 1) | 1.3 (n/a, 1) |
| | | $K_C$ | 1.3 (n/a, 1) | 1.4 (n/a, 1) | 0.9 (n/a, 1) |
| MSTM0109 | Proximal | S | 130 (19, 8) | 138 (15, 12) | 132 (13, 10) |
| | | E | 12.6 (1.7, 8) | 12.9 (0.7, 12) | 12.9 (0.7, 10) |
| | | W | 3.2 (0.7, 8) | 4.5 (1.4, 12) | 3.6 (0.7, 10) |
| | | $K_C$ | 2.2 (0.3, 8) | 2.5 (0.2, 10) | 2.3 (0.2, 10) |
| | Middle | S | — | — | — |
| | | E | | | |
| | | W | | | |
| | | $K_C$ | | | |
| MSW0164 | Proximal | S | 96 (18, 9) | 111 (13, 11) | 106 (17, 5) |
| | | E | 8.6 (0.9, 9) | 9.8 (1.1, 11) | 9.7 (1.4, 5) |
| | | W | 3.2 (1.0, 9) | 4.2 (1.0, 11) | 4.9 (1.5, 5) |
| | | $K_C$ | 2.1 (0.2, 9) | 2.3 (0.2, 10) | 2.1 (0.2, 5) |
| | Middle | S | — | — | — |
| | | E | | | |
| | | W | | | |
| | | $K_C$ | | | |
| MSW0033 | Proximal | S | — | 132 (15, 12) | 153 (24, 9) |
| | | E | | 11.9 (1.3, 12) | 12.6 (1.0, 9) |
| | | W | | 5.3 (1.3, 12) | 8.0 (3.4, 9) |
| | | $K_C$ | | 2.1 (0.2, 12) | 2.3 (0.4, 8) |
| | Middle | S | 125 (9, 10) | — | — |
| | | E | 11.7 (0.7, 10) | | |
| | | W | 4.9 (1.3, 10) | | |
| | | $K_C$ | 1.9 (0.3, 9) | | |

Strength, S; Young's modulus, E; work of fracture, W; and fracture toughness, $K_C$. Standard deviation and sample size are reported for each value in parentheses, respectively. — indicates no samples from that body region.

Table A-2. Continued

| Animal | Site | Mechanical variable | Rib position | | |
|---|---|---|---|---|---|
| | | | Cranial | Central | Caudal |
| MNW0207 | Proximal | S (MPa) | 133 (13, 9) | 123 (33, 4) | 139 (17, 3) |
| | | E (GPa) | 12.3 (0.8, 9) | 11.5 (1.0, 4) | 12.9 (0.5, 3) |
| | | W ($MJ \cdot m^{-3}$) | 4.9 (0.9, 9) | 4.7 (2.9, 4) | 6.1 (1.0, 3) |
| | | $K_C$ ($MPa \cdot m^{1/2}$) | 2.4 (0.3, 9) | 2.3 (0.5,4) | 2.3 (0.1, 2) |
| | Middle | S | — | 128 (12, 12) | 118 (11, 9) |
| | | E | | 11.5 (1.1, 12) | 10.5 (1.0, 9) |
| | | W | | 4.8 (1.0, 12) | 3.9 (0.7, 9) |
| | | $K_C$ | | 2.5 (0.2, 10) | 2.3 (0.2, 9) |
| MSW0227 | Proximal | S | 116 (24, 9) | 145 (16, 12) | 145 (21, 5) |
| | | E | 12.1 (1.7, 9) | 14.0 (1.4, 12) | 13.2 (0.6, 5) |
| | | W | 2.9 (1.3, 9) | 5.1 (1.7, 12) | 8.3 (2.2, 5) |
| | | $K_C$ | 2.3 (0.2, 9) | 2.6 (0.2, 10) | 2.6 (0.3, 5) |
| | Middle | S | — | 111 (25, 12) | 112 (7, 10) |
| | | E | | 11.1 (2.7, 12) | 11.4 (0.7, 10) |
| | | W | | 3.2 (1.1, 12) | 3.1 (0.5, 10) |
| | | $K_C$ | | 2.4 (0.4, 10) | 2.3 (0.2, 10) |
| SWFTM0114 | Proximal | S | 120 (24, 13) | 140 (18, 19) | 125 (14, 11) |
| | | E | 11.9 (1.9, 13) | 12.7 (1.7, 19) | 11.6 (1.2, 11) |
| | | W | 3.3 (1.3, 13) | 5.7 (1.8, 19) | 4.6 (1.1, 11) |
| | | $K_C$ | 2.2 (0.3, 10) | 2.5 (0.3, 19) | 2.4 (0.3, 10) |
| | Middle | S | — | 106 (10, 23) | — |
| | | E | | 9.4 (1.0, 23) | |
| | | W | | 4.5 (1.0, 23) | |
| | | $K_C$ | | 2.1 (0.3, 14) | |
| MSW0057 | Proximal | S | 155 (27, 9) | 162 (16, 6) | 117 (4, 2) |
| | | E | 9.8 (1.8, 9) | 10.0 (1.4, 6) | 7.9 (0.1, 2) |
| | | W | 4.4 (1.0, 9) | 7.1 (1.5, 6) | 4.0 (2.4, 2) |
| | | $K_C$ | 2.9 (0.3, 5) | 2.9 (0.2, 3) | 2.3 (0.0, 1) |
| | Middle | S | 154 (30, 10) | 149 (12, 6) | 151 (10, 3) |
| | | E | 9.6 (1.7, 10) | 9.7 (1.0, 6) | 9.1 (1.2, 3) |
| | | W | 5.7 (1.7, 10) | 5.4 (1.1, 6) | 5.9 (1.9, 3) |
| | | $K_C$ | 2.8 (0.5, 5) | 2.4 (0.3, 4) | 2.3 (0.2, 3) |

Table A-2. Continued

| Animal | Site | Mechanical variable | Rib position | | |
|---|---|---|---|---|---|
| | | | Cranial | Central | Caudal |
| MSW0134 | Proximal | S (MPa) | 125 (22, 14) | 141 (24, 12) | 145 (18, 6) |
| | | E (GPa) | 12.0 (1.7,14) | 12.5 (0.9, 12) | 12.2 (0.5, 6) |
| | | W ($MJ \cdot m^{-3}$) | 4.5 (1.9, 14) | 5.6 (2.1, 12) | 6.9 (2.9, 6) |
| | | $K_C$ ($MPa \cdot m^{1/2}$) | 2.1 (0.5, 14) | 2.1 (0.3, 11) | 2.4 (0.4, 4) |
| | Middle | S | — | — | 125 (14, 26) |
| | | E | | | 10.6 (0.9, 26) |
| | | W | | | 5.7 (1.8, 26) |
| | | $K_C$ | | | 2.0 (0.3, 25) |
| MSE0205 | Proximal | S | 151 (19, 14) | 148 (18, 19) | 140 (13, 18) |
| | | E | 14.9 (0.8, 14) | 13.5 (1.0, 19) | 12.7 (0.6, 18) |
| | | W | 4.5 (1.2, 14) | 5.2 (1.5, 19) | 5.3 (1.9, 18) |
| | | $K_C$ | 2.9 (0.2, 10) | 2.8 (0.2, 10) | 2.6 (0.2, 10) |
| | Middle | S | 123 (27, 14) | 122 (12, 26) | 131 (11, 23) |
| | | E | 12.2 (2.1, 14) | 11.2 (0.9, 26) | 12.0 (0.8, 23) |
| | | W | 3.5 (1.3, 14) | 3.8 (1.2, 26) | 4.3 (1.3, 23) |
| | | $K_C$ | 2.4 (0.2, 10) | 2.5 (0.3, 13) | 2.5 (0.2, 10) |
| MSW0160 | Proximal | S | 179 (20, 19) | 167 (13, 23) | 142 (20, 19) |
| | | E | 16.5 (1.2, 19) | 15.7 (1.0, 23) | 14.0 (1.0, 19) |
| | | W | 5.7 (1.5, 19) | 5.6 (2.2, 23) | 4.4 (2.5, 19) |
| | | $K_C$ | 3.0 (0.3, 10) | 2.9 (0.2, 10) | 2.6 (0.2, 10) |
| | Middle | S | 160 (14, 34) | 153 (13, 36) | — |
| | | E | 15.1 (1.0, 34) | 13.8 (1.1, 36) | |
| | | W | 5.3 (2.1, 34) | 6.4 (2.2, 36) | |
| | | $K_C$ | 2.8 (0.3, 10) | 2.7 (0.2, 10) | |
| MSTM0102 | Proximal | S | 155 (20, 32) | 164 (15, 24) | 161 (16, 15) |
| | | E | 15.5 (2.0, 32) | 15.8 (1.2, 24) | 16.2 (1.2, 15) |
| | | W | 4.2 (1.0, 32) | 5.3 (1.4, 24) | 5.2 (1.3, 15) |
| | | $K_C$ | 2.4 (0.5, 31) | 2.5 (0.3, 24) | 2.7 (0.4, 14) |
| | Middle | S | 155 (22, 32) | 153 (22, 28) | 155 (16, 38) |
| | | E | 15.1 (1.5, 32) | 14.8 (1.0, 28) | 15.3 (1.3, 38) |
| | | W | 4.2 (1.5, 32) | 3.7 (0.8, 28) | 4.0 (0.7, 38) |
| | | $K_C$ | 2.8 (0.3, 26) | 2.6 (0.2, 23) | 2.6 (0.3, 37) |

Table A-2. Continued

| Animal | Site | Mechanical variable | Rib position | | |
|---|---|---|---|---|---|
| | | | Cranial | Central | Caudal |
| MSW0165 | Proximal | S (MPa) | 125 (38, 21) | 156 (23, 32) | 163 (20, 20) |
| | | E (GPa) | 12.6 (3.3, 21) | 15.7 (1.9, 32) | 16.0 (1.7, 20) |
| | | W ($MJ \cdot m^{-3}$) | 3.4 (1.3, 21) | 4.5 (1.8, 32) | 5.2 (1.8, 20) |
| | | $K_C$ ($MPa \cdot m^{1/2}$) | 2.7 (0.2, 10) | 2.7 (0.4, 10) | 2.7 (0.3, 9) |
| | Middle | S | 160 (26, 31) | 164 (13, 27) | 137 (21, 26) |
| | | E | 14.9 (2.4, 31) | 14.7 (1.0, 27) | 13.0 (2.4, 26) |
| | | W | 4.5 (1.2, 31) | 5.4 (0.8, 27) | 4.5 (1.1, 26) |
| | | $K_C$ | 2.9 (0.3, 10) | 2.9 (0.2, 10) | 2.5 (0.6, 10) |
| MEC0220 | Proximal | S | 132 (52, 20) | 148 (15, 23) | 153 (24, 22) |
| | | E | 13.3 (4.9, 20) | 14.4 (1.2, 23) | 15.0 (2.0, 22) |
| | | W | 3.2 (1.5, 20) | 3.9 (1.1, 23) | 4.4 (1.6, 22) |
| | | $K_C$ | 2.6 (0.3, 10) | 2.7 (0.2, 10) | 2.6 (0.3, 10) |
| | Middle | S | 137 (37, 22) | 142 (13, 28) | 134 (14, 28) |
| | | E | 14.5 (3.4, 22) | 14.4 (0.9, 28) | 13.5 (0.9, 28) |
| | | W | 3.2 (1.2, 22) | 3.3 (0.7, 28) | 3.1 (0.9, 28) |
| | | $K_C$ | 2.8 (0.3, 10) | 2.5 (0.3, 10) | 2.4 (0.2, 9) |
| MSW0251 | Proximal | S | 145 (25, 24) | 158 (26, 21) | 157 (21, 12) |
| | | E | 17.0 (1.5, 24) | 17.1 (1.8, 21) | 16.8 (1.5, 12) |
| | | W | 2.7 (0.7, 24) | 4.0 (1.2, 21) | 3.7 (0.8, 12) |
| | | $K_C$ | 2.5 (0.3, 10) | 2.8 (0.4, 10) | 2.8 (0.4, 10) |
| | Middle | S | 162 (22, 28) | 177 (21, 30) | 153 (17, 27) |
| | | E | 18.0 (1.1, 28) | 19.0 (1.3, 30) | 17.1 (1.0, 27) |
| | | W | 3.7 (1.2, 28) | 4.0 (1.2, 30) | 3.4 (1.2, 27) |
| | | $K_C$ | 2.8 (0.3, 28) | 3.1 (0.3, 30) | 2.7 (0.4, 26) |
| MSW0225 | Proximal | S | 142 (23, 16) | 157 (19, 32) | 147 (32, 24) |
| | | E | 15.9 (1.9, 16) | 16.5 (1.4, 32) | 15.9 (1.2, 24) |
| | | W | 3.0 (0.9, 16) | 4.0 (1.3, 32) | 3.9 (1.0, 24) |
| | | $K_C$ | 2.5 (0.3, 10) | 2.7 (0.3, 10) | 2.6 (0.3, 10) |
| | Middle | S | 142 (17, 26) | 158 (18, 32) | 149 (13, 30) |
| | | E | 15.6 (1.3, 26) | 16.2 (2.0, 32) | 15.8 (1.0, 30) |
| | | W | 3.4 (0.8, 26) | 4.3 (0.9, 32) | 3.8 (0.7, 30) |
| | | $K_C$ | 2.5 (0.3, 26) | 3.0 (0.3, 30) | 2.8 (0.3, 28) |

Table A-2. Continued

| Animal | Site | Mechanical variable | Rib position | | |
|---|---|---|---|---|---|
| | | | Cranial | Central | Caudal |
| MSW0223 | Proximal | S (MPa) | 152 (18, 25) | 157 (23, 32) | 156 (17, 32) |
| | | E (GPa) | 15.6 (1.2, 25) | 16.0 (1.4, 32) | 15.3 (1.3, 32) |
| | | W ($MJ \cdot m^{-3}$) | 3.8 (0.6, 25) | 4.1 (1.2, 32) | 4.3 (1.0, 32) |
| | | $K_C$ ($MPa \cdot m^{1/2}$) | 2.7 (0.3, 10) | 2.8 (0.3, 10) | 3.0 (0.4, 10) |
| | Middle | S | 150 (16, 30) | 151 (13, 33) | 150 (12, 32) |
| | | E | 15.7 (0.9, 30) | 15.2 (1.1, 33) | 15.3 (0.6, 32) |
| | | W | 3.7 (1.2, 30) | 3.9 (0.8, 33) | 4.2 (1.1, 32) |
| | | $K_C$ | 2.7 (0.2, 10) | 2.8 (0.2, 10) | 2.7 (0.2, 10) |
| MSW0208 | Proximal | S | 140 (24, 26) | 156 (16, 28) | 160 (16, 21) |
| | | E | 15.0 (2.1, 26) | 16.4 (1.2, 28) | 16.8 (1.2, 21) |
| | | W | 3.5 (1.0, 26) | 4.3 (0.9, 28) | 5.0 (1.2, 21) |
| | | $K_C$ | 2.6 (0.3, 10) | 2.9 (0.2, 10) | 2.8 (0.2, 10) |
| | Middle | S | 152 (15, 32) | 156 (17, 32) | 156 (20, 36) |
| | | E | 16.1 (1.3, 32) | 15.7 (1.1, 32) | 16.2 (1.5, 36) |
| | | W | 3.9 (0.7, 32) | 4.2 (1.3, 32) | 4.3 (1.4, 36) |
| | | $K_C$ | 2.8 (0.2, 10) | 2.8 (0.2, 10) | 2.7 (0.2, 10) |
| MEC0213 | Proximal | S | 124 (18, 26) | 142 (21, 17) | 149 (25, 18) |
| | | E | 14.8 (1.4, 26) | 15.4 (1.6, 17) | 15.7 (1.6, 18) |
| | | W | 2.1 (0.7, 26) | 3.5 (0.7, 17) | 3.7 (1.3, 18) |
| | | $K_C$ | 2.4 (0.2, 10) | 2.6 (0.2, 10) | 2.8 (0.3, 10) |
| | Middle | S | 136 (16, 22) | 154 (19, 33) | 151 (17, 27) |
| | | E | 15.1 (1.4, 22) | 16.1 (1.2, 33) | 15.8 (1.1, 27) |
| | | W | 2.7 (0.5, 22) | 3.2 (0.6, 33) | 4.0 (1.2, 27) |
| | | $K_C$ | 2.6 (0.2, 10) | 2.7 (0.4, 10) | 2.8 (0.3, 10) |
| MSW0226 | Proximal | S | 129 (28, 20) | 159 (22, 26) | 164 (22, 24) |
| | | E | 15.9 (1.7, 20) | 17.3 (1.6, 26) | 17.4 (1.3, 24) |
| | | W | 2.3 (0.6, 20) | 3.6 (1.0, 26) | 4.1 (1.4, 24) |
| | | $K_C$ | 2.5 (0.3, 10) | 2.8 (0.2, 10) | 2.8 (0.2, 10) |
| | Middle | S | 139 (19, 25) | 154 (14, 32) | 154 (16, 29) |
| | | E | 15.5 (1.7, 25) | 16.8 (0.9, 32) | 16.3 (1.4, 29) |
| | | W | 2.5 (0.6, 25) | 3.1 (0.6, 32) | 3.2 (0.6, 29) |
| | | $K_C$ | 2.5 (0.2, 10) | 2.7 (0.3, 10) | 2.8 (0.2, 10) |

Table A-2. Continued

| Animal | Site | Mechanical variable | Rib position | | |
|---|---|---|---|---|---|
| | | | Cranial | Central | Caudal |
| MSW0239 | Proximal | S (MPa) | 136 (24, 30) | 149 (21, 31) | 165 (16, 28) |
| | | E (GPa) | 15.6 (1.9, 30) | 16.8 (1.3, 31) | 17.1 (1.1, 28) |
| | | W ($MJ \cdot m^{-3}$) | 2.7 (0.8, 30) | 3.7 (1.1, 31) | 5.2 (1.7, 28) |
| | | $K_C$ ($MPa \cdot m^{1/2}$) | 2.6 (0.2, 10) | 2.9 (0.3, 10) | 3.0 (0.1, 10) |
| | Middle | S | 154 (20, 28) | 143 (24, 32) | 153 (18, 32) |
| | | E | 16.5 (1.8, 28) | 15.9 (1.6, 32) | 16.4 (1.2, 32) |
| | | W | 3.6 (0.9, 28) | 3.3 (1.0, 32) | 3.7 (0.8, 32) |
| | | $K_C$ | 2.8 (0.3, 10) | 2.5 (0.5, 10) | 2.9 (0.3, 10) |
| MSW0331 | Proximal | S | 153 (20, 27) | 148 (25, 27) | 151 (22, 25) |
| | | E | 17.4 (2.2, 27) | 17.3 (1.7, 27) | 17.4 (1.2, 25) |
| | | W | 2.7 (0.7, 27) | 3.0 (0.9, 27) | 3.4 (1.2, 25) |
| | | $K_C$ | 2.8 (0.4, 9) | 2.6 (0.4, 10) | 2.7 (0.3, 10) |
| | Middle | S | 148 (19, 30) | 154 (17, 32) | 151 (21, 30) |
| | | E | 16.7 (1.5, 30) | 17.1 (0.8, 32) | 17.3 (2.4, 30) |
| | | W | 3.1 (0.7, 30) | 3.4 (1.0, 32) | 3.4 (1.0, 30) |
| | | $K_C$ | 2.6 (0.3, 29) | 2.5 (0.3, 30) | 2.5 (0.4, 29) |
| MSW0253 | Proximal | S | 145 (29, 31) | 156 (22, 32) | 152 (19, 24) |
| | | E | 16.1 (1.8, 31) | 16.5 (1.5, 32) | 15.4 (1.6, 24) |
| | | W | 3.3 (1.2, 31) | 4.0 (1.2, 32) | 4.2 (1.6, 24) |
| | | $K_C$ | 2.6 (0.5, 10) | 2.8 (0.3, 10) | 2.7 (0.2, 10) |
| | Middle | S | 155 (21, 33) | 152 (18, 36) | 137 (22, 32) |
| | | E | 15.9 (1.7, 33) | 15.6 (1.9, 36) | 14.7 (1.3, 32) |
| | | W | 4.3 (1.2, 33) | 3.9 (1.0, 36) | 3.3 (0.9, 32) |
| | | $K_C$ | 2.8 (0.4, 29) | 2.7 (0.3, 31) | 2.3 (0.4, 29) |
| SWFTM0414 | Proximal | S | 151 (18, 33) | 171 (18, 32) | 165 (19, 32) |
| | | E | 17.3 (1.0, 33) | 18.6 (1.4, 32) | 18.0 (0.5, 32) |
| | | W | 2.9 (1.0, 33) | 3.9 (0.9, 32) | 4.4 (1.5, 32) |
| | | $K_C$ | 2.8 (0.3, 10) | 3.2 (0.2, 10) | 3.0 (0.3, 10) |
| | Middle | S | 150 (22, 32) | 156 (18, 28) | 152 (17, 32) |
| | | E | 16.6 (1.6, 32) | 17.2 (0.7, 28) | 17.0 (1.1, 32) |
| | | W | 3.6 (1.4, 32) | 3.4 (0.9, 28) | 3.6 (0.9, 32) |
| | | $K_C$ | 2.7 (0.3, 10) | 2.9 (0.2, 10) | 2.9 (0.3, 10) |

Table A-2. Continued

| Animal | Site | Mechanical variable | Rib position | | |
|---|---|---|---|---|---|
| | | | Cranial | Central | Caudal |
| MNW0208 | Proximal | S (MPa) | 153 (16, 31) | 159 (24, 27) | 173 (17, 24) |
| | | E (GPa) | 18.6 (1.3, 31) | 18.1 (1.6, 27) | 19.0 (1.3, 24) |
| | | W ($MJ \cdot m^{-3}$) | 2.4 (0.6, 31) | 2.9 (0.8, 27) | 3.5 (0.8, 24) |
| | | $K_C$ ($MPa \cdot m^{1/2}$) | 2.9 (0.3, 10) | 2.9 (0.3, 10) | 3.1 (0.2, 10) |
| | Middle | S | 157 (21, 33) | 162 (19, 27) | 154 (20, 30) |
| | | E | 17.8 (1.7, 33) | 17.7 (1.1, 27) | 17.5 (1.0, 30) |
| | | W | 3.0 (0.9, 33) | 3.1 (0.8, 27) | 2.9 (0.7, 30) |
| | | $K_C$ | 2.8 (0.3, 10) | 2.9 (0.2, 10) | 2.9 (0.3, 10) |
| MSW0245 | Proximal | S | 89 (28, 31) | 154 (19, 32) | 149 (21, 35) |
| | | E | 9.3 (3.3, 31) | 16.8 (1.1, 32) | 16.2 (2.0, 35) |
| | | W | 2.0 (0.9, 31) | 3.2 (0.9, 32) | 3.4 (1.1, 35) |
| | | $K_C$ | 1.9 (0.3, 15) | 2.5 (0.4, 15) | 2.5 (0.3, 8) |
| | Middle | S | 141 (20, 52) | 150 (18, 87) | 149 (17, 70) |
| | | E | 15.9 (1.8, 52) | 16.6 (1.4, 87) | 16.2 (1.5, 70) |
| | | W | 3.2 (0.6, 52) | 3.2 (0.7, 87) | 3.3 (0.8, 70) |
| | | $K_C$ | 2.4 (0.3, 25) | 2.4 (0.3, 22) | 2.3 (0.3, 8) |

Table A-3. Critical crack measurements for whole manatee ribs fractured in impact

| Animal | $K_C$ | A | b | c | $\sqrt{c}$ | Y | σ |
|---|---|---|---|---|---|---|---|
| SWFTM0109 | 2.5 | 0.00190 | 0.00195 | 0.001925 | 0.043873 | 1.24 | 46 |
| MNW0207 | 2.4 | 0.00210 | 0.00165 | 0.001861 | 0.043145 | 1.24 | 45 |
| MSW0227 | 2.3 | 0.00230 | 0.00270 | 0.002492 | 0.049920 | 1.24 | 37 |
| SWFTM0113 | 2.0 | 0.00160 | 0.00150 | 0.001549 | 0.039360 | 1.24 | 41 |
| MSW0057 | 2.2 | 0.00190 | 0.00115 | 0.001478 | 0.038447 | 1.24 | 46 |
| MSE0205 | 2.5 | 0.00230 | 0.00135 | 0.001762 | 0.041977 | 1.24 | 48 |
| MSW0160 | 2.7 | 0.00210 | 0.00150 | 0.001775 | 0.042129 | 1.24 | 52 |
| SWFTM0102 | 2.5 | 0.00170 | 0.00140 | 0.001543 | 0.039278 | 1.24 | 51 |
| MSW0165 | 2.9 | 0.00290 | 0.00250 | 0.002693 | 0.051890 | 1.24 | 45 |
| MEC0220 | 2.4 | 0.00250 | 0.00275 | 0.002622 | 0.051206 | 1.24 | 38 |
| MSW0251 | 3.0 | 0.00250 | 0.00225 | 0.002372 | 0.048700 | 1.24 | 50 |
| MSW0225 | 3.0 | 0.00270 | 0.00220 | 0.002437 | 0.049368 | 1.24 | 49 |
| MSW0223 | 2.7 | 0.00280 | 0.00175 | 0.002214 | 0.047049 | 1.24 | 46 |
| MSW0208 | 2.8 | 0.00270 | 0.00270 | 0.002700 | 0.051962 | 1.24 | 43 |
| MEC0213 | 2.7 | 0.00125 | 0.00190 | 0.001541 | 0.039257 | 1.12 | 61 |
| MSW0226 | 2.7 | 0.00280 | 0.00285 | 0.002825 | 0.053150 | 1.24 | 41 |
| MSW0239 | 2.5 | 0.00140 | 0.00175 | 0.001565 | 0.039563 | 1.12 | 56 |
| MSW0253 | 2.7 | 0.00220 | 0.00240 | 0.002298 | 0.047936 | 1.24 | 45 |
| SWFTM0414 | 2.8 | 0.00140 | 0.00300 | 0.002049 | 0.045270 | 1.24 | 50 |
| MNW0208 #6 | 2.9 | 0.00220 | 0.00250 | 0.002345 | 0.048427 | 1.24 | 48 |
| MNW0208 #9 | 2.9 | 0.00150 | 0.00150 | 0.001500 | 0.038730 | 1.12 | 67 |
| MNW0208 #10 | 2.9 | 0.00400 | 0.00300 | 0.003464 | 0.058857 | 1.24 | 40 |
| MNW0208 #14 | 2.9 | 0.00350 | 0.00350 | 0.003500 | 0.059161 | 1.24 | 40 |
| MSW0245 | 2.4 | 0.00280 | 0.00175 | 0.002214 | 0.047049 | 1.24 | 41 |

a and b are crack depth and half-width (m). Crack size was calculated as $c = (a \cdot b)^{1/2}$. Y is a geometric factor based on crack shape. σ is flexural strength (MPa).

# APPENDIX B
# DERIVATION OF WORK OF FRACTURE

We define the work of fracture (WOF) as the area under the stress-strain curve

$$WOF = \int_0^{\varepsilon_u} \sigma d\varepsilon \tag{B-1}$$

where $\varepsilon_u$ is the ultimate strain, $\sigma$ is stress (MPa). Work of fracture can be calculated from the area under the load displacement curve with the appropriate stress and strain relations applied to the type of loading. For specimens tested in tension, it is calculated as

$$WOF = \frac{W}{2A} \tag{B-2}$$

where W is the area under the load-displacement curve (N m) and A is the apparent area ($m^2$) of the fracture surface. This equation is often inappropriately used to calculate work of fracture for specimens tested in flexure. To correctly calculate work of fracture, the load-displacement curve must be converted to the stress-strain curve for flexure. Stress in 3 point flexure is calculated as

$$\sigma = \frac{3FL}{2BD^2} \tag{B-3}$$

where F is the peak load (Newtons) at failure, l is the distance (m) between the lower supports of the bending fixture, B is the specimen width (m), and D is the specimen depth (m). Strain is calculated as

$$\varepsilon = \frac{\Delta L}{L} = \frac{\delta}{L} \tag{B-4}$$

where $\delta$ is the displacement (m).

If we substitute Equations B-3 and B-4 into Equation B-1 we get

$$\mathrm{WOF} = \int_0^{\varepsilon_u} \frac{3\mathrm{FL}}{2\mathrm{BD}^2} \frac{\mathrm{d}\delta}{\mathrm{L}}, \tag{B-5}$$

which is equivalent to

$$\mathrm{WOF} = \frac{3\mathrm{W}}{2\mathrm{BD}^2} \tag{B-6}$$

where W is the area under the load-displacement curve (N m).

LIST OF REFERENCES

Ackerman, B.B., S.D. Wright, R.K. Bonde, D.K. Odell, and D.J. Banowetz. 1995. Trends and patterns in mortality of manatees in Florida, 1974-1992. Pages 223-258 *in* T.J. O'Shea. B.B. Ackerman, and H.F. Percival, editors. Population biology of the Florida manatee. National Biological Service Information and Technology Report 1. Springfield, VA: National Technical Information Service. 289 p.

Aksel, C., and P.D. Warren. 2003. Work of fracture and fracture surface energy of magnesia-spinel composites. Composites Science and Technology 63:1433-1440.

ASTM Annual Book of Standards. 2001. ASTM D790M-92. Standard test methods for flexural properties of unreinforced plastics and electrical insulating materials. ASTM International.

Batson, E.L., G.C. Reilly, J.D. Currey, and D.S. Balderson. 2000. Postexercise and positional variation in mechanical properties of the radius in young horses. Equine Veterinary Journal 32(2):95-100.

Bellairs, A.D'A., and C.R. Jenkin. 1960. The skeleton of birds. Pages 241-300 *in* A.J.Marshall, editor. Biology and comparative physiology of birds. Volume 1. NewYork, NY: Academic Press. 518 p.

Brear, K., and J.D. Currey. 1993. The mechanical design of the tusk of the narwhal (*Monodon monoceros*: Cetacea). Journal of Zoology, London 230:411-423.

Budker, P. 1971. The life of sharks. New York, NY: Columbia University Press. 222 p.

Burr, D.B. 2002. The contribution of the organic matrix to bone's material properties. Bone 31(1):8-11.

Carter, D.R., and G.S. Beaupré. 2001. Skeletal Function and Form. Cambridge: Cambridge University Press. 318 p.

Compagno, L.J.V. 1999. Endoskeleton. Pages 69-92 *in* W.C Hamlett, editor. Sharks, skates, and rays: the biology of elasmobranch fishes. Baltimore,MD: Johns Hopkins University Press. 515 p.

Currey, J.D. 1960. Differences in the blood supply of bone of different histological types. Quarterly Journal of Microscopical Science 101(3):351-370.

Currey, J.D. 1968. The effect of protection on the impact strength of rabbits' bones. Acta Anatomica 71:87-93.

Currey, J.D. 1969. The mechanical consequences of variation in the mineral content of bone. Journal of Biomechanics 2:1-11.

Currey, J.D. 1975. The effects of strain rate, reconstruction and mineral content on some mechanical properties of bovine bone. Journal of Biomechanics 8:81-86.

Currey, J.D. 1979a. Mechanical properties of bone tissues with greatly differing functions. Journal of Biomechanics 12:313-319.

Currey, J.D. 1979b. Changes in the impact energy absorption of bone with age. Journal of Biomechanics 12:459-469.

Currey, J.D. 1984. The Mechanical Adaptations of Bones. Princeton, NJ: Princeton University Press. 294 p.

Currey, J.D. 1988a. The effects of drying and re-wetting on some mechanical properties of cortical bone. Journal of Biomechanics 21:439-441.

Currey, J.D. 1988b. Strain rate and mineral content in fracture models of bone. Journal of Orthopaedic Research 6:32-38.

Currey, J.D. 1998. Mechanical properties of vertebrate hard tissues. Proceedings of the Institution of Mechanical Engineers Part H. Journal of Engineering in Medicine 212(H6):399-411.

Currey, J.D. 1999. What determines the bending strength of compact bone? Journal of Experimental Biology 202:2495-2503.

Currey, J.D. 2001. Ontogenetic changes in compact bone material properties. Pages 19.1-16 *in* S.C. Cowin, ed. Bone mechanics handbook. Boca Raton, FL: CRC Press. 980 p.

Currey, J.D. 2002. Bones: structures and mechanics. Princeton, NJ: Princeton University Press. 436 p.

Currey, J.D. 2003. The many adaptations of bone. Journal of Biomechanics 36:1487-1495.

Currey, J.D. 2004a. Incompatible mechanical properties in compact bone. Journal of Theoretical Biology 231:569-580.

Currey, J.D. 2004b. Tensile yield in compact bone is determined by strain, post-yield behaviour by mineral content. Journal of Biomechanics 37:549-556.

Currey, J.D., and K. Brear. 1990. Hardness, Young's modulus and yield stress in mammalian mineralized tissues. Journal of Materials Science: Materials in Medicine 1:14-20.

Currey, J.D., K. Brear, and P. Zioupos. 1994. Dependence of mechanical properties on fibre angle in narwhal tusk, a highly oriented biological composite. Journal of Biomechanics 27:885-897.

Currey, J.D., K. Brear, and P. Zioupos. 1996. The effects of ageing and changes in mineral content in degrading the toughness of human femora. Journal of Biomechanics 29(2):257-260.

Currey, J.D., and G. Butler. 1975. The mechanical properties of bone tissue in children. Journal of Bone and Joint Surgery 57A(6):810-814.

Currey, J.D., and C.M. Pond. 1989. Mechanical properties of very young bone in the axis deer (*Axis axis*) and humans. Journal of Zoology, London 218:59-67.

Currey, J.D., P. Zioupos, and A. Sedman. 1995. Microstructure-property relations in vertebrate bony hard tissues: microdamage and toughness. p. 117-144 i*n*: Sarikaya, M. and Aksay, I.A. eds. Biomimetics: design and processing of materials. Woodbury, NY: AIP Press. 285 p.

Dayoub, S., H. Devlin, and P. Sloan. 2003. Evidence for the formation of metaplastic bone from pericytes in calcifying fibroblastic granuloma. Journal of Oral Pathology and Medicine 32:232-236.

De Buffrenil, V., A. de Ricqles, C.E. Ray, and D.P. Domning. 1990. Bone histology of the ribs of the archaeocetes (Mammalia: Cetacea). Journal of Vertebrate Paleontology 10:455-466.

De Buffrenil, V., and D. Schoevaert. 1989. Donnees quantitatives et observations histologiques sur la pachyostose du squelette du dugong, *Dugong dugon* (Muller) (Sirenia, Dugongidae). Canadian Journal of Zoology 67:2107-2119.

Della Bona, A., T.J. Hill, and J. J. Mecholsky, Jr. 2001. The effect of contour angle on fractal dimension measurement for brittle materials. Journal of Materials Science 36:2645-2650.

Domning, D.P., and V. de Buffrenil. 1991. Hydrostasis in the Sirenia: quantitative data and functional interpretations. Marine Mammal Science 7(4):331-368.

Domning, D.P., and A.C. Myrick, Jr. 1980. Tetracycline marking and the possible layering rate of bone in an Amazonian manatee (*Trichechus inunguis*). Pages 203-207 *in* W.F. Perrin and A.C. Myrick, Jr., editors. Age determination of toothed whales and sirenians. Special Issue 3, Reports of the International Whaling Commission, Cambridge, UK. 229 p.

Eberhardt, L.L., and T. J. O'Shea. 1995. Integration of manatee life history data and population modeling. Pages 269-279 *in* T.J. O'Shea. B.B. Ackerman, and H.F. Percival, editors. Population biology of the Florida manatee. National Biological Service Information and Technology Report 1. Springfield, VA: National Technical Information Service. 289 p.

Enlow, D.H., and S.O. Brown. 1956. A comparative histological study of fossil and recent bone tissues. Part I. Texas Journal of Science 8(4):405-443.

Enlow, D.H., and S.O. Brown. 1957. A comparative histological study of fossil and recent bone tissues. Part II. Texas Journal of Science 9(2):186-214.

Enlow, D.H., and S.O. Brown. 1958. A comparative histological study of fossil and recent bone tissues. Part III. Texas Journal of Science 10(2):187-230.

Evans, G.P., J.C. Behiri, J.D. Currey, and W. Bonfield. 1990. Microhardness and Young's modulus in cortical bone exhibiting a wide range of mineral volume fractions, and in a bone analogue. Journal of Materials Science: Materials in Medicine 1:38-43.

Fang, J., and B.K. Hall. 1997. Chondrogenic cell differentiation from membrane bone periostea. Anatomy and Embryology 196:349-362.

Fawcett, D.W. 1942a. On the amedullary bones of the Florida manatee (*Trichechus latirostris*). Anatomical Record 82:410-411.

Fawcett, D.W. 1942b. The amedullary bones of the Florida manatee (*Trichechus latirostris*). American Journal of Anatomy 71:271-309.

Feldhamer, G.A., L.C. Drickamer, S.H. Vessey, and J.F. Merritt. 1999. Mammalogy: adaptation, diversity, and ecology. Dubuque: McGraw-Hill. 563 p.

Felts, W.J.L., and F.A. Spurrell. 1965. Structural orientation and density in cetacean humeri. American Journal of Anatomy 116:171-203.

Felts, W.J.L., and F.A. Spurrell. 1966. Some structural and developmental characteristics of cetacean (Odontocete) radii. A study adaptive osteogenesis. American Journal of Anatomy 118:103-134.

Fish, F.E., and B.R. Stein. 1991. Functional correlates of differences in bone density among terrestrial and aquatic genera in the family Mustelidae (Mammalia). Zoomorphology 110:339-345.

Florida Department of Natural Resouces. 1989. Recommendations to improve boating safety and manatee protection for Florida waterways. Final report to the Governor and Cabinet, State of Florida. 20 p.

Florida Fish and Wildlife Conservation Commission. 2005. Manatee Mortality Statistics. Florida Marine Research Institute, St. Petersburg, FL. http://floridamarine.org/features/category_sub.asp?id=2241 (last accessed: 8/2005).

Foote, J.S. 1916. A contribution to the comparative histology of the femur. Smithsonian Contributions to Knowledge 35:1-242.

Gallagher, J.C., H.K. Kinyamu, S.E. Fowler, B. Dawson-Hughes, G.P. Dalisky, and S.S. Sherman. 1998. Caliotropic hormones and bone markers in the elderly. Journal of Bone and Mineral research 13(3):475-482.

Goodrich, E.S. 1986. Studies on the structure and development of vertebrates. Chicago, IL: University of Chicago Press. 837 p.

Gundberg, C.M., A.C. Looker, S.D. Nieman, and M.S. Calvo. 2002. Patterns of osteocalcin and bone specific alkaline phosphatase by age, gender, and race or ethnicity. Bone 31(6):703-708.

Hall, B.K. 1984. Development processes underlying the evolution of cartilage and bone. Pages 155-176 *in* M.J.W. Ferguson, editor. The structure, development and evolution of reptiles. London: Zoological Society of London. 697 p.

Hall, B.K. 2005. Bones and cartilage: developmental and evolutionary skeletal biology. London, UK: Elsevier Academic Press. 760 p.

Harvey, K.B., and S.W. Donahue. 2004. Bending properties, porosity, and ash fraction of black bear (*Ursus americanus*) cortical bone are not compromised with aging despite annual periods of disuse. Journal of Biomechanics 37:1513-1520.

Harvey, K.B., and S.W. Donahue. 2005. The tensile strength of black bear (*Ursus americanus*) cortical bone is not compromised with aging despite annual periods of hibernation. Journal of Biomechanics 38:2143-2150.

Hayes, W.C., and M.L. Bouxsein. 1997. Biomechanics of cortical and trabecular bone: Implications for assessment of fracture risk. Pages 69-111 *in* Basic orthopaedic biomechanics. Second Ed. Philadelphia, PA: Lippincott-Raven Publishers. 514 p.

Hildebrand, M. 1988. Analysis of vertebrate structure. Third Ed. New York, NY: John Wiley & Sons. 701 p.

Hill, T.J. 2001. Quantitative fracture analysis of a biological ceramic composite. PhD Dissertation, University of Florida, Gainesville, Florida. 100 p.

Hill, T.J., A. Della Bona, and J.J. Mecholsky, Jr. 2001 Establishing a protocol for measurements of fractal dimensions in brittle materials. Journal of Materials Science 36:2651-2657.

Jackson, A.P. 1992. Bone, nacre, and other ceramics. Pages 33-56 *in* Vincent, J.F.V., editor. Biomechanics- materials: a practical approach. NewYork, NY: Oxford University Press. 247 p.

Jee, W.S.S. 1988. The skeletal tissues. Pages 213-254 *in* L. Weiss, Editor. Cell and tissue biology: a textbook of histology. Sixth Ed. Baltimore, MD: Urban & Schwarzenberg. 1158 p.

Johnson, M.L., J.L.Picconi, and R.R. Recker. 2002. The gene for high bone mass. The Endocrinologist 12(5):445-453.

Kaiser, H.E. 1965. The phylogenetic adaptation of aquatic mammals to their environment. American Zoologist 5:229.

Kaiser, H.E. 1967. Pachyostotic bone conditions in certain regions of the skull of *Odobenus rosmarus L.*, in relation to weight distribution. Anatomical Record 157:366.

Kaufman, J.J., and R.S. Siffert. 2001. Nonivasive measurement of bone integrity. Pages 34.1-34.25 *in* S.C. Cowin, editor. Bone mechanics handbook. Boca Raton, FL: CRC Press. 980 p.

Kawakami, T., T. Kawai, A. Kimura, H. Hasegawa, H. Tsujigiwa, M. Gunduz, H. Nagatsuka, and N. Nagai. 2001. Characteristics of bone morphogenetic protein-induced chondriod bone: histochemical, immunohistochemical and *in situ* hybridization examinations. Journal of International Medical Research 29:480-487.

Kent, G.C., and L. Miller. 1997. Comparative anatomy of the vertebrates. Eighth ed. Dubuque, IA: McGraw Hill. 487 p.

Key West Boats, Inc. 2005. 1760 Stealth. Ridgeville, SC: Key West Boats, Inc. http://www.keywestboatsinc.com/boats/1760stealth.html. (last accessed 12/2005).

Kipps, E.K., W.A McLellan, S.A. Rommel, and D.A Pabst. 2002. Skin density and its influence on buoyancy in the manatee (*Trichechus manatus latirostris*), harbor porpoise (*Phocoena phocoena*), and bottlenose dolphin (*Tursiops truncatus*). Marine Mammal Science 18(3):765-778.

Koay, M.A., and M.A. Brown. 2005. Genetic disorders of the LRP5-Wnt signalling pathway affecting the skeleton. Trends in Molecular Medicine 11(3):129-137.

Les, C.M., S.M. Stover, J.H. Keyak, K.T. Taylor, and A.J. Kaneps. 2002. Stiff and strong compressive properties are associated with brittle post-yield behavior in equine compact bone material. Journal of Orthopaedic Research 20:607-614.

Li, C.Y., B.D. Gelb, K.J. Jepsen, and M.B. Schaffler. 2005a. Cathepsin K-deficiency results in bone fragility in mice. Journal of Bone and Mineral Research 20(1):S295.

Li, Y.P., Y. Abe, R Isoda, R. Moroi, S. Yang, J.Z. Shao, E. Li, and W. Chen. 2005b. Cathepsin K-deficient mice exhibit pycnodysostosis features due to loss of cathepsin K-mediated osteoclast senescence for bone homeostasis. Journal of Bone and Mineral Research 20(1):S253.

Lopez, D., A.C. Duran, A.V. de Andrés, A. Guerrero, M. Blasco, and V. Sans-Coma. 2003. Formation of cartilage in the heart of the Spanish Terrapin, *Mauremys leprosa* (Reptilia, Chelonia). Journal of Morphology 258(1):97-105.

Lucchinetti, E. 2001. Dense bone tissue as a molecular composite. Pages 13.1-15 25 *in* S.C. Cowin, editor. Bone mechanics handbook. Boca Raton, FL: CRC Press. 980 p.

Maes, C., J.J. Haigh, A. Chan, K. Haigh, R. Bouillon, G. Carmeleir, and A. Nagy. 2005. Aberrent bone formation in mice over-expressing specific VEGF isoforms in cartilage. Journal of Bone and Mineral Research 20(1):S39.

Majumdar, S., R.S. Weinstein, and R.R. Prasad. 1993. Application of fractal geometry techniques to the study of trabecular bone. Medical Physics 20(6):1611-1619.

Mako Marine International, Inc. 2005. 171 Center Console. Springfield, MO: Mako Marine International, Inc. http://www.mako-boats.com/boat/index.cfm?fuseaction=boat.specs&nav=193&boat=1678. (last accessed 12/2005).

Malik, C.L., S.M. Stover, R.B. Martin, J.C. Gibeling. 2003. Equine cortical bone exhibits rising R-curve fracture mechanics. Journal of Biomechanics 36:191-198.

Mandelbort, B.B., D.E. Passoja, and A.J. Paullay. 1984. Fractal character of fracture surfaces of metals. Nature 308(19):721-722.

Marieb, E.N.1995. Human anatomy and physiology. Third Ed. Redwood City, CA: Benjamin/Cummings. 1040 p.

Marmontel, M. 1993. Age determination and population biology of the Florida manatee, *Trichechus manatus latirostris*. Ph.D. dissertation, University of Florida, Gainesville. 408 p.

Martin, R.B, and D.B. Burr. 1989. Structure, function, and adaptation of compact bone. New York, NY: Raven Press. 275 p.

Martin, R.B., D.B. Burr, and N.A. Sharkey. 1998. Skeletal tissue mechanics. New York, NY: Springer-Verlag. 392 p.

Maverick Boat Company, Inc. 2004. Maverick 17' Master Angler. Ft. Pierce, FL: Maverick Boat Company, Inc. http://www.maverickboats.com/maverick/boat_specs/17ma.htm. (last accessed 12/2005).

Mecholsky, J.J., Jr. 1986. Fractals—fact or fiction? Earth and Mineral Sciences 55(3):29-33.

Mecholsky, J.J., Jr. 1993. Quantitative fracture surface analysis of glass materials. Pages 483-521 *in* C.J. Simmons and O.H. El-Bayoumi. editors. Experimental techniques of glass science. Westerville: American Ceramic Society. 524 p.

Mecholsky, J.J., Jr. 1996. Fractography, fracture mechanics and fractal geometry: an integration. Pages 385-393 *in* J.R. Varner, V.D. Frechette, and G.D. Quinn, editors. Ceramic Transations. Fractography of glasses and ceramics III. Westerville: American Ceramic Society. 547 p.

Mecholsky, J.J., Jr. 2001. Fractography: brittle materials.Pages 3257-3265 *in* K.H.J. Buchow et al., eds. Encyclopedia of Materials: Science and Technology. Oxford, UK: Pergamon Press. 10,000 p.

Mecholsky, J.J., Jr., D.E. Passoja, and K.S. Feinberg-Ringel. 1989. Quantitative Analysis of Brittle Fracture Surfaces Using Fractal Geometry. Journal of the American Ceramic Society 72(1):60-65.

Mecholsky, J.J., Jr., J.K. West, and D.E. Passoja. 2002. Fractal dimension as a characterization of free volume created during fracture in brittle materials. Philosophical Magazine A 82 (17/18):3163-3176.

Meier, C., U. Meinhardt, M.E. Kraenzlin, J.R. Greenfield, T.V. Nguyen, C.R. Dunstan, and M.J. Seibel. 2005. Serum cathepsin K levels reflect osteoclastic activity in women with postmenopausal osteoporosis and patients with Paget's disease. Journal of Bone and Mineral Research 20(1):S222.

Meister, W. 1962. Histological structure of the long bones of penguins. Anatomical Record 143:377-387.

Moss, M.L. 1961. Osteogenesis of acellular teleost fish bone. American Journal of Anatomy 108:99-110.

Murray, P.D.F. 1936. Bones: a study of the development and structure of the vertebrate skeleton. London: Cambridge University Press. 203 p.

Nah, H.D., M. Pacifici, L.C. Gerstenfeld, S.L. Adams, and T. Kirsch. 2000. Transient chondrogenic phase in the intramembranous pathway during normal skeletal development. Journal of Bone and Mineral Research. 15(3):522-533.

Nalla, R.K., J.J. Kruzic, J.H. Kinney, and R.O. Ritchie. 2004. Effect of aging on the toughness of human cortical bone: evaluation by R-curves. Bone 35:1240-1246.

Nikolić, V., J. Hančević, M. Hudec, and B. Banović. 1975. Absorption of the ipact energy in the palmar soft tissues. Anatomy and Embryology 148:215-221.

Nopcsa, F. von. 1923. Vorläufige notiz über die Pachyostose und Osteosclerose einiger mariner Wirbeltiere. Anatomischer Anzeiger 56(15/16):353-359.

O'Shea, T.J., C.A. Beck, R.K. Bonde, H.I. Kochman, and D.K. Odell. 1985. An analysis of manatee mortality patterns in Florida, 1976-81. Journal of Wildlife Management 49(1):1-11.

Parkkari, J., P. Kannus, J. Poutala, and I. Vuori. 1995. Force attenuation properties of varioustrochanteric padding materials under typical falling conditions of the elderly. Journal of Bone and Mineral Research 9(9):1391-1396.

Parkkari, J., P. Kannus, J. Heikkila, J. Poutala, H. Sievanen, and I. Vuori. 1995. Energy-shunting external hip protector attenuates the peak femoral impact force below the theoretical fracture threshold: an in vitro biomechanical study under falling conditions of the elderly. Journal of Bone and Mineral Research 10(10):1437-1442.

Pelker, R.R., G.E. Friedlaender, T.C. Markham, M.M. Panjabi, and C.J. Moen. 1984. Effects of freezing and freeze-drying on the biomechanical properties of rat bone. Journal of Orthopaedic Research 1:405-411.

Phelps, J.B., G.B. Hubbard, X. Wang, and C.M. Agrawal. 2000. Microstructural heterogeneity and the fracture toughness of bone. Journal of Biomedical Materials Research 51:735-741.

Reilly, G.C., and J.D. Currey. 1999. The development of microcracking and failure in bone depends on the loading mode to which it is adapted. Journal of Experimental Biology 202:543-552.

Reynolds, J.E. III, and D.K. Odell. 1991. Manatees and Dugongs. New York, NY: Facts On File, Inc. 192 p.

Rhodin, A.G.J., J.A. Ogden, and G.J.Conlogue. 1981. Chondro-osseus morphology of *Dermochelys coriacea*, a marine reptile with mammalian skeletal features. Nature 290:244-246.

Riley, W.F., L.D. Sturges, and D.H. Morris. 1999. Mechanics of Materials, 5th Ed. New York, NY: John Wiley and Sons. 1999 p.

Robinovitch, S.N., T.A. McMahon, and W.C. Hayes. 1995. Force attenuation in trochanteric soft tissues during impact from a fall. Journal of Orthopaedic Research 13:956-962.

Romer, A.S., and T.S. Parsons. 1977. The vertebrate body. Fifth ed. Philadelphia, PA: Saunders College Publishing. 624 p.

Russ, J.C. 1994. Fractal surfaces. New York, NY: Plenum Press. 309 p.

SAS Institute Inc. 1989. SAS/STAT User's Guide, Version 6, Fourth Edition, Volume 2. Cary, NC:SAS Institute Inc. 846 p.

Savage, R.J.G. 1976. Review of early Sirenia. Systematic Zoology 25:344-351.

Schaffler, M.B., and D.B. Burr. 1988. Stiffness of compact bone: effects of porosity and density. Journal of Biomechanics 21(1):13-16.

Schryver, F. 1978. Bending properties of cortical bone of the horse. American Journal of Veterinary Research 39(1):25-28.

Sedlin, E.D., and C. Hirsch. 1966. Factors affecting the determination of the physical properties of femoral cortical bone. Acta orthop. Scandinavia 37:29-48.

Shapiro, F. 1993. Osteopetrosis- Current clinical considerations. Clinical Orthopaedics and Related Research 294:34-44.

Sickenberg, O. 1931. Morphologie und stammesgeschichte der Sirenen I. Die einflüsse des Wasserlebens auf die innere secretion und formgestaltung der Sirenen. Paleobiologica (Wien) 4(6/7):405-444.

Siomin, V., R. Willinsky, P. Shannon, and A.Guha1. 2003. Metaplastic bone formation in a low grade conus glioma: case report and review of the literature. Journal of Neuro-Oncology 62: 275–280.

Stein, B.R. 1989. Bone density and adaptation in semiaquatic mammals. Journal of Mammalogy 70(3):467-476.

Steinbrech, D.S, B.J. Mehrara, P.B. Saadeh, G. Chin, M.E. Dudziak, R.P. Gerrets, G.K. Gittes, and M.T. Longaker. 1999. Hypoxia regulates VEGF expression and cellular proliferation by osteoblasts in vitro. Plastic and Reconstructive Surgery 104(3):738-747.

Swartz, S.M., and P. Watts. 1999. Structural design of finger bones of bats. American Zoologist 39(5):101A.

Thompson, D.W. 1942. On growth and form: the revised edition. Mineola, NY: Dover Publications, Inc. 1116 p.

Tolar, J., S.L. Teitelbaum, P.J. Orchard. 2004. Osteopetrosis. New England Journal of Medicine 351:2839-2849.

Turner, C.H., and D.B. Burr. 1993. Basic biomechanical measurements of bone: a tutorial. Bone 14:595-608.

U.S.Coast Guard. 2005. Boating statistics-2004. Washington, DC: United States Coast Guard. 47p. http://www.uscgboating.org/statistics/Boating_Statistics_2004.pdf (last accessed 11/05).

U.S. Fish and Wildlife Service. 1996. Florida manatee (*Trichechus manatus latirostris*) recovery plan. U.S. Fish and Wildlife Service, Atlanta, Ga. 160 p.

U.S. Fish and Wildlife Service. 2000. Technical/Agency Draft, Florida Manatee recovery Plan, (*Trichechus manatus latirostris*), Third Revision. Atlanta, GA: U.S. Fish and Wildlife Service. 145 p.

Vashishth, D. 2004. Rising crack-growth-resistance behavior in cortical bone: implications for toughness measurements. Journal of Biomechanics 37:943-946.

Vashishth, D., J.C. Behiri, and W. Bonfield. 1997. Crack growth resistance in cortical bone: concept of microcrack toughening. Journal of Biomechanics 30(8): 763-769.

Vincent, J.F.V. 1990. Structural Biomaterials. Princeton, NJ: Princeton University Press. 244 p.

Wainwright, S.A., W.D. Biggs, J.D. Currey, and J.M. Gosline. 1982. Mechanical Design in Organisms. Princeton, NJ: Princeton University Press. 423 p.

Wall, W.P. 1983. The correlation between high limb-bone density and aquatic habits in recent mammals. Journal of Paleontology 57(2):197-203.

Wang, X., R.A. Bank, J.M. TeKoppele, and C.M. Agrawal. 2001. The role of collagen in determining bone mechanical properties. Journal of Orthopaedic Research 19:1021-1026.

Wang, X., X. Shen, X. Li, and C. M. Agrawal. 2002. Age-related changes in the collagen network and toughness of bone. Bone 31(1):1-7.

Warren, S.M., D.S. Steinbrech, B.J. Mehrara, P.B. Saadeh, J.A. Greenwald, J.A. Spector, P.J. Bouletreau, and M.T. Longaker. 2001. Hypoxia regulates osteoblast gene expression. Journal of Surgical Research 99:147-155.

West, J.K., J.J. Mecholsky, Jr., and L.L. Hench. 1999. The application of fractal and quantum geometry to brittle fracture. Journal of Non-Crystalline Solids 260:99-108.

Witten, P.E., and B.K. Hall. 2002. Differentiation and growth of kype skeletal tissues in anadromous male Atlantic Salmon (*Salmo salar*). International Journal of Developmental Biology 46:719-730.

Witten, P.E., and B.K. Hall. 2003. Seasonal changes in the lower jaw skeleton in male Atlantic salmon (*Salmo salar* L.): remodelling and regression of the kype after spawning. Journal of Anatomy 203:435-450.

Wright, S.D., B.B. Ackerman, R.K. Bonde, C.A. Beck, and D.J. Banowetz. 1995. Analysis of watercraft-related mortality of manatees in Florida, 1979-1991. Pages 259-268 *in* T.J. O'Shea, B.B. Ackerman, and H.F. Percival, editors. Population biology of the Florida manatee. National Biological Service Information and Technology Report 1. Springfield, VA: National Technical Information Service. 289 p.

Yan, J. 2002. Biomechanical properties of manatee rib bone and analytical study using finite element analysis. Master thesis, University of Florida, Gainesville, Florida. 115 p.

Yan, J. 2005. Elastic-plastic fracture mechanics of compact bone. PhD Dissertation, University of Florida, Gainesville, Florida. 110 p.

Yan, J., K.B. Clifton, R.L. Reep, and J.J. Mecholsky, Jr. 2005. Fracture toughness of manatee rib and bovine femur using a Chevron-notched beam test. Journal of Biomechanics. Accepted February 15, 2005.

Yeni, Y.N., C.U. Brown, and T.L. Norman. 1998. Influence of bone composition and apparent density on fracture toughness of the human femur and tibia. Bone 22(1):79-84.

Zar, J.H. 1996. Biostatistical Analysis. Third Edition. Upper Saddle River: Prentice Hall. 662 p.

Zioupos, P. 1998. Recent developments in the study of failure of solid biomaterials and bone: 'fracture' and 'pre-fracture' toughness. Materials Science and Engineering C 6:33-40.

Zioupos, P., and J.D. Currey. 1998. Changes in the stiffness, strength, and toughness of human cortical bone with age. Bone 22(1):57-66.

Zioupos, P., J.D. Currey, A. Casinos, and V. de Buffrenil. 1997. Mechanical properties of the rostrum of the whale *Mesoplodon densirostris*, a remarkably dense bony tissue. Journal of Zoology, London 241:725-737.

Zioupos, P., J.D. Currey, and A.J. Hamer. 1999. The role of collagen in the declining mechanical properties of aging human cortical bone. Journal of biomedical Materials Research 45(2):108-116.

## BIOGRAPHICAL SKETCH

Kari Beth Clifton was born in Chicago, Illinois, and grew up in the near west suburb of Oak Park. She attended Valparaiso University where she majored in biology and French, and minored in chemistry. While there she spent a semester studying in Paris, and another term working with marine mammals at Brookfield Zoo in Chicago. She also played field hockey, served as an editor for the school's literary publication, and learned to SCUBA dive. Kari graduated in 1988 with a Bachelor of Science degree. After graduation Kari moved to Tampa, Florida to attend graduate school at the University of South Florida. Her research topic was entitled "Ecomorphological relationships of five species of labrids (Labridae, Teleostei) in a coral reef community." She graduated with a Master of Science in zoology in 1993. In January 1992, Kari began working for the (former) Florida Department of Natural Resources tagging redfish and mullet. After 2 months, she moved to the Endangered and Threatened Species program, where she began work on the population biology of the Florida manatee. During her 7 years with the state, she flew aerial surveys of manatees and right whales, and participated in radiotelemetry, captures, rescues, and necropsies. In 1996 she undertook a study on manatee bone mechanics that eventually led her to Gainesville. In 1998, Kari resigned her position to enter the PhD program at the University of Florida's College of Veterinary Medicine, to continue the bone research full time. Kari has accepted a postdoctoral position at the Mayo Clinic, where she will continue to do bone research.